

AREAS OF CONTACT AND PRESSURE DISTRIBUTION
IN BOLTED JOINTS

H.H. Gould

B.B. Mikic

Final Technical Report

Prepared for

George C. Marshall Space Flight Center
Marshall Space Flight Center
Alabama 35812

under

Contract NAS 8-24867

June 1970

DSR Project 71821-68

Engineering Projects Laboratory
Department of Mechanical Engineering
Massachusetts Institute of Technology
Cambridge, Massachusetts 02139

ABSTRACT

When two plates are bolted (or riveted) together these will be in contact in the immediate vicinity of the bolt heads and separated beyond it. The pressure distribution and size of the contact zone is of considerable interest in the study of heat transfer across bolted joints.

The pressure distributions in the contact zones and the radii at which flat and smooth axisymmetric, linear elastic plates will separate were computed for several thicknesses as a function of the configuration of the bolt load by the finite element method. The radii of separation were also measured by two experimental methods. One method employed autoradiographic techniques. The other method measured the polished area around the bolt hole of the plates caused by sliding under load in the contact zone. The sliding was produced by rotating one plate of a mated pair relative to the other plate with the bolt force acting.

The computational and experimental results are in agreement and these yield smaller zones of contact than indicated by the literature. It is shown that the discrepancy is due to an assumption made in the previous analyses.

In addition to the above results this report contains the finite element and heat transfer computer programs used in this study. Instructions for the use of these programs are also included.

ACKNOWLEDGMENTS

This report was supported by the NASA Marshall Space Flight Center under contract NAS 8-24867 and sponsored by the Division of Sponsored Research at M.I.T.

TABLE OF CONTENTS

	<u>Page</u>
Title Page	1
Abstract	2
Acknowledgments	3
Table of Contents	4
List of Tables and Figures	6
Nomenclature	8
Chapter I: Introduction	10
Chapter II: Analysis	15
A. Problem Statement	15
B. Method of Analysis	18
Chapter III: Experimental Method	23
Chapter IV: Results	28
A. Pressure Distribution and Radii of Separation from Single Plate and Two Plate Finite Element Models	28
B. Radii of Separation from Experiment and Their Pre- dicted Values from the Two Plate Finite Element Computation	29
Chapter V: Application	32
Chapter VI: Conclusions	35
References	37
Appendices	
A. Finite Element Analysis of Axisymmetric Solids	39

	<u>Page</u>
B. Finite Element Program for the Analysis of Isotropic Elastic Axisymmetric Plates	44
C. Finite Element Program for the Analysis of Isotropic Elastic Axisymmetric Plates — Thermal Strains Included	68
D. Steady State Heat Transfer Program for Bolted Joint	94

LIST OF TABLES AND FIGURES

<u>Table</u>		<u>Page</u>
1	Separation Radius Comparison - Single and Two Plate Models	100
2	Test and Analytical Results for Radii of Separation of Bolted Plates	101
 <u>Figure</u>		
1	Bolted Joint	102
2	Roetscher's Rule of Thumb for Pressure Distribution in a Bolted Joint	102
3	Furnlund's Sequence of Superposition	103
4	Finite Element Idealization of Two Plates in Contact	107
5	Finite Element Models	108
6	Examples of Unacceptable Solutions	109
7	Plate Specimen, Bolt and Nuts, Fixture and Tools	110
8	Footprints on the Mating Surface of 1/16 - 1/16, 1/8 - 1/8, 3/16 - 3/16, 1/4 - 1/4, and 1/8 - 1/4 Pairs	111
9	Footprint of Nut on Plate	116
10	X-Ray Photographs of Contamination Transferred from Radioactive Plate to Mated Plate. 1/16, 1/4, 3/16, 1/4 Inch Pairs	117
11	Free Body Diagram for Two Plates in Contact	119
12	Single Plate Analysis-Midplane σ_z Stress Distribution	120
13	Single Plate Analysis-Midplane σ_z Stress Distribution	121
14	Single Plate Analysis-Midplane σ_z Stress Distribution	122

<u>Figure</u>		<u>Page</u>
15	Interface Pressure Distribution in a Bolted Joint	123
16	Interface Pressure Distribution in a Bolted Joint	124
17	Interface Pressure Distribution in a Bolted Joint	125
18	Finite Element Analysis Results for 1/4 Inch Plate Pair	126
19	Pressure in Joint, Triangular Loading	127
20	Variations of Loading and Boundary Conditions	128
21	Pressure in Joint, Uniform Displacement Under Nut	129
22	Deflection of Plate Under Nut	130
23	Finite Element Analysis Results for 3/16 Inch Plate Pair	131
24	Finite Element Analysis Results for 1/8 Inch Plate Pair	132
25	Gap Deformation for Free and Fixed Edges — Finite Element Analysis, 1/8 inch Plate Pair.	133
26	Finite Element Analysis Result for 1/16 Inch Plate Pair	134
27	Finite Element Analysis Results for 1/8 Inch Plate Mated With 1/4 Inch Plate	135
28	Comparison Between Tested and Measured Separation Radii	136
29	Location of Nodes — Steady State Heat Transfer Analysis	137

NOMENCLATURE

A, B, C	radii
D	thickness
E	modulus of elasticity
G	shear modulus
h_c, h_f	heat transfer coefficients
H	hardness
k, k_1, k_2	thermal conductivities
P, p	pressure
r	coordinate
R_o	radius of separation
u, w	displacement in r and z directions
x	coordinate
X_c	length of contact
y	coordinate
y'	slope
z	coordinate
δ	deflection
ϵ	dilation
$\epsilon_r, \epsilon_t, \epsilon_{rz}$	strains
$\sigma, \sigma_1, \sigma_2$	standard deviations
$\sigma_r, \sigma_t, \sigma_z$	stresses

λ, μ	Lame's constants
ν	Poisson's ratio
τ	shear stress
θ	angle

Subscripts

r	radial direction
t	tangential direction
z	z-direction

Chapter I

INTRODUCTION

When two plates are bolted (or riveted) together, these will be in contact in the immediate vicinity of the bolt heads and separated beyond it. The pressure distribution in the contact area and the separation of the plates is of considerable interest in the study of heat transfer across joints. Cooper, Mikic and Yovanovich [1] show that with assumed Gaussian distribution of surface heights, the microscopic contact conductance is related to the interface pressure, surface characteristics and the hardness of the softer material in

$$h_c = 1.45 \frac{\tan \theta}{\sigma} k \left(\frac{P}{H} \right)^{0.985} \quad (1.1)$$

where

$$k \equiv \frac{2k_1 k_2}{k_1 + k_2} \quad (1.2)$$

and k_1 and k_2 represent the thermal conductivities of two bodies in contact; σ is the combined standard deviation for the two surfaces which can be expressed as

$$\sigma = (\sigma_1^2 + \sigma_2^2)^{1/2} \quad (1.3)$$

where σ_1 and σ_2 are the individual standard deviation of height for the respective surfaces; $\tan \theta$ is the mean of the absolute value of slope for the combined profile and it is related, for normal distribution of slope, to the individual mean of absolute values of slopes as

$$\tan \theta = (\tan^2 \theta_1 + \tan^2 \theta_2)^{1/2} \quad (1.4)$$

where

$$\tan \theta_i = \lim_{L \rightarrow \infty} \frac{1}{L} \int_0^L |y'_i| dx; \quad i = 1, 2 \quad (1.5)$$

and y' is the slope of the respective surface profiles; P represents the local interface pressure; and H is the hardness of the softer material.

Relation (1.1), as written above, is applicable for contact in a vacuum. One can modify the expression by simply adding to it

$$h_f \equiv \frac{\text{conductivity of interstitial fluid}}{\text{average distance between the surfaces}} \quad (1.6)$$

in order to account approximately for the presence of the interstitial fluid.

All parameters in relation (1.1), except for the pressure, are functions of the material and geometry and can be easily obtained. The determination of the pressure distribution and the extent of the contact area between two plates present both mathematical and experimental

difficulties. From the mathematical point of view, the difficulty stems from the fact that the theory of elasticity will yield a three dimensional (axisymmetric) problem with mixed boundary conditions. Experimentally, the discrimination between contact and gaps of the order of millionths of an inch is required.

Roetscher [2] proposed in 1927, a rule of thumb that the pressure distribution of two bolted plates, Fig.1, is limited to the two frustums of the cones with a half cone angle of 45 degrees as shown in Fig. 2 and that at any level within the cone the pressure is constant. Also, for symmetric plates, according to Roetscher, separation will occur at the circle which is defined by the contact plane and the 45 degree truncated cone emanating from the outer radius of the bolt head.

Since 1961 Fernlund [3], Greenwood [4] and Lardner [5] among others reported solutions based upon the theory of elasticity. Although their solutions also yield separation radii at approximately 45 degrees as in Roetscher's rule, their solutions yield a much more reasonable pressure distribution as compared to Roetscher's constant pressure at each level of the frustrum. These investigators have made use of the Hankel transform method demonstrated by Sneddon [6] in his solution for the elastic stresses produced in a thick plate of infinite radius by the application of pressure to its free surfaces. The basic assumption in their approach is that two bolted plates can be represented by a single plate of the same thickness as the combined thickness of the two plates under the same external loading. It then follows that the z -stress distribution at the parting plane can be approximated by the z -stress distribution in the same plane of the single plate. It also follows that separation will occur at the smallest radius in that plane for which

the z -stress is tensile. In the case of two plates of equal thickness the σ_z stress at the midplane of the equivalent single plate is the stress of interest.

Fernlund [3], for example, used the method of superposition in the sequence shown in Figs. 3(a) to 3(c) to obtain annular loading. Then by superposition of shear and radial stresses at radius A , Figs. 3(d) and 3 (e), opposite in sign of those due to the annular loading at the free surfaces, Fernlund obtained the solution for a single plate with a hole under annular loading (Fig. 3(f)).

Experimental work in this area included Bradley's [7] measurements of the stress field by three dimensional photoelasticity techniques, and the use of introducing pressurized oil at various radii in the contact zone and measuring the pressure at which oil leaks out from the joint [3,8]. Both of these experimental methods have uncertainties as indicated by the authors.

Because of the cumbersomness of the Hankel transform solution and experimental difficulties, the body of work in this area has been very limited and definite verification of analytical results by experiment is not cited in the literature.

The research described in the succeeding chapters was undertaken with the following primary objectives:

- a) To provide a method of solution for the case of two bolted plates without the simplifying assumption of the single plate substitution.
- b) To devise a test to validate the two plate analysis.
- c) To test the validity of the single plate substitution.

A finite element computer program has been assembled for the analytical solution of two-plate problems. Experiments have been performed to verify the analytical results. Since in heat transfer calculations the extent of the radius of contact is of primary importance, and since by restricting the experimental effort to the verification of only this parameter, (rather than the verification of the entire pressure distribution,) many experimental uncertainties should be eliminated, the experiments were designed only for the determination of the contact area.

Agreement between analysis and experiment was obtained and the results show that the single plate substitution is not justified and the 45 degree rule is not valid for the flat and smooth surfaces studied.

Chapter II

ANALYSIS

A. Problem Statement

The objective of the analysis was to solve the linear elasticity problem of two plates in contact defined mathematically by the following equations for each plate:

The equations of equilibrium

$$\frac{\partial}{\partial r} (r \sigma_r) - \sigma_t + r \frac{\partial \tau}{\partial z} = 0 \quad (2.1)$$

$$\frac{\partial}{\partial r} (r \tau) + \frac{\partial}{\partial z} (r \sigma_z) = 0$$

where $\tau_{rz} = \tau_{zr} = \tau$ and $\tau_{rt} = \tau_{tr} = \tau_{zt} = \tau_{tz} = 0$.

The stress - strain relations, using standard notation for stress and strain,

$$\begin{aligned} \sigma_r &= \lambda \epsilon + 2 \mu \epsilon_r \\ \sigma_t &= \lambda \epsilon + 2 \mu \epsilon_t \\ \sigma_z &= \lambda \epsilon + 2 \mu \epsilon_z \\ \tau &= 2 \mu \epsilon_{rz} \end{aligned} \quad (2.2)$$

where λ and μ are Lamé's constants and

$$\lambda = \frac{2 G \nu}{1 - 2\nu} \quad (2.3)$$

$$\mu = G$$

if G is the modulus of elasticity in shear and ν is Poisson's ratio;
and ϵ the volume expansion is defined by

$$\epsilon = \frac{\partial u}{\partial r} + \frac{u}{r} + \frac{\partial w}{\partial z} \quad (2.4)$$

where u is the displacement in the radial direction and w is the displacement in the axial direction.

The strain - displacement relations

$$\begin{aligned} \epsilon_r &= \frac{\partial u}{\partial r} \\ \epsilon_t &= \frac{u}{r} \\ \epsilon_z &= \frac{\partial w}{\partial z} \\ \epsilon_{rz} &= \frac{1}{2} \left(\frac{\partial u}{\partial z} + \frac{\partial w}{\partial r} \right) \end{aligned} \quad (2.5)$$

The above equations can be combined to yield the equilibrium equations in terms of displacements

$$\begin{aligned} \nabla^2 u - \frac{u}{r^2} + \frac{1}{1 - 2\nu} \frac{\partial \epsilon}{\partial r} &= 0 \\ \nabla^2 w + \frac{1}{1 - 2\nu} \frac{\partial \epsilon}{\partial z} &= 0 \end{aligned} \quad (2.6)$$

The applicable boundary conditions are (see Fig. 11)

$$\begin{aligned}
 \sigma_r^{(1)}(A, z) &= \sigma_r^{(2)}(A, z) = 0 \\
 \tau^{(1)}(A, z) &= \tau^{(2)}(A, z) = 0 \\
 \sigma_r^{(1)}(C, z) &= \sigma_r^{(2)}(C, z) = 0 \\
 \tau^{(1)}(C, z) &= \tau^{(2)}(C, z) = 0 \\
 \tau^{(1)}(r, D_1) &= \tau^{(2)}(r, -D_2) = 0, \\
 \tau^{(1)}(r, 0) &= \tau^{(2)}(r, 0), \quad A \leq r \leq R_0 \\
 \sigma_z^{(1)}(r, D_1) &= \sigma_z^{(2)}(r, -D_2) = 0, \quad B \leq r \leq C \\
 \tau^{(1)}(r, 0) &= \tau^{(2)}(r, 0) = 0, \quad R_0 \leq r \leq C \\
 \sigma_z^{(1)}(r, 0) &= \sigma_z^{(2)}(r, 0), \quad A \leq r \leq R_0 \\
 \sigma_z^{(1)}(r, 0) &= \sigma_z^{(2)}(r, 0) = 0, \quad R_0 \leq r \leq R \\
 \sigma_z^{(1)}(r, D_1) &= \sigma_z^{(2)}(r, -D_2) = P(r), \quad A \leq r \leq B \\
 w^{(1)}(r, 0) &= w^{(2)}(r, 0), \quad A \leq r \leq R_0
 \end{aligned} \tag{2.7}$$

$$2\pi \int_A^B Pr \, dr = 2\pi \int_A^{R_0} pr \, dr$$

Inspection of the above equations shows that the above constitutes a mixed boundary value problem and the most appropriate technique for solution is the finite element method.

B. Method of Analysis

A finite element computer program was assembled for the analytical solution of bolted plates. Descriptions of the finite element method are given in references [9,10], but for completeness, an outline of the mathematical formulation for this case is presented in Appendix A. A listing of the computer program and instructions for its use may be found in Appendix B. Appendix C contains user's instructions and a listing of the finite element program modified to include thermal strains.

As in the previous work axial symmetry and isotropic linear elastic material behavior were assumed. However, the computer programs accommodate plates with different material properties in a bolted pair.

The basic concept of the finite element method is that a body may be considered to be an assemblage of individual elements. The body then consists of a finite number of such elements interconnected at a finite number of nodal points or nodal circles. The finite character of the structural connectivity makes it possible to obtain a solution by means of simultaneous algebraic equations. When the problem, as is the case here, is expressed in a cylindrical coordinate system and in the presence of axial symmetry in geometry and load, tangential displacements do not exist, and the three-dimensional annular ring finite element is then reduced to the characteristics of a two-dimensional finite element.

The analysis consists of (a) structural idealization, (b) evaluation of the element properties, and (c) structural analysis of the assemblage of the elements. Items (b) and (c) are covered in the appendices and in the references quoted. The structural idealization and the criteria for acceptable solutions will be described in this chapter.

Fig. 4(a) shows two circular plates in contact under arbitrary axisymmetric loading. The plates are subdivided into a number of annular ring elements which are defined by the corner nodal circles (or node points when represented in a plane) as shown in Figs. 4(b) and 4(c). Unlike the cases described in Chapter I, which have been solved by the Hankel transform method, all plates solved by the finite element method have finite radii. The cross sections of each annular ring element is either a general quadrilateral or triangle. To improve accuracy smaller elements are used in zones where rapid variations in stress are anticipated than in zones of constant stress; thus the different size elements shown in Fig. 4(b). (However, the total number of elements allowable are subject to computer capacity.)

Figure 4(b) shows the two plates in contact for the radial distance X_c and separated beyond it. It is to be noted that the nodal points on the parting line and within the length of contact X_c are common to elements in both plates. The other elements adjacent to the parting line on each plate are separated from their corresponding elements in the mating plate and these elements have no common nodal points. Physically, it is equivalent to the welding together of the two plates in the contact zone. Mathematically, we are imposing the condition that

in the contact zone the displacements in the z and r directions be identical for both plates. In the case of bolted plates of equal thickness, i.e. in the presence of symmetry about the parting plane, these conditions apply exactly. Furthermore, because of this symmetry, one needs to analyze only one plate, as shown in Fig. 5(b), with the imposed boundary conditions on the contact zone of zero displacement in the z -direction and freedom to displace in the r -direction. It can also be observed that the solution of two plates with symmetry about the parting plane is equivalent to the solution of one of these plates under the same loading conditions, but resting on a frictionless infinitely rigid plane. Also, under the above conditions the shear stress in the contact zone is identically zero.

In the case of bolted plates of unequal thickness the model includes both plates as shown in Fig. 5(c). This model is an approximation because, in general, two plates of unequal thickness do not have the same displacement in the r -direction on the contact surface. The solution yields, therefore, a shearing stress distribution in the contact zone. The solution, however, should be exactly compatible with the physical model if the frictional forces in the joint prevent sliding.

The critical aspect of the approach used herein is the determination of the largest nodal circle on the parting plane which is common to an element on each plate. This nodal circle defines the contact zone and the radius, R_o , at which separation occurs.

The output of the finite element computer program includes the displacement of each node in the r and z directions and the average

σ_z , σ_r , σ_t and τ_{rz} stresses for each element.

The computation is iterative and the objective is to achieve the lowest possible compressive σ_z stress in the outermost elements bordering the contact zone. Unacceptable solutions are shown in Fig. 6(a) and 6(b). If R_o for a given external load distribution is too small, then the solution will show that the two plates intersect (Fig. 6(a)). On the other hand, if R_o is assumed too large, the solution will show that the outer portion of the contact zone sustains a tensile σ_z stress (Fig. 6(b)). Neither of these two situations is physically feasible. In general, the procedure employed was to commence the iterations with a value for R_o which would yield a tensile σ_z stress in the outer elements adjacent to the contact zone and then move R_o inward. The iteration ended as soon as no tensile σ_z stress was present at the contact zone. For example, for the case shown in Fig. 5(b), if the σ_z stress for the element in the last row and to the left of the last roller is tensile, then the following iteration will proceed without the last roller. Thus, the resolution is one nodal interval. Finer resolution can be obtained by reducing the interval between nodal circles by introducing more elements or shifting the grid locally. The same criteria apply to the model shown in Fig. 5(c).

In the finite element analysis of the Fernlund (3) model, i.e. single plate with external loads at the faces $z = \pm D$ no iteration is required and the rollers shown in Fig. 5(c) would extend to the outer radius of the plate. (Although Fernlund's computations are based on infinite plates, computations show that there is no distinction between infinite plates and plates of radius greater than five times of the outer

radius, B , of the load. See Fig. 5(a).

Convergence was tested by subdividing elements further, with nodal points in the coarser grid remaining nodal points in the finer grid. Changing the mesh from 180 elements to 360 elements have shown no improvement in accuracy. Meshes from 180 to 300 elements were used in this analysis. Typical spacings between nodal points were 0.015 inch radially and 0.03 inch in the z -direction.

Chapter III

EXPERIMENTAL METHOD

The objective of the experiment was to determine the extent of contact between two plates when bolted together. Sixteen type 304 stainless steel plates, 4 inches in diameter, were machined to nominal thicknesses of $1/16$, $1/8$, $3/16$ and $1/4$ inch, 4 plates for each thickness. After rough machining these plates were stress relieved at 1875°F and ground flat to 0.0002 inch. One side of each plate was then lapped flat to better than one fringe of sodium light (11 micro-inches) in the case of the $1/8$, $3/16$ and $1/4$ inch plates, and to better than two fringes in the case of the $1/16$ inch plates. Disregarding scratches, the finish of the lapped surfaces was 5 micro-inches rms. Each plate had a central hole, 0.257 inch in diameter, for a $1/4 - 20$ bolt, and two notches and two holes on the periphery (see Fig. 7). Two techniques were employed in determining the area of contact when two of these plates were bolted together. The first technique entailed the following procedure (see Fig. 7):

- (a) The plates were cleaned with alcohol and lens tissue.
- (b) One plate was placed on the base of the fixture shown in Fig. 7, lapped surface up and the two holes on the periphery of the plates engaged with two pins on the fixture. Spacers between the fixture base and plate prevented the pins from extending beyond the top surface of the plate.

- (c) A second plate was placed on top of the first plate, lapped surfaces mating. The notches on the two plates were lined up with each other and with notches in the base of the fixture. Thus, rotation of the plates was prevented.
- (d) A standard $1/4 - 20$ hex-nut with its annular bearing surface (0.42 inch O.D.) lapped flat was engaged on a high strength $1/4 - 20$ bolt. The nut was located about two threads away from the head of the bolt and served in lieu of the bolt head. The lapped surface of the nut faced away from the bolt head and since the nut was not sent home against the bolt head, the looseness of fit between nut and bolt offered a degree of self alignment.
- (e) The bolt and nut assembly described in (d) above was then inserted through the $1/4$ inch central holes of the two plates and a second $1/4 - 20$ lapped nut was engaged on the bolt. Thus the two plates were captured by the two $1/4 - 20$ nuts with the lapped surfaces of the nuts bearing against the plates.
- (f) With the torque wrench shown on the right in Fig. 7, the nuts were torqued down to 70 pound-inches of torque to yield a 1100 pound force in the bolt [11].
- (g) The position of the keys was changed to engage with only the lower plate and the fixture and a special spanner wrench, as shown in Fig. 7, was engaged with the top plate. The spanner wrench was restrained to move in the horizontal plane and it was set into motion by the screw pressing against the wrench handle.

- (h) With the aid of the spanner wrench the upper plate was rotated relative to the lower plate several times approximately ± 5 degrees.

Thus, the above procedure allowed for the rubbing of one plate relative to its mate while under a bolt force of approximately 1100 lbs. The remaining steps were the disassembly and the measurement of the extent of the contact zone which was defined by the shine due to the rubbing in the contact zone. It is to be noted that the boundaries of the contact zone as measured by the naked eye and by searching for marks of "polished" or "damaged" surface under a 10.5 power magnification are essentially the same.

The above test was performed on 5 pairs of specimen. These were

1. One 0.07 in. plate mated to a 0.65 in. plate
2. One 0.126 in. plate mated to a 0.126 in. plate
3. One 0.191 in. plate mated to a 0.192 in. plate
4. One 0.253 in. plate mated to a 0.256 in. plate
5. One 0.124 in. plate mated to a 0.257 in. plate

The identical tests were repeated for

1. One 0.124 in. plate mated to a 0.126 in. plate; and
2. One 0.191 in. plate mated to a 0.192 in. plate,

but in lieu of the 1/4 - 20 nuts in direct contact with the plates special washers, 1.000 in. O.D., 0.257 in. I.D. and 0.620 in. high, were interposed between the bolt head and nut.

The diameters of the contact zones were measured with a machinist ruler with 100 divisions to the inch and with a Jones and Lamston Vertac 14 Optical Comparator.

The second technique used the same parts and fixture, but it involved autoradiographic measurements.

Four plates, 1/4, 3/16, 1/8 and 1/16 inch thick were sent to Tracerlab, Inc., Waltham, Mass., for electrolytic plating with radioactive silver $\text{Ag } 110^{\text{M}}$ (half life of 8 months). Each plate was masked except for an area on the lapped face one inch in radius. The plates then received a plating of copper about 5 microinches thick and then approximately a 5 microinch plating of silver containing the radioactive isotope. The resultant activity on each plate was about 2 millicuries.

These plates were then mated to plates of equal thickness (not plated) and assembled in a shielded hood as indicated in steps (a) to (h) above except that in the case of the pair of 1/4 inch plates care was taken not to rotate the plates during and after assembly and in the remaining cases the rotation specified in step (h) was done only once in one direction.

The plates were then disassembled and the radioactive contamination on the plates which were in contact with the radioactive plates measured. The transferred activity was:

1/4 in. plate	approximately	0.05 microcuries
3/16 in. plate	approximately	3. microcuries
1/8 in. plate	approximately	0.1 microcuries
1/16 in. plate	approximately	0.4 microcuries

It was also observed in handling that the adhesion of the silver on the 3/16 in. plate was poor.

Kodak type R single coated industrial x-ray film was then placed on the contaminated plates under darkroom conditions. The sensitive side of the film was pressed against the radioactive sides of the plates with a uniform load of about five pounds and left for exposure for three days. After three days, the film was removed and developed. The results are shown in Fig. 10.

Chapter IV

RESULTS

A. Pressure Distribution and Radii of Separation from Single Plate and Two Plate Finite Element Models.

Using the finite element procedure described in Chapter II, the midplane stress distribution of single circular plates of thickness $2D$, outer radii of 1.54 in., inner radii of 0.1 in., Poisson ratio of 0.3, and loaded by a constant pressure between radii A and B , Fig. 3(f), was computed. Computations were performed for D values of 0.1, 0.1333 and 0.2 in. For each value of D the radius B , which defines the region of the symmetric external load, assumed the values of 0.31, 0.22, 0.16 and 0.13 in. The σ_z stress distribution at the midplane, from the inner radius to the radius at which the above stress is no longer compressive, is shown in Figs. 12, 13 and 14 as a function of radius.

The identical cases were then recomputed, using again the finite element method, in accordance with the two plate model shown in Figs. 4(b) and 5(b). These results are given in Figs. 15, 16 and 17.

Inspection of the above figures show that the two plate model yields a somewhat different stress distribution in the contact zone than the stress distribution approximated from the single plate model, and more significantly, from the heat transfer point of view, the two plate model yields a lower value for the radius of separation, R_o , which

results in a reduction in area for heat transfer. Table 1 gives a comparison of the values for R_o obtained from the two models.

It may be observed that the single plate result of Fernlund (Ref. 3, pp. 56, 124) is in fair agreement with the finite element results obtained for the single plate model.

B. Radii of Separation from Experiment and Their Predicted Values from the Two Plate Finite Element Computation.

As described in Chapter III, stainless steel circular plate specimen (Fig. 7) were bolted together, rotated relative to each other with the bolt force acting, and after disassembly the contact area of the joint was determined by measuring the footprints (the shiny, polished areas) on each plate due to the plates rubbing against each other. Photographs of these footprints are shown in Fig. 8. Fig. 9 also shows a typical footprint of the annular bearing surface of the 1/4 - 20 nut against a plate. All plates tested were of 304 stainless steel, 4 inch O.D., .257 I.D., and the nominal thicknesses of the plates were 1/16, 1/8, 3/16 and 1/4 inch. In addition to the plates fastened with standard nuts which gave a loading circle of radius B (Fig. 5) of 0.211 inch, plates fastened by the special nuts described in Chapter III for which B was 0.5 inch were also tested.

Figure 10 shows the results of the autoradiographic tests described in Chapter III. For all plate pairs tested, i.e. 1/16, 1/8, 3/16 and 1/4 inch nominal, the value of B was 0.211 inch.

The pressure distributions and radii of separation for all the

above test cases were computed independently by the two plate model finite element analysis. Table 2 gives the test and analytical results for all test cases. The test results are an average of all measurements (minimum of six readings). A description of the analyses follows.

Figure 18 shows the results of a two plate and a single plate model analysis for the 0.253 inch bolted test specimen. For Figure 19 the external pressure distribution between radii A and B is triangular. (The total force, however, is equal to the force exerted in the case of uniform pressure.) In one case, the peak external pressure is at A, Fig. 20(a), and in the other case at B, Fig. 20(b). Results of another computation which assumed a uniform displacement of 50 microinches under each nut is shown in Fig. 21. It is interesting to note that the point of separation obtained by using the two plate model for all variations of loading given above occurs in the range of r/A values of 2.73 to 2.93 while the two plate model yields separation at a value for r/A of 3.5. The computed deflections under the nuts are given in Fig. 22.

The finite element analysis results for the 0.191 in. plate pair specimen are given in Fig. 23. Figures 24 and 25 show the computed pressure distribution and deflection patterns in the joint, respectively, for the 1/8 in. plate pair. In order to investigate the possible influence misalignments of the spanner wrench, i.e. vertical forces or restraints exerted at edge of plate, may have on the results of the experiment, the extreme case of fixing the outer edges of the plate as shown in Fig. 20(c) was considered. As Fig. 24 shows, within the

resolution of the finite element grid size, the effect is negligible. This model, Fig. 20(c), and result also indicate that the influence of additional fasteners 2 inches away would not have an influence on the contact zone for the geometry considered. (However, if the distance between bolts is considerably reduced, then the contact area should increase.) The computed results for the 1/16 inch plate pair is given in Fig. 26.

Figure 27 gives the finite element analysis results for the asymmetric case of a 1/8 in. plate bolted to a 1/4 in. plate. The model shown in Fig. 5(c) was used and as discussed in Chapter II, this model is strictly valid only if the friction in the joint prevents sliding between the plates. Nevertheless, the percent discrepancy between the computed value and tested value (see Table 2) falls within the range of the symmetric cases analyzed and tested.

In summary, the results obtained from the two plate finite element model and from experiment are in good agreement (Fig. 28).

Chapter V

APPLICATION

An application of the above results for the evaluation of the thermal contact conductance, h_c , and the determination of the heat transferred in a specific, but typical, lap joint section is illustrated in this chapter.

An aluminum lap joint in a vacuum environment, the relevant section and boundary conditions as shown in Fig. 29, was analyzed by means of a nodal analysis. The plate thickness was 0.1 in. and the hole diameter, 2A, was 0.2 in. The bearing surface of the bolt, 2B, was 0.26 in. in diameter. Because of the high conductivity and small thickness of the plates, no z dependence (see Fig. 29) was assumed for the temperature in the main body of the plate. However, heat flow in the z -direction in the nodes above and below the contact zone is considered. Qualitatively, the heat flow in the joint proceeds in the x - y plane from the left end (Fig. 29) toward the 0.2 in. diameter hole. In the vicinity of the hole, a macroscopic constriction for heat flow is encountered because the flow is being channeled toward the small contact zone. The flow of heat then encounters the microscopic constrictions at the contacting asperities (which determine h_c) in the contact zone; spreads out in the x - y directions in the second plate; and continues to the right edge of the lap joint.

The material properties assumed were (refer to equation 1.1):

$$\begin{aligned} H &= 150,000 \text{ psi} \\ k &= 100 \text{ Btu/hr-}^\circ\text{F-ft} \quad (k_1 = k_2 = 100) \\ \sigma &= 5.9 \times 10^{-6} \text{ ft.} \quad (\sigma_1 = \sigma_2 = 50 \times 10^{-6} \text{ in.}) \\ \tan \theta &= 0.1 \end{aligned}$$

Assuming further, a uniform load of 46,500 psi on the loading surface (#10 screw; 1000 lb. bolt force) and referring to Fig. 15, curve $\frac{B}{A} = 1.3$, the following interface stresses, σ_z , contact heat transfer coefficient, h_c , and conductance, (area) $\cdot (h_c)$, were obtained as a function of inner and outer radii. (These radii define increments of area, the sum of which define one quarter of the contact zone.):

$\underline{r_{\text{outer}}}$ <u>inch</u>	$\underline{r_{\text{inner}}}$ <u>inch</u>	$\underline{\sigma_z}$ <u>psi</u>	$\underline{h_c}$ Btu/hr- $^\circ$ F-ft ²	Area x $\underline{h_c}$ Btu/hr- $^\circ$ F-ft ²
.13	.1	27,900	446,000	16.6
.16	.13	14,000	223,000	10.6
.175	.16	3,950	63,100	1.7

The conductance between nodal points were then computed and with the aid of the steady state heat transfer program listed in Appendix D, the nodal temperatures for the conditions given in Fig. 29 were computed. The heat transferred from the edge maintained at 20 $^\circ$ F to the edge at 0 $^\circ$ F (Fig. 29) for this case was 2.88 Btu/hour. The same computation was repeated for the case of a bearing surface between the plate

and the bolt (2B) of 0.44 in. in diameter, but the bolt force was left unchanged. The heat transferred from the 20°F edge to the 0°F edge in this case was 3.15 Btu/hour. In the absence of the joint the heat transfer along an equivalent 7 inch length of solid aluminum would have been 3.58 Btu/hour. This data shows that the thermal resistance of the contact zone (not entire 7 inch lap joint) was decreased from 1.52 to 0.92 °F-hr/Btu by the increase of the effective bolt head diameter from .26 to .44 in. It should be observed that the change in thermal resistance of the joint is primarily due to the increase in contact area and the resulting decrease in macroscopic constriction resistance at the hole. Also, the heat flux in this example is mainly controlled by the 7 inch length and 0.1 inch thickness rather than the joint resistance. This emphasizes the importance of a balanced thermal design.

For large heat fluxes where thermal strains may have an influence on the radii of separation, the finite element program given in Appendix C may be used. Also, in a non-vacuum environment the effect of the interstitial fluid is added in two ways. Firstly, equation (1.6) is applied to account for the presence of interstitial fluid in the contact zone, and secondly, conduction across the gaps between the plates and convection from the plates is considered. (Radiation heat transfer, if applicable, should also be included.)

Chapter VI

CONCLUSIONS

The finite element technique used in this work for the analysis of the pressure distribution and deformation of smooth and flat bolted plates under conditions of axial symmetry predicts contact areas in joints considerably lower than reported previously in the literature. These results were verified experimentally. The discrepancy between the previously reported results and the results reported here is due to the simplifying assumption made by earlier researchers that a joint can be modeled as a single plate.

The computer programs listed in the appendices will also accommodate joints made up of plates of dissimilar materials and the presence of thermal gradients.

Of the eleven tests performed, only one (case 3, autoradiographic) yielded inconsistent results. (This data point could probably be ignored because of the poor adhesion of the plating material which manifested itself by the high radioactive contamination count during test.)

The finite element analysis performed for the test specimen show that the gap between the $1/4$ inch bolted steel specimen is 98.6 microinches at the outer radius of the plate of 2 inches, and $1/32$ of an inch away from the radius of separation (0.35 in.), the gap is

only 3 microinches for the test load. This data indicates the difficulties previous workers have encountered in their experiments. (This also explains the oval shape of several of the footprints.) Furthermore, this data shows that the effects of surface roughness and the lack of flatness could have a significant effect on the size of contour area.

An application of the above work to a heat transfer problem is illustrated in Chapter V.

REFERENCES

1. Cooper, M.G., Mikic, B.B., and Yovanovich, M.M., "Thermal Contact Conductance," International Journal of Heat and Mass Transfer, Vol. 12, No. 3 (March 1969), 279-300.
2. Roetscher, F., Die Maschinenelemente, Erster Band. Berlin: Julius Springer, 1927.
3. Fernlund, I., "A Method to Calculate the Pressure Between Bolted or Riveted Plates," Transactions of Chalmers, University of Technology. Gothenburg, Sweden, No. 245, 1961.
4. Greenwood, J.A., "The Elastic Stresses Produced in the Mid-Plane of a Slab by Pressure Applied Symmetrically at its Surface," Proc. Camb. Phil. Soc. Cambridge, England, Vol. 60, 1964, 159-169.
5. Lardner, T.J., "Stresses in a Thick Plate with Axially Symmetric Loading," J. of Applied Mechanics, Trans. ASME, Series E, Vol. 32, June 1965 (458-459).
6. Sneddon, I.N., "The Elastic Stresses Produced in a Thick Plate by the Application of Pressure to its Free Surfaces," Proc. Camb. Phil. Soc. Cambridge, England, Vol. 42, 1946 (260-271).
7. Bradley, T.L., "Stress Analysis for Thermal Contact Resistance Across Bolted Joints," M.S. Thesis, Massachusetts Institute of Technology, Mechanical Engineering Department, Cambridge, Mass. August 1968.
8. Louisiana State University, Division of Engineering Research, The Thermal Conductance of Bolted Joints. NASA Grant No. 19-001-035, C.A. Whitehurst, Dir. Baton Rouge: LSU Div. of Eng. Res., May 1968.
9. Zienkiewicz, O.C., The Finite Element Method in Structural and Continuum Mechanics. London: McGraw-Hill Publishing Co., Ltd., 1967.
10. Przemieniecki, J.S., Theory of Matrix Structural Analysis. New York: McGraw-Hill Book Co., 1968.
11. Cobb, B.J., "Preloading of Bolts," Product Engineering, August 19, 1963 (62-66).
12. Wilson, E.L., "Structural Analysis of Axisymmetric Solids," AIAA Journal, Vol. 3, No. 12, (Dec. 1965), 2269-2274.

13. Jones, R.M. and Crose, J.G., SAAS II Finite Element Stress Analysis of Axisymmetric Solids. United States Air Force Report No. SAMSO-TR-68-455 (Sept. 1968).
14. Christian, J.T. and others, FEAST-1 and FEAST-3 Programs. Cambridge: Computer Program Library, M.I.T. Department of Civil Engineering, Soil Mechanics Division, 1969.
15. Clough, R.W., "The Finite Element Method in Structural Mechanics," Ch. 7, Stress Analysis, Zienkiewicz, O.C. and Holister, G.S., editors. London: John Wiley and Sons, Ltd., 1965.

APPENDIX A

FINITE ELEMENT ANALYSIS OF AXISYMMETRIC SOLIDS

The finite element method and the equations which govern the stresses and displacements in axisymmetric solids is given in the literature [9,10,12,13,15] and the procedure will be briefly summarized in this appendix.

The procedure for the standard stiffness analysis method is as follows [15]:

- (a) The internal displacements, v , are expressed as

$$\{v(r,z)\} = [M(r,z)] \{\alpha\} \quad (A.1)$$

where M is a displacement function and α are the generalized coordinates representing the amplitudes of the displacement functions.

- (b) The nodal displacements v_i are expressed in terms of the generalized coordinates

$$\{v_i\} = [A] \{\alpha\} \quad (A.2)$$

where A is obtained by substituting the coordinates of the nodal points into M .

- (c) The generalized coordinates are expressed in terms of the nodal displacements

$$\{\alpha\} = [A]^{-1} \{v_i\} \quad (A.3)$$

(d) The element strains, ϵ , are evaluated

$$\{\epsilon\} = [B(r,z)] \{\alpha\} \quad (A.4)$$

where B is obtained from the appropriate differentiation of M .

(e) The element stresses are expressed in terms of the stress-strain relation D

$$\{\sigma(r,z)\} = [D] \{\epsilon\} = [D] [B] \{\alpha\} \quad (A.5)$$

(f) Assuming a virtual strain $\bar{\epsilon}$ and a generalized virtual coordinate displacement $\bar{\alpha}$ the internal virtual work, W_i , in the differential volume, dV , is given by

$$dW_i = \{\epsilon\}^T \{\sigma\} dV = \{\alpha\}^T [B]^T [D] [B] \{\alpha\} dV \quad (A.6)$$

and the total internal virtual work is

$$W_i = \{\bar{\alpha}\}^T \left[\int_{Vol} [B]^T [D] [B] dV \right] \alpha \quad (A.7)$$

(g) The external work, W_e , associated with the generalized displacement $\bar{\alpha}$ is

$$W_e = \{\alpha\}^T \{\beta\} \quad (A.8)$$

where β are generalized forces corresponding with the displacements α .

(h) After equating W_i and W_e and setting the $\bar{\alpha}$ displacement to unity

$$\{\beta\} = \left[\int_{Vol} [B]^T [D] [B] \right] \alpha = [\bar{k}] \{\alpha\} \quad (A.9)$$

$$\text{where } [\bar{k}] = \int_{Vol} [B]^T [D] [B] dV \quad (A.10)$$

and which transforms to the nodal point surfaces

$$k = [A^{-1}] [\bar{k}] [A^{-1}] \quad (A.11)$$

(i) The stiffness matrix for the complete system is then

$$[K] = \sum_{m=1}^n [k]_m \quad (A.12)$$

where n equals the number of elements and the equilibrium relationship becomes

$$\{Q\} = [K] \{v_i\} \quad (A.13)$$

where

$$\{Q\} = \sum_{m=1}^n \{R\}_m \quad (A.14)$$

$$\{R\} = \int_{Area} [A^{-1}]^T [M]^T \{P\}_m dA \quad (A.15)$$

and P are the surface forces.

The above procedure applies with minor modification to problems with thermal and body force loading.

The expression

$$\{Q\} = [K] \{v_i\} \quad (A.16)$$

represents the relationship between all nodal point forces and all nodal point displacements. Mixed boundary conditions are considered by rewriting this equation in the partitioned form

$$\begin{Bmatrix} Q_a \\ Q_b \end{Bmatrix} = \begin{bmatrix} K_{aa} & K_{ab} \\ K_{ba} & K_{bb} \end{bmatrix} \begin{Bmatrix} u_a \\ u_b \end{Bmatrix} \quad (A.17)$$

where $v_i = u$.

The first part of the partitioned equation can be written as

$$\{Q_a\} = [K_{aa}] \{u_a\} + [K_{ab}] \{u_b\} \quad (A.18)$$

and then expressed in the reduced form

$$\{Q^*\} = [K_{aa}] \{u_a\} \quad (A.19)$$

where

$$\{Q^*\} = \{Q_a\} - [K_{ab}] \{u_b\} \quad (A.20)$$

The matrix equation (A.19) is solved for the nodal point displacements by standard techniques. Once the displacement are known the strains are evaluated from the strain displacement relationship and the stresses in turn are evaluated from the stress strain relations.

Both triangular and quadrilateral elements are used. The displacements in the r - z plane in the element are assumed to be of the form

$$\begin{aligned} v_r &= \alpha_1 + \alpha_2 r + \alpha_3 z \\ v_z &= \alpha_4 + \alpha_5 r + \alpha_6 z \end{aligned} \tag{A.21}$$

This linear displacement field assures continuity between elements since lines which are initially straight remain straight in their displaced position. Six equilibrium equations are developed for each triangular element.

A quadrilateral element is composed of four triangular elements and ten equilibrium equations correspond to each element.

APPENDIX B

FINITE ELEMENT PROGRAM FOR THE ANALYSIS OF ISOTROPIC ELASTIC AXISYMMETRIC PLATES (ref. 13,14)

Input Instructions:

<u>Card Sequence</u>	<u>Item</u>	<u>Format</u>	<u>Columns</u>
1	Title	18A4	1-72
2	Total number of nodal points	I5	1-5
	Total number of elements	I5	6-10
	Total number of materials	I5	11-15
	Normalizing stress (NORM)	I5	16-20
	Number of pressure cards	I5	21-25

(If NORM = 0, put in value of E in material card;

if NORM = 1, put in value $E/\sigma_{\text{vertical}}$;

if NORM = -1, put in value $E/\sigma_{\text{octahedral}}$;

NOTE: Use NORM = 0 for this application.)

3 (Material property cards - one set of
(a) and (b) for each material)

(a) 1st card



Material No.	I5	1-5
Initial σ_z stress	F10.0	6-15
Initial σ_r stress	F10.0	16-25

(b) Second Card

E	F10.0	1-10
ν	F10.0	11-20

<u>Card Sequence</u>	<u>Item</u>	<u>Format</u>	<u>Column</u>
4	Nodal point information (One for each node)	2I5,4F10.0	
	Node number		1-5
	CODE		6-10
	r-coordinate		11-20
	z-coordinate		21-30
	XR		31-40
	XZ		41-50

If the number in column 10 is

		<u>Condition</u>
0	XR is the specified R-load and XZ is the specified Z-load	free
1	XR is the specified R-displacement and XZ is the specified Z-load	
2	XR is the specified R-load and XZ is the specified Z-displacement.	
3	XR is the specified R-displacement and XZ is the specified Z-displacement.	fixed

Remarks

The following restrictions are placed on the size of problems which can be handled by the program.

<u>Item</u>	<u>Maximum Number</u>
Nodal Points	450
Elements	450
Materials	25
Boundary Pressure Cards	200

All loads are considered to be total forces acting on a one radian segment. Nodal point cards must be in numerical sequence. If cards are omitted, the omitted nodal points are generated at equal intervals along a straight line between the defined nodal points. The boundary code (column 10), XR and XZ are set equal to zero.

If the number in columns 6-10 of the nodal point cards is other than 0, 1, 2 or 3, it is interpreted as the magnitude of an angle in degrees. The terms in columns 31-50 of the nodal point card are then interpreted as follows:

XR is the specified load in the s-direction

XZ is the specified displacement in the n-direction

The angle must always be input as a negative angle and may range from -.001 to -180 degrees. Hence, +1.0 degree is the same as -179.0 degrees. The displacements of these nodal points which are printed by the program are

u_r = the displacement in the s-direction

u_z = the displacement in the n-direction

Element cards must be in element number sequence. If element cards are omitted, the program automatically generates the omitted information by incrementing by one the preceding I, J, K and L. The material identification code for the generated cards is set equal to the value given on the last card. The last element card must always be supplied.

Triangular elements are also permissible; they are identified by repeating the last nodal point number (i.e. I, J, K, K).

One card for each boundary element which is subjected to a normal pressure is required. The boundary element must be on the left as one

progresses from I to J. Surface tensile force is input as a negative pressure.

Printed output includes:

1. Reprint of input data.
2. Nodal point displacement
3. Stresses at the center of each element.

Nodal point numbers must be entered counterclockwise around the element when coding element data.

The maximum difference between the nodal point numbers on an element must be less than 25. However, on a nodal diagram elements and nodes need not be numbered sequentially.


```

      WRITE (6,2051) (E(J,MTYPE),J=1,2)
      80 CONTINUE
      C *****
      C READ AND PRINT NODAL POINT DATA
      C *****
      100 WRITE (6,2013)
         L=0
      105 READ (5,1006) N,ICODE(N),R(N),Z(N),UR(N),UZ(N)
      106 NL=L+1
         IF (L.EQ.0) GO TO 110
         ZX=N-L
         DR=(R(N)-R(L))/ZX
         DZ=(Z(N)-Z(L))/ZX
      110 L=L+1
         IF (N-L) 113,112,111
      111 ICODE(L)=0
         R(L)=R(L-1)+DR
         Z(L)=Z(L-1)+DZ
         UR(L)=0.0
         UZ(L)=0.0
         GO TO 110
      112 WRITE (6,2014) (K,ICODE(K),R(K),Z(K),UR(K),UZ(K),K=NL,N)
      113 WRITE (6,2015) N
         GO TO 900
      C *****
      C READ AND PRINT ELEMENT PROPERTIES
      C *****
      120 WRITE (6,2016)
         N=0
      130 READ (5,1007) M,(IX(M,I),I=1,5)
      140 N=N+1
         IF (M-N) 170,170,150
      150 IX(N,1)=IX(N-1,1)+1
         IX(N,2)=IX(N-1,2)+1
         IX(N,3)=IX(N-1,3)+1

```

FENT0037
 FENT0038
 FENT0039
 FENT0040
 FENT0041
 FENT0042
 FENT0043
 FENT0044
 FENT0045
 FENT0046
 FENT0047
 FENT0048
 FENT0049
 FENT0050
 FENT0051
 FENT0052
 FENT0053
 FENT0054
 FENT0055
 FENT0056
 FENT0057
 FENT0058
 FENT0059
 FENT0060
 FENT0061
 FENT0062
 FENT0063
 FENT0064
 FENT0065
 FENT0066
 FENT0067
 FENT0068
 FENT0069
 FENT0070
 FENT0071
 FENT0072

```

      IX(N,4)=IX(N-1,4)+1
      IX(N,5)=IX(N-1,5)
170  WRITE (6,2017) N,(IX(N,I),I=1,5)
      IF (M-N) 180,180,140
180  IF (NUMEL-N) 300,300,130
C    *****
C    READ AND PRINT THE PRESSURE CARDS
C    *****
300  IF (NUMPC) 290,210,290
290  WRITE(6,9000)
      DO 200 L=1,NUMPC
      READ(5,9001) IRC(L),JRC(L),PR(L)
200  WRITE(6,9002) IRC(L),JRC(L),PR(L)
210  CONTINUE
C    *****
C    DETERMINE PAND WIDTH
C    *****
      J=0
      DO 340 N=1,NUMEL
      DO 340 I=1,4
      DO 325 L=1,4
      KK=IX(N,I)-IX(N,L)
      IF (KK.LT.0) KK=-KK
      IF (KK.GT.J) J=KK
325  CONTINUE
340  CONTINUE
      MRAND=2*J+2
C    *****
C    SOLVE FOR DISPLACEMENTS AND STRESSES
C    *****
      KSW=0
      CALL STIFF
      IF (KSW.NE.0) GO TO 900
C
      CALL BANSCL
      WRITE(6,2052)

```

```

FENT0073
FENT0074
FENT0075
FENT0076
FENT0077
FENT0078
FENT0079
FENT0080
FENT0081
FENT0082
FENT0083
FENT0084
FENT0085
FENT0086
FENT0087
FENT0088
FENT0089
FENT0090
FENT0091
FENT0092
FENT0093
FENT0094
FENT0095
FENT0096
FENT0097
FENT0098
FENT0099
FENT0100
FENT0101
FENT0102
FENT0103
FENT0104
FENT0105
FENT0106
FENT0107
FENT0108

```

	WRITE (6,2025) (N,B	(2*N-1),B	(2*N),N=1,NUMNP)	FENTO109
C				FENTO110
	450 CALL STRESS(SPLOT)			FENTO111
C	*****			FENTO112
C	PROCESS ALL DECKS EVEN IF ERROR			FENTO113
C	*****			FENTO114
	GO TO 910			FENTO115
	900 WRITE (6,4000)			FENTO116
	910 WRITE (6,4001) HED			FENTO117
C				FENTO118
	920 READ (5,1000) CHK			FENTO119
	IF (CHK.NE.STRS) GO TO 920			FENTO120
	GO TO 50			FENTO121
	950 CONTINUE			FENTO122
	WRITE (6,4002)			FENTO123
	CALL EXIT			FENTO124
C	*****			FENTO125
C	*****			FENTO126
	1000 FORMAT (18A4)			FENTO127
	1001 FORMAT (12I5)			FENTO128
	1002 FORMAT (15,2F10.0)			FENTO129
	1003 FORMAT(2F10.0)			FENTO130
	1004 FORMAT (2F10.0)			FENTO131
	1005 FORMAT (3F10.0)			FENTO132
	1006 FORMAT (2I5,4F10.0)			FENTO133
	1007 FORMAT (6I5)			FENTO134
C	*****			FENTO135
	2000 FORMAT (1H1,20A4)			FENTO136
	2006 FORMAT (28HONUMBER OF NODAL POINTS----- I3/			FENTO137
	1 28H NUMBER OF ELEMENTS----- I3)			FENTO138
	2007 FORMAT (20HOMATERIAL NUMBER----- I3/			FENTO139
	1 25H INITIAL VERTICAL STRESS= F10.3 ,5X,			FENTO140
	2 26HINITIAL HORIZONTAL STRESS= F10.3)			FENTO141
	2013 FORMAT (12H1NODAL POINT ,4X, 4HTYPE ,4X, 10HR-ORDINATE ,4X,			FENTO142
	1 10HZ-ORDINATE ,10X, 6HR-LOAD ,10X, 6HZ-LOAD)			FENTO143
	2014 FORMAT (I12,I8,2F14.3,2E16.5)			FENTO144

2015	FORMAT (26HONODAL POINT CARD ERROR N= I5)	FENT0145
2016	FORMAT (49H1ELEMENT NO. I J K L MATERIAL)	FENT0146
2017	FORMAT (11I13,4I6,1I12)	FENT0147
2025	FORMAT (12HONODAL POINT ,6X, 14HR-DISPLACEMENT ,6X, 14HZ-DISPLACEMENT / (I12,1P2D20.7))	FENT0148
2041	FORMAT (76HOMODULUS AND YIELD STRESS NORMALIZED WITH RESPECT TO INITIAL VERTICAL STRESS)	FENT0149
2051	FORMAT(1H0,10X,'E',8X,'NU',/,3X,F11.1,F10.4/)	FENT0150
2052	FORMAT(1H1)	FENT0151
C	*****	FENT0152
3003	FORMAT (16I5)	FENT0153
C	*****	FENT0154
4000	FORMAT (//// ' ABNORMAL TERMINATION')	FENT0155
4001	FORMAT (//// ' END OF PROBLEM ' 20A4)	FENT0156
4002	FORMAT (////' END OF JOB')	FENT0157
C	*****	FENT0158
9000	FORMAT(29HOPRESSURE BOUNDARY CONDITIONS/ 24H I J PRESSURE)	FENT0159
9001	FORMAT(2I5,F10.0)	FENT0160
9002	FORMAT(2I6,F12.3)	FENT0161
	END	FENT0162
	SUBROUTINE STIFF	FENT0163
C		FENT0164
	IMPLICIT REAL*8 (A-H,O-Z)	FENT0165
	IMPLICIT INTEGER*2(I-N)	FENT0166
	COMMON STTCP,HED(18),SIGIR(25),SIGIZ(25),GAMMA(25),ZKNOT(25),	FENT0167
	1 DEPTH(25),E(10,25),SIG(7),R(450),Z(450),UR(450),	FENT0168
	2 UZ(450),STOTAL(450,4),KSW	FENT0169
	COMMON /INTEGR/ NUMNP,NUMEL,NUMMAT,NDEPTH,NORM,MTYPE,ICODE(450)	FENT0170
	COMMON /ARG/ RRR(5),ZZZ(5),S(10,10),P(10),LM(4),DD(3,3),	FENT0171
	1 HH(6,10),RR(4),ZZ(4),C(4,4),H(6,10),D(6,6),F(6,10),TP(6),XI(6),	FENT0172
	2 EE(10),IX(450,5)	FENT0173
	COMMON /BANARG/ B(900),A(900,54),MBAND	FENT0174
	COMMON/PRFSS/ IBC(200),JBC(200),PR(200),NUMPC	FENT0175
	DIMENSION CODE(450)	FENT0176
C	*****	FENT0177
		FENT0178
		FENT0179
		FENT0180

```

FENT0181
FENT0182
FENT0183
FENT0184
FENT0185
FENT0186
FENT0187
FENT0188
FENT0189
FENT0190
FENT0191
FENT0192
FENT0193
FENT0194
FENT0195
FENT0196
FENT0197
FENT0198
FENT0199
FENT0200
FENT0201
FENT0202
FENT0203
FENT0204
FENT0205
FENT0206
FENT0207
FENT0208
FENT0209
FENT0210
FENT0211
FENT0212
FENT0213
FENT0214
FENT0215
FENT0216

C INITIALIZATION
C *****
NR=27
ND=2*NB
ND2=2*NUMNP
DO 50 N=1,ND2
  B(N)=0.0
DO 50 M=1,ND
  A(N,M)=0.0
  *****
  FORM STIFFNESS MATRIX
  *****
DO 210 N=1,NUMEL
  *****
  90 CALL QUAD(N,VOL)
  IF (VOL) 142,142,144
  142 WRITE (6,2003) N
  KSW=1
  GO TO 210
  *****
  144 IF (IX(N,3)-IX(N,4)) 145,165,145
  145 DO 150 II=1,9
    CC=S(II,10)/S(10,10)
    DO 150 JJ=1,9
      150 S(II,JJ)=S(II,JJ)-CC*S(10,JJ)
      *****
    DO 160 II=1,8
      CC=S(II,9)/S(9,9)
      DO 160 JJ=1,8
        160 S(II,JJ)=S(II,JJ)-CC*S(9,JJ)
        *****
      ADD ELEMENT STIFFNESS TO TOTAL STIFFNESS
      *****
    165 DO 166 I=1,4
    166 LM(I)=2*IX(N,I)-2
    *****

```



```

C
DO 200 I=1,4
DO 200 K=1,2
II=LM(I)+K
KK=2*I-2+K
DO 200 J=1,4
DO 200 L=1,2
JJ=LM(J)+L-II+1
LL=2*J-2+L
IF (JJ) 200,200,175
175 IF (ND-JJ) 180,195,195
180 WRITE (6,2004) N
KSW=1
GO TO 210
195 A(II,JJ)=A(II,JJ)+S(KK,LL)
200 CONTINUE
210 CONTINUE
IF(KSW.EQ.1) GO TO 500
C
ADD CONCENTRATED FORCES
C
DO 250 N=1,NUMNP
K=2*N
B(K)=B(K)+U7(N)
R(K-1)=B(K-1)+UR(N)
250 CONTINUE
C
PRESSURE BOUNDARY CONDITIONS
C
IF(NUMPC) 260,310,260
260 DO 300 L=1,NUMPC
I=IRC(L)
J=JRC(L)
CODE(I)=ICCODE(I)
CODE(J)=ICCODE(J)

```

FENT0217
 FENT0218
 FENT0219
 FENT0220
 FENT0221
 FENT0222
 FENT0223
 FENT0224
 FENT0225
 FENT0226
 FENT0227
 FENT0228
 FENT0229
 FENT0230
 FENT0231
 FENT0232
 FENT0233
 FENT0234
 FENT0235
 FENT0236
 FENT0237
 FENT0238
 FENT0239
 FENT0240
 FENT0241
 FENT0242
 FENT0243
 FENT0244
 FENT0245
 FENT0246
 FENT0247
 FENT0248
 FENT0249
 FENT0250
 FENT0251
 FENT0252

```

FENT0253
FENT0254
FENT0255
FENT0256
FENT0257
FENT0258
FENT0259
FENT0260
FENT0261
FENT0262
FENT0263
FENT0264
FENT0265
FENT0266
FENT0267
FENT0268
FENT0269
FENT0270
FENT0271
FENT0272
FENT0273
FENT0274
FENT0275
FENT0276
FENT0277
FENT0278
FENT0279
FENT0280
FENT0281
FENT0282
FENT0283
FENT0284
FENT0285
FENT0286
FENT0287
FENT0288

PP=PR(L)/6.
DZ=(Z(I)-Z(J))*PP
DR=(R(J)-R(I))*PP
RX=2.0*R(I)+R(J)
ZX=R(I)+2.0*R(J)
264 II=2*I
JJ=2*J
270 SINA=0.0
COSA=1.0
IF(CODE(I)) 271,272,272
271 SINA=DSIN(CODE(I))
COSA=DCCS(CODE(I))
272 B(II-1)=B(II-1)+RX*(COSA*DZ+SINA*DR)
B(II)=B(II)-RX*(SINA*DZ-COSA*DR)
290 SINA=0.0
COSA=1.0
IF(CODE(J)) 291,292,292
291 SINA=DSIN(CODE(I))
COSA=DCOS(CODE(I))
292 B(JJ-1)=B(JJ-1)+ZX*(COSA*DZ+SINA*DR)
B(JJ)=B(JJ)-ZX*(SINA*DZ-COSA*DR)
300 CONTINUE
310 CONTINUE
DISPLACEMENT B.C.
C
C
DO 400 M=1,NUMNP
U=UR(M)
N=2*M-1
KX=ICOD(M)+1
GO TO (400,370,390,380),KX
370 CALL MODIFY(N,U,ND2)
GO TO 400
380 CALL MODIFY(N,U,ND2)
390 U=UZ(M)
N=N+1
CALL MODIFY(N,U,ND2)

```

```

400 CONTINUE
C
500 RETURN
C *****
2003 FORMAT (26HNEGATIVE AREA ELEMENT NO. I4)
2004 FORMAT (29HOBAND WIDTH EXCEEDS ALLOWABLE I4)
C *****
END
SUBROUTINE QUAD(N,VOL)
C
  IMPLICIT REAL*8 (A-H,O-Z)
  IMPLICIT INTEGER*2(I-N)
  COMMON      STTOP,HED(18),SIGIR(25),SIGIZ(25),GAMMA(25),ZKNOT(25),
1 DEPTH(25),E(10,25),SIG(7),R(450),Z(450),UR(450),
2 UZ(450),STOTAL(450,4),KSW
  COMMON /INTEGR/ NUMNP,NUMEL,NUMMAT,NDEPTH,NORM,MTYPE,ICODE(450)
  COMMON /ARG/ RRR(5),ZZZ(5),S(10,10),P(10),LM(4),DD(3,3),
1 HH(6,10),RR(4),ZZ(4),C(4,4),H(6,10),D(6,6),F(6,10),TP(6),XI(6),
2 FE(10),IX(450,5)
  COMMON /BANARG/ B(900),A(900,54),MBAND
C *****
  I=IX(N,1)
  J=IX(N,2)
  K=IX(N,3)
  L=IX(N,4)
C
  I1=1
  I2=2
  I3=3
  I4=4
  I5=5
C *****
C DETERMINE ELASTIC CONSTANTS AND STRESS-STRAIN RELATIONSHIP
C *****
C
  CALL MPROP(N)

```

```

FENT0289
FENT0290
FENT0291
FENT0292
FENT0293
FENT0294
FENT0295
FENT0296
FENT0297
FENT0298
FENT0299
FENT0300
FENT0301
FENT0302
FENT0303
FENT0304
FENT0305
FENT0306
FENT0307
FENT0308
FENT0309
FENT0310
FENT0311
FENT0312
FENT0313
FENT0314
FENT0315
FENT0316
FENT0317
FENT0318
FENT0319
FENT0320
FENT0321
FENT0322
FENT0323
FENT0324

```



```

C      DO 140 II=1,6
      DO 140 JJ=1,10
      140 HH(II,JJ)=HH(II,JJ)/4.0
C
C      160 RETURN
C      ***
C      2000 FORMAT (' ZERO AREA      ELEMENT',I5)
      END
      SUBROUTINE TRISTF(II,JJ,KK)
      IMPLICIT REAL*8 (A-H,O-Z)
      IMPLICIT INTEGER*2(I-N)
      COMMON      STOP,HED(18),SIGIR(25),SIGIZ(25),GAMMA(25),ZKNOT(25),
      1 DEPTH(25),E(10,25),SIG(7),R(450),Z(450),UR(450),
      2 UZ(450),STOTAL(450,4),KSW
      COMMON /INTEGR/ NUMNP,NUMEL,NUMMAT,NDEPTH,NORM,MTYPE,ICODE(450)
      COMMON /ARG/ RRR(5),ZZZ(5),S(10,10),P(10),LM(4),DD(3,3),
      1 HH(6,10),RR(4),ZZ(4),C(4,4),H(6,10),D(6,6),F(6,10),TP(6),XI(6),
      2 EE(10),IX(450,5)
      COMMON /BANARG/ R(900),A(900,54),MBRAND
C      *****
C      INITIALIZATION
C
      LM(1)=II
      LM(2)=JJ
      LM(3)=KK
C
      RR(1)=RRR(II)
      RR(2)=RRR(JJ)
      RR(3)=RRR(KK)
      RR(4)=RRR(II)
      ZZ(1)=ZZZ(II)
      ZZ(2)=ZZZ(JJ)
      ZZ(3)=ZZZ(KK)
      ZZ(4)=ZZZ(II)

```

FENT0361
 FENT0362
 FENT0363
 FENT0364
 FENT0365
 FENT0366
 FENT0367
 FENT0368
 FENT0369
 FENT0370
 FENT0371
 FENT0372
 FENT0373
 FENT0374
 FENT0375
 FENT0376
 FENT0377
 FENT0378
 FENT0379
 FENT0380
 FENT0381
 FENT0382
 FENT0383
 FENT0384
 FENT0385
 FENT0386
 FENT0387
 FENT0388
 FENT0389
 FENT0390
 FENT0391
 FENT0392
 FENT0393
 FENT0394
 FENT0395
 FENT0396

```

C      85 DO 100 I=1,6
          DO 90 J=1,10
            F(I,J)=0.0
          90 H(I,J)=0.0
          DO 100 J=1,6
            100 D(I,J)=0.0
C
C      FORM INTEGRAL (G)T*(C)*(G)
C      CALL INTER(XI,RR,ZZ)
C
          D(2,6)=XI(1)*(C(1,2)+C(2,3))
          D(3,5)=XI(1)*C(4,4)
          D(5,5)=D(3,5)
          D(6,6)=XI(1)*C(2,2)
          D(1,1)=XI(3)*C(3,3)
          D(1,2)=XI(2)*(C(1,3)+C(3,3))
          D(1,3)=XI(5)*C(3,3)
          D(1,6)=XI(2)*C(2,3)
          D(2,2)=XI(1)*(C(1,1)+2.0*C(1,3)+C(3,3))
          D(2,3)=XI(4)*(C(1,3)+C(3,3))
          D(3,3)=XI(6)*C(3,3)+XI(1)*C(4,4)
          D(3,6)=XI(4)*C(2,3)
          DO 110 I=1,6
          DO 110 J=1,6
          110 D(J,I)=D(I,J)
C
C      FORM COEFFICIENT-DISPLACEMENT MATRIX
C
          COMM=RR(2)*(ZZ(3)-ZZ(1))+RR(1)*(ZZ(2)-ZZ(3))+RR(3)*(ZZ(1)-ZZ(2))
          DD(1,1)=(RR(2)*ZZ(3)-RR(3)*ZZ(2))/COMM
          DD(1,2)=(RR(3)*ZZ(1)-RR(1)*ZZ(3))/COMM
          DD(1,3)=(RR(1)*ZZ(2)-RR(2)*ZZ(1))/COMM
          DD(2,1)=(ZZ(2)-ZZ(3))/COMM
          DD(2,2)=(ZZ(3)-ZZ(1))/COMM
FENT0397
FENT0398
FENT0399
FENT0400
FENT0401
FENT0402
FENT0403
FENT0404
FENT0405
FENT0406
FENT0407
FENT0408
FENT0409
FENT0410
FENT0411
FENT0412
FENT0413
FENT0414
FENT0415
FENT0416
FENT0417
FENT0418
FENT0419
FENT0420
FENT0421
FENT0422
FENT0423
FENT0424
FENT0425
FENT0426
FENT0427
FENT0428
FENT0429
FENT0430
FENT0431
FENT0432

```

```

DD(2,3)=(ZZ(1)-ZZ(2))/COMM
DD(3,1)=(RR(3)-RR(2))/COMM
DD(3,2)=(RR(1)-RR(3))/COMM
DD(3,3)=(RR(2)-RR(1))/COMM
C
DO 120 I=1,3
J=2*LM(I)-1
H(1,J)=DD(1,I)
H(2,J)=DD(2,I)
H(3,J)=DD(3,I)
H(4,J+1)=DD(1,I)
H(5,J+1)=DD(2,I)
120 H(6,J+1)=DD(3,I)
C
FORM STIFFNESS MATRIX (H)T*(D)*(H)
C
DO 130 J=1,10
DO 130 K=1,6
IF (H(K,J)) 128,130,128
128 DO 129 I=1,6
129 F(I,J)=F(I,J)+D(I,K)*H(K,J)
130 CONTINUE
C
DO 140 I=1,10
DO 140 K=1,6
IF (H(K,I)) 138,140,138
138 DO 139 J=1,10
139 S(I,J)=S(I,J)+H(K,I)*F(K,J)
140 CONTINUE
C
FORM STRAIN TRANSFORMATION MATRIX
C
DO 410 I=1,6
DO 410 J=1,10
410 HH(I,J)=HH(I,J)+H(I,J)
C

```

FENT0433
FENT0434
FENT0435
FENT0436
FENT0437
FENT0438
FENT0439
FENT0440
FENT0441
FENT0442
FENT0443
FENT0444
FENT0445
FENT0446
FENT0447
FENT0448
FENT0449
FENT0450
FENT0451
FENT0452
FENT0453
FENT0454
FENT0455
FENT0456
FENT0457
FENT0458
FENT0459
FENT0460
FENT0461
FENT0462
FENT0463
FENT0464
FENT0465
FENT0466
FENT0467
FENT0468

```

C      500 RETURN
      FND
      SUBROUTINE MPRCP(N)
      IMPLICIT REAL*8 (A-H,O-Z)
      IMPLICIT INTEGER*2(I-N)
      COMMON      STQCP,HED(18),SIGIR(25),SIGIZ(25),GAMMA(25),ZKNOT(25),
1 DEPTH(25),E(10,25),SIG(7),R(450),Z(450),UR(450),
2 UZ(450),STOTAL(450,4),KSW
      COMMON /INTEGR/ NUMNP,NUMEL,NUMMAT,NDEPTH,NORM,MTYPE,ICODE(450)
      COMMON /ARG/ RRR(5),ZZZ(5),S(10,10),P(10),LM(4),DD(3,3),
1 HH(6,10),RR(4),ZZ(4),C(4,4),H(6,10),E(6,6),F(6,10),IP(6),XI(6),
2 EE(10),IX(450,5)
      COMMON /BANARG/ B(900),A(900,54),MBAND
      *****
      I=IX(N,1)
      J=IX(N,2)
      K=IX(N,3)
      L=IX(N,4)
      MTYPE=IX(N,5)
      *****
C      DO 5 II=1,4
C      DO 5 JJ=1,4
C      5 C(II,JJ)=0.0
C      *****
C      DETERMINE ELASTIC CONSTANTS
C      *****
C      DO 55 KK=1,2
C      55 EF(KK)=E(KK,MTYPE)
C      60 IF (NORM) 65,75,65
C      65 FF(1)=EE(1)*SIGIZ(MTYPE)
C      *****
C      FORM STRESS STRAIN RELATIONSHIP
C      *****
C      75 COFF=FF(1)/(1.-EE(2)-2.*EE(2)*EE(2))

```

```

FENT0469
FENT0470
FENT0471
FENT0472
FENT0473
FENT0474
FENT0475
FENT0476
FENT0477
FENT0478
FENT0479
FENT0480
FENT0481
FENT0482
FENT0483
FENT0484
FENT0485
FENT0486
FENT0487
FENT0488
FENT0489
FENT0490
FENT0491
FENT0492
FENT0493
FENT0494
FENT0495
FENT0496
FENT0497
FENT0498
FENT0499
FENT0500
FENT0501
FENT0502
FENT0503
FENT0504

```



```

C(1,1)=COEF*(1.-EE(2))
C(1,2)=COEF*EE(2)
C(1,3)=EE(2)*COEF
C(2,1)=C(1,2)
C(2,2)=C(1,1)
C(2,3)=C(1,2)
C(3,1)=C(1,3)
C(3,2)=C(1,2)
C(3,3)=C(1,1)
C(4,4)=COEF*(0.5-EE(2))
RETURN
END

```

```

SUBROUTINE MODIFY(N,U,ND2)

```

C

```

IMPLICIT REAL*8 (A-H,O-Z)
IMPLICIT INTEGER*2(I-N)
COMMON /BANARG/ R(900),A(900,54),MBAND
DO 250 M=2,MBAND
  K=N-M+1

```

```

  IF (K) 235,235,230
  230 R(K)=R(K)-A(K,M)*U
  A(K,M)=0.0

```

```

  235 K=N-M-1

```

```

  IF (ND2-K) 250,240,240

```

```

  240 R(K)=R(K)-A(N,M)*U

```

```

  A(N,M)=0.0

```

```

  250 CONTINUE

```

```

  A(N,1)=1.0

```

```

  R(N)=U

```

```

  RETURN

```

```

  END

```

```

SUBROUTINE BANSOL

```

C

```

IMPLICIT REAL*8 (A-H,O-Z)
IMPLICIT INTEGER*2(I-N)
COMMON STOP,HED(18),SIGIR(25),SIGIZ(25),GAMMA(25),ZKNOT(25),

```

FENT0505
FENT0506
FENT0507
FENT0508
FENT0509
FENT0510
FENT0511
FENT0512
FENT0513
FENT0514
FENT0515
FENT0516
FENT0517
FENT0518
FENT0519
FENT0520
FENT0521
FENT0522
FENT0523
FENT0524
FENT0525
FENT0526
FENT0527
FENT0528
FENT0529
FENT0530
FENT0531
FENT0532
FENT0533
FENT0534
FENT0535
FENT0536
FENT0537
FENT0538
FENT0539
FENT0540

```

1 DEPTH(25),E(10,25),SIG(7),R(450),7(450),UR(450),
2 UZ(450),STOTAL(450,4),KSW
COMMON /INTEGR/ NUMNP,NUMEL,NUMMAT,NDEPTH,NORM,MTYPE,ICODE(450)
COMMON /BANARG/ B(900),A(900,54),MBAND
ND2=2*NUMNP
C
DO 280 N=1,ND2
DO 260 L=2,MBAND
C=A(N,L)/A(N,1)
I=N+L-1
C
IF (ND2.LT.1) GO TO 260
J=0
DO 250 K=L,MBAND
J=J+1
250 A(I,J)=A(I,J)-C*A(N,K)
R(I)=B(I)-C*B(N)
260 A(N,L)=C
280 B(N)=B(N)/A(N,1)
C
BACKSUBSTITUTION
C
N=ND2
300 N=N-1
C
IF (N.LE.0) GO TO 500
DO 400 K=2,MRAND
L=N+K-1
IF (ND2.LT.L) GO TO 400
B(N)=B(N)-A(N,K)*B(L)
400 CONTINUE
C
GO TO 300
C
500 RETURN

```

FENT0541
FENT0542
FENT0543
FENT0544
FENT0545
FENT0546
FENT0547
FENT0548
FENT0549
FENT0550
FENT0551
FENT0552
FENT0553
FENT0554
FENT0555
FENT0556
FENT0557
FENT0558
FENT0559
FENT0560
FENT0561
FENT0562
FENT0563
FENT0564
FENT0565
FENT0566
FENT0567
FENT0568
FENT0569
FENT0570
FENT0571
FENT0572
FENT0573
FENT0574
FENT0575
FENT0576


```
FENT0613
FENT0614
FENT0615
FENT0616
FENT0617
FENT0618
FENT0619
FENT0620
FENT0621
FENT0622
FENT0623
FENT0624
FENT0625
FENT0626
FENT0627
FENT0628
FENT0629
FENT0630
FENT0631
FENT0632
FENT0633
FENT0634
FENT0635
FENT0636
FENT0637
FENT0638
FENT0639
FENT0640
FENT0641
FENT0642
FENT0643
FENT0644
FENT0645
FENT0646
FENT0647
FENT0648
```

```
C      JJ=2*IX(N,I)
C      P(II-1)=B(JJ-I)
C      120 P(II)=B(JJ)
C
C      P(9)=0.0
C      P(10)=0.0
C      130 DO 150 I=1,2
C          RR(I)=P(I+8)
C          DO 150 K=1,8
C              150 RR(I)=RR(I)-S(I+8,K)*P(K)
C
C      COMM=S(9,9)*S(10,10)-S(9,10)*S(10,9)
C      IF (COMM) 155,160,155
C      155 P(9)=(S(10,10)*RR(1)-S(9,10)*RR(2))/COMM
C      P(10)=(-S(10,9)*RR(1)+S(9,9)*RR(2))/COMM
C
C      160 DO 170 I=1,6
C          TP(I)=0.0
C          DO 170 K=1,10
C              170 TP(I)=TP(I)+HH(I,K)*P(K)
C
C      RR(1)=TP(2)
C      RR(2)=TP(6)
C      RR(3)=(TP(1)+TP(2)*RRR(5)+TP(3)*ZZZ(5))/RRR(5)
C      RR(4)=TP(3)+TP(5)
C
C      COMPUTE STRESSES
C
C      DO 180 I=1,4
C          SIG(I)=0.0
C          DO 180 K=1,4
C              180 SIG(I)=SIG(I)+C(I,K)*RR(K)
C
C      COMPUTE PRINCIPLE STRESSES
C
C      CC=(SIG(1)+SIG(2))/2.0
```

C

```

FENT0685
FENT0686
FENT0687
FENT0688
FENT0689
FENT0690
FENT0691
FENT0692
FENT0693
FENT0694
FENT0695
FENT0696
FENT0697
FENT0698
FENT0699
FENT0700
FENT0701
FENT0702
FENT0703
FENT0704
FENT0705
FENT0706
FENT0707
FENT0708
FENT0709
FENT0710
FENT0711
FENT0712
FENT0713
FENT0714
FENT0715
FENT0716
FENT0717
FENT0718
FENT0719
FENT0720

XX(3)=XX(1)
XX(4)=.1323941527884
XX(5)=XX(4)
XX(6)=XX(4)
XX(7)=.225
XX(8)=.696140478028
XX(9)=.410426152314
R(7)=(RR(1)+RR(2)+RR(3))/3.
Z(7)=(ZZ(1)+ZZ(2)+ZZ(3))/3.

C
DO 100 I=1,3
J=I+3
R(I)=XX(8)*RR(I)+(1.-XX(8))*R(7)
R(J)=XX(9)*RR(I)+(1.-XX(9))*R(7)
Z(I)=XX(8)*Z(I)+(1.-XX(8))*Z(7)
100 Z(J)=XX(9)*Z(I)+(1.-XX(9))*Z(7)

C
DO 200 I=1,7
200 XM(I)=XX(I)*R(I)

C
DO 300 I=1,6
300 XI(I)=0.

C
AREA=.5*(RR(1)*(ZZ(2)-ZZ(3))+RR(2)*(ZZ(3)-ZZ(1))+RR(3)*(ZZ(1)-ZZ(2)
1))

C
DO 400 I=1,7
XI(1)=XI(1)+XM(I)
XI(2)=XI(2)+XM(I)/R(I)
XI(3)=XI(3)+XM(I)/(R(I)**2)
XI(4)=XI(4)+XM(I)*Z(I)/R(I)
XI(5)=XI(5)+XM(I)*Z(I)/(R(I)**2)
400 XI(6)=XI(6)+XM(I)*(Z(I)**2)/(R(I)**2)

C
DO 500 I=1,6
500 XI(I)=XI(I)*AREA

```

FENT0721
FENT0722
FENT0723

RETURN
END

C

APPENDIX C

FINITE ELEMENT PROGRAM FOR THE ANALYSIS OF ISOTROPIC ELASTIC AXISYMMETRIC PLATES - THERMAL STRAINS INCLUDED (Ref. 13, 14)

Program Capabilities:

The following restrictions are placed on the size of problems which can be handled by the program.

<u>Item</u>	<u>Maximum Number</u>
Nodal Points	450
Elements	450
Materials	25
Boundary Pressure Cards	200

Printed output includes:

1. Reprint of Input Data
2. Nodal Point Displacements
3. Stresses at the center of each element.

Input Data Format:

A. Identification card - (18A4)

Columns 1 to 72 of this card contain information to be printed with results.

B. Control card - (5I5,F10.0)

Columns	1 - 5	Number of nodal points
	6 - 10	Number of elements
	11 - 15	Number of different materials

- 16 - 20 Normalizing stress (see NORM, Appendix B)
- 21 - 25 Number of boundary pressure cards
- 26 - 35 Reference temperature (stress free temperature)

C. Material Property information

The following group of cards must be supplied for each different material:

First Card - (2I5, 2F10.0)

- Columns 1 - 5 Materials identification - any number from 1 to 12.
- 6 - 10 Number of different temperatures for which properties are given = 8 maximum.
- 11 - 20 Initial Z stress.
- 21 - 30 Initial R stress.

Following Cards - (4F10.0) One card for each temperature



- Columns 1 - 10 Temperature
- 11 - 20 Modulus of elasticity - E
- 21 - 30 Poisson's ratio - ν
- 31 - 40 Coefficient of thermal expansion

D. Nodal Point Cards - (2I5, 5F10.0)

One card for each nodal point with the following information:

- Columns 1 - 5 Nodal point number
- 10 Number which indicates if displacements or forces are to be specified.
- 11 - 20 R - ordinate
- 21 - 30 Z - ordinate
- 31 - 40 XR
- 41 - 50 XZ
- 51 - 60 Temperature

If the number in column 10 is

		<u>Condition</u>
0	XR is the specified R-load and XZ is the specified Z - load	free
1	XR is the specified R-displacement and XZ is the specified Z-load.	
2.	XR is the specified R-load and XZ is the specified Z-displacement.	
3	XR is the specified R-displacement and XZ is the specified Z- displacement.	fixed

All loads are considered to be total forces acting on a one radian segment. Nodal point cards must be in numerical sequence. If cards are omitted, the omitted nodal points are generated at equal intervals along a straight line between the defined nodal points. The necessary temperatures are determined by linear interpolation. The boundary code (column 10), XR and XZ are set equal to zero.

Skew Boundaries:

If the number in columns 5-10 of the nodal point cards is other than 0, 1, 2 or 3, it is interpreted as the magnitude of an angle in degrees. The terms in columns 31-50 of the nodal point card are then interpreted as follows:

XR is the specified load in the s-direction

XZ is the specified displacement in the n-direction

The angle must always be input as a negative angle and may range from -.001 to -180 degrees. Hence, +1.0 degree is the same as -179.0 degrees. The displacements of these nodal points which are printed by the program are

u_r = the displacement in the s-direction

u_z = the displacement in the n-direction

E. Element Cards - (6I5)

One card for each element

Columns	1 - 5	Element number	1. Order nodal points counter-clockwise around element.
	6 - 10	Nodal Point I	
	11 - 15	Nodal Point J	
	16 - 20	Nodal Point K	2. Maximum difference between nodal point I.D. must be less than 25.
	21 - 25	Nodal Point L	
	26 - 30	Material Identification	

Element cards must be in element number sequence. If element cards are omitted, the program automatically generates the omitted information by incrementing by one the preceding I, J, K and L. The material identification code for the generated cards is set equal to the value given on the last card. The last element card must always be supplied.

Triangular elements are also permissible; they are identified by repeating the last nodal point number (i.e., I, J, K, K).

F. Pressure Cards - (2I5, 1F10.0)

One card for each boundary element which is subjected to a normal pressure.

Columns	1 - 5	Nodal Point I
	6 - 10	Nodal Point J
	11 - 20	Normal Pressure

The boundary element must be on the left as one progresses from I to J. Surface tensile force is input as a negative pressure.

Listing:

C	*****	FEWT0001
C	FINITE ELEMENT PROGRAM FOR THE ANALYSIS OF ISOTROPIC ELASTIC	FEWT0002
C	AXYSYMMETRIC PLATES REF FEAST 1,3 SAAS 2	FEWT0003
C	*****	FEWT0004
C		FEWT0005
	IMPLICIT REAL*8 (A-H,O-Z)	FEWT0006
	IMPLICIT INTEGER*2(I-N)	FEWT0007
	COMMON STTOP,HED(18),SIGIR(25),SIGIZ(25),GAMMA(25),ZKNOT(25),	FEWT0008
	1DEPTH(25),F(8,4,25),SIG(7),R(450),Z(450),UR(450),TT(3),	FEWT0009
	2 U7(450),STOTAL(450,4),	FEWT0010
	3 T(450),TEMP,Q,KSW	FEWT0011
	COMMON /INTEGR/ NUMNP,NUMEL,NUMMAT,NDEPTH,NORM,MTYPE,ICODE(450)	FEWT0012
	COMMON /ARG/ RRR(5),ZZZ(5),S(10,10),P(10),LM(4),DD(3,3),	FEWT0013
	1 HH(6,10),RR(4),ZZ(4),C(4,4),H(6,10),D(6,6),F(6,10),TP(6),XI(6),	FEWT0014
	2 EE(10),IX(450,5)	FEWT0015
	COMMON /BANARG/ R(900),A(900,54),MBAND	FEWT0016
	COMMON/PRESS/ IBC(200),JBC(200),PR(200),NUMPC	FEWT0017
	DATA STRS /'*****'/	FEWT0018
C	*****	FEWT0019
C	READ AND PRINT CONTROL INFORMATION	FEWT0020
C	*****	FEWT0021
	50 READ (5,1000,END=950) HED	FEWT0022
	WRITE (6,2000) HED	FEWT0023
C		FEWT0024
	READ(5,1001) NUMNP,NUMEL,NUMMAT,NORM,NUMPC,Q	FEWT0025
	WRITE(6,2006) NUMNP,NUMEL,NUMMAT,NUMPC,Q	FEWT0026
	IF (NORM) 65,65,66	FEWT0027
	66 WRITE (6,2041)	FEWT0028
C	*****	FEWT0029
C	READ AND PRINT MATERIAL PROPERTIES	FEWT0030
C	*****	FEWT0031
	65 CONTINUE	FEWT0032
C		FEWT0033
	DO 80 M=1,NUMMAT	FEWT0034
	READ(5,1012) MTYPE,NUMTC,SIGIZ(MTYPE),SIGIR(MTYPE)	FEWT0035
	WRITE(6,2011) MTYPE,NUMTC,SIGIZ(MTYPE),SIGIR(MTYPE)	FEWT0036

```

      READ(5,1011) ((E(I,J,MTYPE),J=1,4),I=1,NUMTC)
      WRITE(6,2010) ((E(I,J,MTYPE),J=1,4),I=1,NUMTC)
      DO 81 I=NUMTC,8
      DO 81 J=1,4
      81 E(I,J,MTYPE)=E(NUMTC,J,MTYPE)
      80 CONTINUE
      *****
      C READ AND PRINT NODAL POINT DATA
      *****
      C
      100 WRITE (6,2013)
      L=0
      105 READ(5,1006) N,ICODE(N),R(N),Z(N),UR(N),UZ(N),T(N)
      106 NL=L+1
      IF (L,FO,0) GO TO 110
      ZX=N-L
      DR=(R(N)-R(L))/ZX
      DZ=(Z(N)-Z(L))/ZX
      DT=(T(N)-T(L))/ZX
      110 L=L+1
      IF (N-L) 113,112,111
      111 ICODE(L)=0
      R(L)=R(L-1)+DR
      Z(L)=Z(L-1)+DZ
      T(L)=T(L-1)+DT
      UR(L)=0.0
      UZ(L)=0.0
      GO TO 110
      112 WRITE(6,2014) (K,ICODE(K),R(K),Z(K),UR(K),UZ(K),T(K),K=NL,N)
      IF (NUMNP-N) 113,120,105
      113 WRITE (6,2015) N
      GO TO 900
      *****
      C READ AND PRINT ELEMENT PROPERTIES
      *****
      C
      120 WRITE (6,2016)
      N=0
      FEWT0037
      FEWT0038
      FEWT0039
      FEWT0040
      FEWT0041
      FEWT0042
      FEWT0043
      FEWT0044
      FEWT0045
      FEWT0046
      FEWT0047
      FEWT0048
      FEWT0049
      FEWT0050
      FEWT0051
      FEWT0052
      FEWT0053
      FEWT0054
      FEWT0055
      FEWT0056
      FEWT0057
      FEWT0058
      FEWT0059
      FEWT0060
      FEWT0061
      FEWT0062
      FEWT0063
      FEWT0064
      FEWT0065
      FEWT0066
      FEWT0067
      FEWT0068
      FEWT0069
      FEWT0070
      FEWT0071
      FEWT0072

```

130	READ (5,1007) M,(IX(M,I),I=1,5)	FEWT0073
140	N=N+1	FEWT0074
	IF (M-N) 170,170,150	FEWT0075
150	IX(N,1)=IX(N-1,1)+1	FEWT0076
	IX(N,2)=IX(N-1,2)+1	FEWT0077
	IX(N,3)=IX(N-1,3)+1	FEWT0078
	IX(N,4)=IX(N-1,4)+1	FEWT0079
	IX(N,5)=IX(N-1,5)	FEWT0080
170	WRITE (6,2017) N,(IX(N,I),I=1,5)	FEWT0081
	IF (M-N) 180,180,140	FEWT0082
180	IF (NUMEL-N) 300,300,130	FEWT0083
C	*****	FEWT0084
C	READ AND PRINT THE PRESSURE CARDS	FEWT0085
C	*****	FEWT0086
300	IF(NUMPC) 290,210,290	FEWT0087
290	WRITE(6,9000)	FEWT0088
	DO 200 L=1,NUMPC	FEWT0089
	READ(5,9001) IBC(L),JBC(L),PR(L)	FEWT0090
200	WRITE(6,9002) IBC(L),JBC(L),PR(L)	FEWT0091
210	CONTINUE	FEWT0092
C	*****	FEWT0093
C	DETERMINE BAND WIDTH	FEWT0094
C	*****	FEWT0095
	J=0	FEWT0096
	DO 340 N=1,NUMEL	FEWT0097
	DO 340 I=1,4	FEWT0098
	DO 325 L=1,4	FEWT0099
	KK=IX(N,I)-IX(N,L)	FEWT0100
	IF (KK.LT.0) KK=-KK	FEWT0101
	IF (KK.GT.J) J=KK	FEWT0102
325	CONTINUE	FEWT0103
340	CONTINUE	FEWT0104
	MBAND=2*J+2	FEWT0105
C	*****	FEWT0106
C	SOLVE FOR DISPLACEMENTS AND STRESSES	FEWT0107
C	*****	FEWT0108

	KSW=0	FEWT0109
	CALL STIFF	FEWT0110
	IF (KSW.NE.0) GO TO 900	FEWT0111
C		FEWT0112
	CALL BANSOL	FEWT0113
	WRITE(6,2052)	FEWT0114
	WRITE (6,2025) (N,B (2*N-1),B (2*N),N=1,NUMNP)	FEWT0115
C		FEWT0116
450	CALL STRESS(SPLOT)	FEWT0117
C	*****	FEWT0118
C	PROCESS ALL DECKS EVEN IF ERROR	FEWT0119
C	*****	FEWT0120
	GO TO 910	FEWT0121
900	WRITE (6,4000)	FEWT0122
910	WRITE (6,4001) HED	FEWT0123
C		FEWT0124
920	READ (5,1000) CHK	FEWT0125
	IF (CHK.NE.STRS) GO TO 920	FEWT0126
	GO TO 50	FEWT0127
950	CONTINUE	FEWT0128
	WRITE (6,4002)	FEWT0129
	CALL EXIT	FEWT0130
C	*****	FEWT0131
C	*****	FEWT0132
1000	FORMAT (18A4)	FEWT0133
1001	FORMAT(5I5,F10.0)	FEWT0134
1002	FORMAT (I5,2F10.0)	FEWT0135
1003	FORMAT(2F10.0)	FEWT0136
1004	FORMAT (2F10.0)	FEWT0137
1005	FORMAT (3F10.0)	FEWT0138
1006	FORMAT(2I5,5F10.0)	FEWT0139
1007	FORMAT (6I5)	FEWT0140
1011	FORMAT(4F10.0)	FEWT0141
1012	FORMAT(2I5,2F10.0)	FEWT0142
C	*****	FEWT0143
2000	FORMAT (1H1,20A4)	FEWT0144

```

2006 FORMAT (//,
  1 30H0 NUMBER OF NODAL POINTS----- I3 /
  2 30H0 NUMBER OF ELEMENTS----- I3 /
  3 30H0 NUMBER OF DIFF. MATERIALS--- I3 /
  4 30H0 NUMBER OF PRESSURE CARDS---- I3 /
  5 30H0 REFERENCE TEMPERATURE----- F12.4)
2010 FORMAT (15H0 TEMPERATURE 15X 5HE      15X 6HNU      15X 6HALPHA      9X
  1/4F20.8)
2011 FORMAT (17H0MATERIAL NUMBER= I3, 30H, NUMBER OF TEMPERATURE CARDS=
  1 I3,25H INITIAL VERTICAL STRESS= F10.3,5X,
  2 27H INITIAL HORIZONTAL STRESS= F10.3)
2013 FORMAT (12H1NODAL POINT ,4X, 4HTYPE ,4X, 10HR-ORDINATE ,4X,
  1 10HZ-ORDINATE ,10X,6HR-LOAD ,10X, 6HZ-LOAD,10X,4HTEMP )
2014 FORMAT(I12,I8,2F14.3,2F16.5,F14.3)
2015 FORMAT (26H0NODAL POINT CARD ERROR N= I5)
2016 FORMAT (49H1ELEMENT NO.      I      J      K      L      MATERIAL )
2017 FORMAT (11I13,4I6,1I12)
2025 FORMAT (12H0NODAL POINT ,6X, 14HR-DISPLACEMENT ,6X, 14HZ-DISPLACEM
  1ENT / (I12,1P2D20.7))
2041 FORMAT (76H0MODULUS AND YIELD STRESS NORMALIZED WITH RESPECT TO IN
  1ITIAL VERTICAL STRESS )
2051 FORMAT(1H0,10X,'E',8X,'NU',/,3X,F11.1,F10.4/)
2052 FORMAT(1H1)
C *****
3003 FORMAT (16I5)
C *****
4000 FORMAT (//// ' ABNORMAL TERMINATION')
4001 FORMAT (//// ' END OF PROBLEM ' 20A4)
4002 FORMAT (//// ' END OF JOB')
C *****
9000 FORMAT(29H0PRESSURE BOUNDARY CONDITIONS/ 24H      I      J      PRESSU
  1RE )
9001 FORMAT(2I5,F10.0)
9002 FORMAT(2I6,F12.3)
      END
      SUBROUTINE STIFF

```

```

FEWT0145
FEWT0146
FEWT0147
FEWT0148
FEWT0149
FEWT0150
FEWT0151
FEWT0152
FEWT0153
FEWT0154
FEWT0155
FEWT0156
FEWT0157
FEWT0158
FEWT0159
FEWT0160
FEWT0161
FEWT0162
FEWT0163
FEWT0164
FEWT0165
FEWT0166
FEWT0167
FEWT0168
FEWT0169
FEWT0170
FEWT0171
FEWT0172
FEWT0173
FEWT0174
FEWT0175
FEWT0176
FEWT0177
FEWT0178
FEWT0179
FEWT0180

```



```

C      IMPLICIT REAL*8 (A-H,C-Z)
      IMPLICIT INTEGER*2(I-N)
      COMMON      STTOP,HED(18),SIGIR(25),SIGIZ(25),GAMMA(25),ZKNCT(25),
1DEPTH(25),E(8,4,25),SIG(7),R(450),Z(450),UR(450),TT(3),
2 UZ(450),STOTAL(450,4),
3 T(450),TEMP,Q,KSW
      COMMON /INTEGR/ NUMNP,NUMEL,NUMMAT,NDEPTH,NORM,MTYPE,ICODE(450)
      COMMON /ARG/ RRR(5),ZZZ(5),S(10,10),P(10),LM(4),DD(3,3),
1 HH(6,10),RR(4),ZZ(4),C(4,4),H(6,10),D(6,6),F(6,10),TP(6),XI(6),
2 EE(10),IX(450,5)
      COMMON /BANARG/ B(900),A(900,54),MBAND
      COMMON/PRESS/ IBC(200),JBC(200),PR(200),NUMPC
      DIMENSION CODE(450)
C      *****
C      INITIALIZATION
C      *****
      NB=27
      ND=2*NB
      ND2=2*NUMNP
      DO 50 N=1,ND2
      B(N)=0.0
      DO 50 M=1,ND
50  A(N,M)=0.0
C      *****
C      FORM STIFFNESS MATRIX
C      *****
      DO 210 N=1,NUMEL
C
C
90  CALL QUAD(N,VOL)
      IF (VOL) 142,142,144
142 WRITE (6,2003) N
      KSW=1
      GO TO 210
C

```

```

FEWT0181
FEWT0182
FEWT0183
FEWT0184
FEWT0185
FEWT0186
FEWT0187
FEWT0188
FEWT0189
FEWT0190
FEWT0191
FEWT0192
FEWT0193
FEWT0194
FEWT0195
FEWT0196
FEWT0197
FEWT0198
FEWT0199
FEWT0200
FEWT0201
FEWT0202
FEWT0203
FEWT0204
FEWT0205
FEWT0206
FEWT0207
FEWT0208
FEWT0209
FEWT0210
FEWT0211
FEWT0212
FEWT0213
FEWT0214
FEWT0215
FEWT0216

```

```

144 IF (IX(N,3)-IX(N,4)) 145,165,145
145 DO 150 II=1,9
    CC=S(II,10)/S(10,10)
    P(II)=P(II)-CC*P(10)
    DO 150 JJ=1,9
150 S(II,JJ)=S(II,JJ)-CC*S(10,JJ)
C
    DO 160 II=1,8
    CC=S(II,9)/S(9,9)
    P(II)=P(II)-CC*P(9)
    DO 160 JJ=1,8
160 S(II,JJ)=S(II,JJ)-CC*S(9,JJ)
C
C      ADD ELEMENT STIFFNESS TO TOTAL STIFFNESS
C
165 DO 166 I=1,4
166 LM(I)=2*IX(N,I)-2
C
    DO 200 I=1,4
    DO 200 K=1,2
    II=LM(I)+K
    KK=2*I-2+K
    B(II)=R(II)+P(KK)
    DO 200 J=1,4
    DO 200 L=1,2
    JJ=LM(J)+L-II+1
    LL=2*J-2+L
    IF (JJ) 200,200,175
175 IF (ND-JJ) 180,195,195
180 WRITE (6,2004) N
    KSW=1
    GO TO 210
195 A(II,JJ)=A(II,JJ)+S(KK,LL)
200 CONTINUE
210 CONTINUE
    IF (KSW.EQ.1) GO TO 500
FEWT0217
FEWT0218
FEWT0219
FEWT0220
FEWT0221
FEWT0222
FEWT0223
FEWT0224
FEWT0225
FEWT0226
FEWT0227
FEWT0228
FEWT0229
FEWT0230
FEWT0231
FEWT0232
FEWT0233
FEWT0234
FEWT0235
FEWT0236
FEWT0237
FEWT0238
FEWT0239
FEWT0240
FEWT0241
FEWT0242
FEWT0243
FEWT0244
FEWT0245
FEWT0246
FEWT0247
FEWT0248
FEWT0249
FEWT0250
FEWT0251
FEWT0252

```

```

C
C      ADD CONCENTRATED FORCES
C
C      DO 250 N=1,NUMNP
C      K=2*N
C      R(K)=R(K)+UZ(N)
C      B(K-1)=R(K-1)+UR(N)
C      250 CONTINUE

C
C      PRESSURE BOUNDARY CONDITIONS
C
C      IF(NUMPC) 260,310,260
260 DO 300 L=1,NUMPC
      I=IBC(L)
      J=JBC(L)
      CODE(I)=ICODE(I)
      CODE(J)=ICODE(J)
      PP=PR(L)/6.
      DZ=(Z(I)-Z(J))*PP
      DR=(R(J)-R(I))*PP
      RX=2.0*R(I)+R(J)
      RX=R(I)+2.0*R(J)
264 IT=2*I
      JJ=2*J
270 SINA=0.0
      COSA=1.0
      IF(CODE(I)) 271,272,272
271 SINA=DSIN(CODE(I))
      COSA=DCOS(CODE(I))
272 R(I-1)=R(I-1)+RX*(COSA*DZ+SINA*DR)
      R(I)=B(I)-RX*(SINA*DZ-COSA*DR)
290 SINA=C.0
      COSA=1.0
      IF(CODE(J)) 291,292,292
291 SINA=DSIN(CODE(I))

```

```

FEWTO253
FEWTO254
FEWTO255
FEWTO256
FEWTO257
FEWTO258
FEWTO259
FEWTO260
FEWTO261
FEWTO262
FEWTO263
FEWTO264
FEWTO265
FEWTO266
FEWTO267
FEWTO268
FEWTO269
FEWTO270
FEWTO271
FEWTO272
FEWTO273
FEWTO274
FEWTO275
FEWTO276
FEWTO277
FEWTO278
FEWTO279
FEWTO280
FEWTO281
FEWTO282
FEWTO283
FEWTO284
FEWTO285
FEWTO286
FEWTO287
FEWTO288

```

	COSA=DCOS(CODE(I))	FEWT0289
292	B(JJ-1)=B(JJ-1)+ZX*(COSA*DZ+SINA*DR)	FEWT0290
	B(JJ)=B(JJ)-ZX*(SINA*DZ-COSA*DR)	FEWT0291
300	CONTINUE	FEWT0292
310	CONTINUE	FEWT0293
C	DISPLACEMENT B.C.	FEWT0294
C		FEWT0295
	DO 400 M=1,NUMNP	FEWT0296
	U=UR(M)	FEWT0297
	N=2*M-1	FEWT0298
	KX=ICODE(M)+1	FEWT0299
	GO TO (400,370,390,380),KX	FEWT0300
370	CALL MODIFY(N,U,ND2)	FEWT0301
	GO TO 400	FEWT0302
380	CALL MODIFY(N,U,ND2)	FEWT0303
390	U=UZ(M)	FEWT0304
	N=N+1	FEWT0305
	CALL MODIFY(N,U,ND2)	FEWT0306
400	CONTINUE	FEWT0307
C		FEWT0308
500	RETURN	FEWT0309
C	*****	FEWT0310
2003	FORMAT (26H0NEGATIVE AREA ELEMENT NO. I4)	FEWT0311
2004	FORMAT (29H0BAND WIDTH EXCEEDS ALLOWABLE I4)	FEWT0312
C	*****	FEWT0313
	END	FEWT0314
	SUBROUTINE QUAD(N,VOL)	FEWT0315
C		FEWT0316
	IMPLICIT REAL*8 (A-H,O-Z)	FEWT0317
	IMPLICIT INTEGER*2(I-N)	FEWT0318
	COMMON STTOP,HED(18),SIGIR(25),SIGIZ(25),GAMMA(25),ZKNOT(25),	FEWT0319
	1DEPTH(25),E(8,4,25),SIG(7),R(450),Z(450),UR(450),TT(3),	FEWT0320
	2 UZ(450),STOTAL(450,4),	FEWT0321
	3 T(450),TEMP,Q,KSW	FEWT0322
	COMMON /INTEGR/ NUMNP,NUMEL,NUMMAT,NDEPTH,NORM,MTYPE,ICODE(450)	FEWT0323
	COMMON /ARG/ RRR(5),ZZZ(5),S(10,10),P(10),LM(4),DD(3,3),	FEWT0324

	1 HH(6,10),RR(4),ZZ(4),C(4,4),H(6,10),D(6,6),F(6,10),TP(6),XI(6),	FEWT0325
	2 EE(10),IX(450,5)	FEWT0326
	COMMON /BANARG/ B(900),A(900,54),MBAND	FEWT0327
C	*****	FEWT0328
	I=IX(N,1)	FEWT0329
	J=IX(N,2)	FEWT0330
	K=IX(N,3)	FEWT0331
	L=IX(N,4)	FEWT0332
C		FEWT0333
	I1=1	FEWT0334
	I2=2	FEWT0335
	I3=3	FEWT0336
	I4=4	FEWT0337
	I5=5	FEWT0338
C	THERMAL STRESSES	FEWT0339
	TEMP=(T(I)+T(J)+T(K)+T(L))/4.0	FEWT0340
	DO 103 M=2,8	FEWT0341
	IF(E(M,1,MTYPE)-TEMP) 103,104,104	FEWT0342
103	CONTINUE	FEWT0343
104	RATIO=0.0	FEWT0344
	DEN=E(M,1,MTYPE)-E(M-1,1,MTYPE)	FEWT0345
	IF(DEN) 70,71,70	FEWT0346
70	RATIO=(TEMP-E(M-1,1,MTYPE))/DEN	FEWT0347
71	DO 105 KK=1,3	FEWT0348
105	FE(KK)=E(M-1,KK+1,MTYPE)+RATIO*(E(M,KK+1,MTYPE)-E(M-1,KK+1,MTYPE))	FEWT0349
	TEMP=TEMP-Q	FEWT0350
C	*****	FEWT0351
C	DETERMINE ELASTIC CONSTANTS AND STRESS-STRAIN RELATIONSHIP	FEWT0352
C	*****	FEWT0353
C		FEWT0354
	CALL MPROP(N)	FEWT0355
C		FEWT0356
	88 DO 110 M=1,3	FEWT0357
110	TT(M)=(C(M,1)+C(M,2)+C(M,3))*EE(3)*TEMP	FEWT0358
C	*****	FEWT0359
C	FORM QUADRILATERAL STIFFNESS MATRIX	FEWT0360

```

C      ** ** ** ** ** ** ** ** ** ** ** ** ** ** ** ** ** ** ** ** ** ** ** ** ** ** ** ** ** ** ** ** ** ** ** ** ** ** ** ** ** ** ** ** ** ** ** ** ** ** ** ** ** ** ** ** ** ** ** ** ** ** ** ** ** ** ** ** ** ** ** ** ** ** ** ** ** ** ** ** ** ** ** ** ** ** ** ** ** ** **
210 RRR(5)=(R(I)+R(J)+R(K)+R(L))/4.0
ZZZ(5)=(Z(I)+Z(J)+Z(K)+Z(L))/4.0
DO 94 M=1,4
MM=IX(N,M)
IF(R(MM).EQ.0..AND.ICODE(MM).EQ.0) ICODE(MM)=1
93 RRR(M)=R(MM)
94 ZZZ(M)=Z(MM)
C
DO 100 II=1,10
P(II)=0.0
DO 95 JJ=1,6
95 HH(JJ,II)=0.0
DO 100 JJ=1,10
100 S(II,JJ)=0.0
IF (K-L) 125,120,125
120 CALL TRISTF(I1,I2,I3)
RRR(5)=(RRR(1)+RRR(2)+RRR(3))/3.0
ZZZ(5)=(ZZZ(1)+ZZZ(2)+ZZZ(3))/3.0
VOL=XI(1)
GO TO 160
125 VOL=0.0
CALL TRISTF(I4,I1,I5)
IF(XI(1).EQ.0.) WRITE(6,2000) N
VOL=VOL+XI(1)
CALL TRISTF(I1,I2,I5)
IF(XI(1).EQ.0) WRITE(6,2000) N
VOL=VOL+XI(1)
CALL TRISTF(I3,I4,I5)
IF(XI(1).EQ.0) WRITE(6,2000) N
VOL=VOL+XI(1)
CALL TRISTF(I2,I3,I5)
IF(XI(1).EQ.0) WRITE(6,2000) N
VOL=VOL+XI(1)
C
DO 140 II=1,6

```

FEWT0361

FEWT0362

FEWT0363

FEWT0364

FEWT0365

FEWT0366

FEWT0367

FEWT0368

FEWT0369

FEWT0370

FEWT0371

FEWT0372

FEWT0373

FEWT0374

FEWT0375

FEWT0376

FEWT0377

FEWT0378

FEWT0379

FEWT0380

FEWT0381

FEWT0382

FEWT0383

FEWT0384

FEWT0385

FEWT0386

FEWT0387

FEWT0388

FEWT0389

FEWT0390

FEWT0391

FEWT0392

FEWT0393

FEWT0394

FEWT0395

FEWT0396

```

DO 140 JJ=1,10
140 HH(II,JJ)=HH(II,JJ)/4.0
C
C
160 RETURN
C ***
2000 FORMAT (' ZERO AREA ELEMENT',I5)
END
SUBROUTINE TRISTF(II,JJ,KK)
IMPLICIT REAL*8 (A-H,O-Z)
IMPLICIT INTEGER*2(I-N)
COMMON STTOP,HED(18),SIGIR(25),SIGIZ(25),GAMMA(25),ZKNCT(25),
1 DEPTH(25),E(8,4,25),SIG(7),R(450),Z(450),UR(450),TT(3),
2 UZ(450),STOTAL(450,4),
3 T(450),TEMP,Q,КСW
COMMON /INTEGR/ NUMNP,NUMEL,NUMMAT,NDEPTH,NORM,MIYPE,ICODE(450)
COMMON /ARG/ RRR(5),ZZZ(5),S(10,10),P(10),LM(4),DD(3,3),
1 HH(6,10),RR(4),ZZ(4),C(4,4),H(6,10),D(6,6),F(6,10),TP(6),XI(6),
2 EE(10),IX(450,5)
COMMON /BANARG/ R(900),A(900,54),MBAND
C *****
C INITIALIZATION
C
LM(1)=II
LM(2)=JJ
LM(3)=KK
C
RR(1)=RRR(II)
RR(2)=RRR(JJ)
RR(3)=RRR(KK)
RR(4)=RRR(II)
ZZ(1)=ZZZ(II)
ZZ(2)=ZZZ(JJ)
ZZ(3)=ZZZ(KK)
ZZ(4)=ZZZ(II)
C

```

FEWT0397
FEWT0398
FEWT0399
FEWT0400
FEWT0401
FEWT0402
FEWT0403
FEWT0404
FEWT0405
FEWT0406
FEWT0407
FEWT0408
FEWT0409
FEWT0410
FEWT0411
FEWT0412
FEWT0413
FEWT0414
FEWT0415
FEWT0416
FEWT0417
FEWT0418
FEWT0419
FEWT0420
FEWT0421
FEWT0422
FEWT0423
FEWT0424
FEWT0425
FEWT0426
FEWT0427
FEWT0428
FEWT0429
FEWT0430
FEWT0431
FEWT0432

FEWT0433
FEWT0434
FEWT0435
FEWT0436
FEWT0437
FEWT0438
FEWT0439
FEWT0440
FEWT0441
FEWT0442
FEWT0443
FEWT0444
FEWT0445
FEWT0446
FEWT0447
FEWT0448
FEWT0449
FEWT0450
FEWT0451
FEWT0452
FEWT0453
FEWT0454
FEWT0455
FEWT0456
FEWT0457
FEWT0458
FEWT0459
FEWT0460
FEWT0461
FEWT0462
FEWT0463
FEWT0464
FEWT0465
FEWT0466
FEWT0467
FEWT0468

85 DO 100 I=1,6
DO 90 J=1,10
F(I,J)=0.0
90 H(I,J)=0.0
DO 100 J=1,6
100 D(I,J)=0.0

C
C
C
FORM INTEGRAL (G)T*(C)*(G)
CALL INTER(XI,RR,ZZ)

C
D(2,6)=XI(1)*(C(1,2)+C(2,3))
D(3,5)=XI(1)*C(4,4)
D(5,5)=D(3,5)
D(6,6)=XI(1)*C(2,2)
D(1,1)=XI(3)*C(3,3)
D(1,2)=XI(2)*(C(1,3)+C(3,3))
D(1,3)=XI(5)*C(3,3)
D(1,6)=XI(2)*C(2,3)
D(2,2)=XI(1)*(C(1,1)+2.0*C(1,3)+C(3,3))
D(2,3)=XI(4)*(C(1,3)+C(3,3))
D(3,3)=XI(6)*C(3,3)+XI(1)*C(4,4)
D(3,6)=XI(4)*C(2,3)

DO 110 I=1,6
DO 110 J=1,6
110 D(J,I)=D(I,J)

C
C
C
C

FORM COEFFICIENT-DISPLACEMENT MATRIX

COMM=RR(2)*(ZZ(3)-ZZ(1))+RR(1)*(ZZ(2)-ZZ(3))+RR(3)*(ZZ(1)-ZZ(2))
DD(1,1)=(RR(2)*ZZ(3)-RR(3)*ZZ(2))/COMM
DD(1,2)=(RR(3)*ZZ(1)-RR(1)*ZZ(3))/COMM
DD(1,3)=(RR(1)*ZZ(2)-RR(2)*ZZ(1))/COMM
DD(2,1)=(ZZ(2)-ZZ(3))/COMM
DD(2,2)=(ZZ(3)-ZZ(1))/COMM
DD(2,3)=(ZZ(1)-ZZ(2))/COMM


```

C      60 IF (NORM) 65,75,65
      65 FE(1)=EE(1)*SIGIZ(MTYPE)
C      *****
C      FORM STRESS STRAIN RELATIONSHIP
C      *****
      75 COEF=EE(1)/(1.-EE(2))-2.*EE(2)*EE(2)
        C(1,1)=COEF*(1.-EE(2))
        C(1,2)=COEF*EE(2)
        C(1,3)=EE(2)*COEF
        C(2,1)=C(1,2)
        C(2,2)=C(1,1)
        C(2,3)=C(1,2)
        C(3,1)=C(1,3)
        C(3,2)=C(1,2)
        C(3,3)=C(1,1)
        C(4,4)=COEF*(0.5-EE(2))
        RETURN
      END
C      SUBROUTINE MODIFY(N,U,ND2)
        IMPLICIT REAL*8 (A-H,O-Z)
        IMPLICIT INTEGER*2(I-N)
        COMMON /BANARG/ R(900),A(900,54),MBAND
        DO 250 M=2,MBAND
          K=N-M+1
          IF (K) 235,235,230
          230 R(K)=R(K)-A(K,M)*U
              A(K,M)=0.0
          235 K=N-M-1
          IF (NC2-K) 250,240,240
          240 B(K)=R(K)-A(N,M)*U
              A(N,M)=0.0
          250 CONTINUE
              A(N,1)=1.0
              R(N)=U

```

```

FEWT0541
FEWT0542
FEWT0543
FEWT0544
FEWT0545
FEWT0546
FEWT0547
FEWT0548
FEWT0549
FEWT0550
FEWT0551
FEWT0552
FEWT0553
FEWT0554
FEWT0555
FEWT0556
FEWT0557
FEWT0558
FEWT0559
FEWT0560
FEWT0561
FEWT0562
FEWT0563
FEWT0564
FEWT0565
FEWT0566
FEWT0567
FEWT0568
FEWT0569
FEWT0570
FEWT0571
FEWT0572
FEWT0573
FEWT0574
FEWT0575
FEWT0576

```

```

FEWT0577
FEWT0578
FEWT0579
FEWT0580
FEWT0581
FEWT0582
FEWT0583
FEWT0584
FEWT0585
FEWT0586
FEWT0587
FEWT0588
FEWT0589
FEWT0590
FEWT0591
FEWT0592
FEWT0593
FEWT0594
FEWT0595
FEWT0596
FEWT0597
FEWT0598
FEWT0599
FEWT0600
FEWT0601
FEWT0602
FEWT0603
FEWT0604
FEWT0605
FEWT0606
FEWT0607
FEWT0608
FEWT0609
FEWT0610
FEWT0611
FEWT0612

      RETURN
      END
      SUBROUTINE BANSOL
C
      IMPLICIT REAL*8 (A-H,O-Z)
      IMPLICIT INTEGER*2(I-N)
      COMMON STTOP,HED(18),SIGIR(25),SIGIZ(25),GAMMA(25),ZKNCT(25),
1DEPTH(25),E(8,4,25),SIG(7),R(450),Z(450),UR(450),TT(3),
2UZ(450),STOTAL(450,4),
3T(450),TEMP,Q,KSW
      COMMON /INTEGR/ NUMNP,NUMEL,NUMMAT,NDEPTH,NORM,MTYPE,ICODE(450)
      COMMON /BANARG/ B(900),A(900,54),MBAND
      ND2=2*NUMNP
C
      DO 280 N=1,ND2
      DO 260 L=2,MBAND
      C=A(N,L)/A(N,1)
      I=N+L-1
C
      IF (ND2.LT.1) GO TO 260
      J=0
      DO 250 K=L,MBAND
      J=J+1
      250 A(I,J)=A(I,J)-C*A(N,K)
      B(I)=B(I)-C*B(N)
      260 A(N,L)=C
      280 B(N)=B(N)/A(N,1)
C
      BACKSUBSTITUTION
C
      N=ND2
      300 N=N-1
C
      IF (N.LE.0) GO TO 500
      DO 400 K=2,MBAND

```



```

ZZZ(5)=(Z(I1)+Z(J1)+Z(K1)+Z(L1))/4.0
GO TO 100
50 RRR(5)=(R(I1)+R(J1)+R(K1))/3.0
ZZZ(5)=(Z(I1)+Z(J1)+Z(K1))/3.0
C
C      COMPUTE STRAINS
C
100 DO 120 I=1,4
    II=2*I
    JJ=2*IX(N,I)
    P(II-1)=B(JJ-1)
    120 P(II)=B(JJ)
C
    P(9)=0.0
    P(10)=0.0
130 DO 150 I=1,2
    RR(I)=P(I+8)
    DO 150 K=1,8
    150 RR(I)=RR(I)-S(I+8,K)*P(K)
C
    COMM=S(9,9)*S(10,10)-S(9,10)*S(10,9)
    IF (COMM) 155,160,155
155 P(9)=(S(10,10)*RR(1)-S(9,10)*RR(2))/COMM
    P(10)=(-S(10,9)*RR(1)+S(9,9)*RR(2))/COMM
C
160 DO 170 I=1,6
    TP(I)=0.0
    DO 170 K=1,10
    170 TP(I)=TP(I)+HH(I,K)*P(K)
C
    RR(1)=TP(2)
    RR(2)=TP(6)
    RR(3)=(TP(1)+TP(2)*RRR(5)+TP(3)*ZZZ(5))/RRR(5)
    RR(4)=TP(3)+TP(5)
C
C      COMPUTE STRESSES

```

FEWT0649
FEWT0650
FEWT0651
FEWT0652
FEWT0653
FEWT0654
FEWT0655
FEWT0656
FEWT0657
FEWT0658
FEWT0659
FEWT0660
FEWT0661
FEWT0662
FEWT0663
FEWT0664
FEWT0665
FEWT0666
FEWT0667
FEWT0668
FEWT0669
FEWT0670
FEWT0671
FEWT0672
FEWT0673
FEWT0674
FEWT0675
FEWT0676
FEWT0677
FEWT0678
FEWT0679
FEWT0680
FEWT0681
FEWT0682
FEWT0683
FEWT0684


```

FEWT0721
FEWT0722
FEWT0723
FEWT0724
FEWT0725
FEWT0726
FEWT0727
FEWT0728
FEWT0729
FEWT0730
FEWT0731
FEWT0732
FEWT0733
FEWT0734
FEWT0735
FEWT0736
FEWT0737
FEWT0738
FEWT0739
FEWT0740
FEWT0741
FEWT0742
FEWT0743
FEWT0744
FEWT0745
FEWT0746
FEWT0747
FEWT0748
FEWT0749
FEWT0750
FEWT0751
FEWT0752
FEWT0753
FEWT0754
FEWT0755
FEWT0756

END
SUBROUTINE INTER(XI,RR,ZZ)
IMPLICIT REAL*8 (A-H,C-Z)
IMPLICIT INTEGER*2(I-N)
DIMENSION RR(1),ZZ(1),XI(1)
DIMENSION XM(7),R(7),Z(7),XX(9)

C
XX(1)=.1259391805448
XX(2)=XX(1)
XX(3)=XX(1)
XX(4)=.1323941527884
XX(5)=XX(4)
XX(6)=XX(4)
XX(7)=.225
XX(8)=.696140478028
XX(9)=.410426192314
R(7)=(RR(1)+RR(2)+RR(3))/3.
Z(7)=(ZZ(1)+ZZ(2)+ZZ(3))/3.

C
DO 100 I=1,3
J=I+3
R(I)=XX(8)*RR(I)+(1.-XX(8))*R(7)
R(J)=XX(9)*RR(I)+(1.-XX(9))*R(7)
Z(I)=XX(8)*ZZ(I)+(1.-XX(8))*Z(7)
100 Z(J)=XX(9)*ZZ(I)+(1.-XX(9))*Z(7)

C
DO 200 I=1,7
200 XM(I)=XX(I)*R(I)

C
DO 300 I=1,6
300 XI(I)=0.

C
AREA=.5*(RR(1)*(ZZ(2)-ZZ(3))+RR(2)*(ZZ(3)-ZZ(1))+RR(3)*(ZZ(1)-ZZ(2)
1)))

C
DO 400 I=1,7

```



```

      XI(1)=XI(1)+XM(I)
      XI(2)=XI(2)+XM(I)/R(I)
      XI(3)=XI(3)+XM(I)/(R(I)**2)
      XI(4)=XI(4)+XM(I)*Z(I)/R(I)
      XI(5)=XI(5)+XM(I)*Z(I)/(R(I)**2)
      XI(6)=XI(6)+XM(I)*(Z(I)**2)/(R(I)**2)
400  DO 500 I=1,6
      DO 500 I=1,6
      XI(I)=XI(I)*AREA
C
      RETURN
      END
FEMT0757
FEMT0758
FEMT0759
FEMT0760
FEMT0761
FEMT0762
FEMT0763
FEMT0764
FEMT0765
FEMT0766
FEMT0767
FEMT0768

```

APPENDIX D

STEADY STATE HEAT TRANSFER PROGRAM FOR BOLTED JOINT

Program Capacity: 50 nodal points

Output Data:

- (a) Input data
- (b) Inverse of matrix
- (c) Nodal temperature
- (d) Given and calculated augmenting vector and residual error

Input Data Sequence:

- A. Case identification (12A4) followed by two blank cards
- B. Card (11) with a 1
- C. Card (17) with dimension of matrix
- D. Card (11) with a 1
- E. Cards (11, 3(213, E15.8)) with node indices started in the first I3 field followed by conductance between these nodes. Only input from lower node number to higher node number required (since the conductance from node i to j equals the conductance from j to i.) Each card has three groups of z node numbers followed by a conductance value except the last card. Last card could have 1, 2 or 3 groups and has a 1 in column 1.
- F. Cards (11, 3(I6, E15.8) with number of node followed by conductance from the node to ground node which is at specified temperature. Each card has 3 groups of node number followed by conductance. The 11 field is skipped except for the last card for ground conductances which can have 1, 2 or 3 fields and the first column has a 1. A

node can be connected to only one ground node.

- G. Same as F above, but code temperature specified for ground node instead of the conductance value.
- H. Same as F above, but code internal power dissipation for the particular node instead of the conductance value.

Listing:

```

C      STFADY STATE HEAT TRANSFER PROGRAM      BOLTED JOINT
      DIMENSION IDENT(12),A(050,050),AA(050,050),B( 50),BI( 50 ),
      IBC( 50),RES( 50),ACON( 50),TACCN( 50),Q( 50)
101 WRITE(6,23)
41 READ(5,51) K,IDENT
51 FORMAT(11,12A4)
      WRITE(6,111) IDENT
111 FORMAT(12A6)
      IF(K .NE. 1) GO TO 41
      READ(5,55) N,K
55 FORMAT(17/11)
      M = N+1
      DO 3 I = 1,N
      DO 3 J = 1,N
      AA(I,J) = 0.0
      ACON(I)=0.
      Q(I) = 0.
      TACCN(I) = 0.
3 CONTINUE
C      READ IN COEFF. MATRIX ELEMENTS
42 READ(5,52) K,(I,J,AA(I,J),JM=1,3)
52 FORMAT(11,3(2I3,E15.8))
      IF(K .NE. 1) GO TO 42
43 READ(5,53) K,(I,ACON(I),JM=1,3)
      IF(K .NE. 1) GO TO 43
44 READ(5,53) K,(I,TACCN(I),JM=1,3)
      IF(K .NE. 1) GO TO 44
45 READ(5,53) K,(I,Q(I),JM=1,3)
      IF(K .NE. 1) GO TO 45
53 FORMAT(11,3(16,E15.8))
      DO 500 I=1,N
500 B(I) = -(Q(I) + ACON(I) * TACCN(I))
      DO 1000 I=1,N
      DO 1000 J=1,N
1000 AA(J,I) = AA(I,J)
      DO 3000 I=1,N

```

SSHT0001
SSHT0002
SSHT0003
SSHT0004
SSHT0005
SSHT0006
SSHT0007
SSHT0008
SSHT0009
SSHT0010
SSHT0011
SSHT0012
SSHT0013
SSHT0014
SSHT0015
SSHT0016
SSHT0017
SSHT0018
SSHT0019
SSHT0020
SSHT0021
SSHT0022
SSHT0023
SSHT0024
SSHT0025
SSHT0026
SSHT0027
SSHT0028
SSHT0029
SSHT0030
SSHT0031
SSHT0032
SSHT0033
SSHT0034
SSHT0035
SSHT0036

```

SSHT0037
SSHT0038
SSHT0039
SSHT0040
SSHT0041
SSHT0042
SSHT0043
SSHT0044
SSHT0045
SSHT0046
SSHT0047
SSHT0048
SSHT0049
SSHT0050
SSHT0051
SSHT0052
SSHT0053
SSHT0054
SSHT0055
SSHT0056
SSHT0057
SSHT0058
SSHT0059
SSHT0060
SSHT0061
SSHT0062
SSHT0063
SSHT0064
SSHT0065
SSHT0066
SSHT0067
SSHT0068
SSHT0069
SSHT0070
SSHT0071
SSHT0072

IN=I
AA(I,I) = 0.
DO 2001 J=1,N
JN=J
IF (JN.EQ. IN) GO TO 2001
2000 AA(I,I) = AA(I,I) + AA(I,J)
2001 CONTINUE
3000 AA(I,I) = (AA(I,I)+ACGN(I)) * (-1.)
WRITE(6,26)
26 FORMAT(1H1,27X,1H1,12X,1HQ,15X,1CHGRD. COND.,10X,1CHGRD. TEMP.//)
WRITE(6,25)(I,Q(I),ACGN(I),TACGN(I),I=1,N)
25 FORMAT(1H ,26X,I3,7X,F10.5,10X,F10.5,10X,F10.5,10X)
MM = 1
DO 4 I=1,N
DO 4 J = 1,N
A(I,J) = AA(I,J)
4 CONTINUE
WRITE(6,5)
5 FCRMAT( 1H1,39X17HA = COEFF. MATRIX //
1 40X21HB = AUGMENTING VECTOR //
2 40X19HT = SOLUTION VECTOR //
3 40X16HAI= INVERSE OF A //
4 40X33HRC = AUGMENTING VECTOR CALCULATED //
5 40X21H( A ) * ( T ) = ( R ) /// )
DO 7 I = 1,N
7 WRITE(5,6)( I,J,A(I,J), J = 1,N )
6 FORMAT(1H / (4( 5H A(I3,1H,I3,2H)=F10.5,5X)))
DO 8 I = 1,N
BI(I) = B(I)
8 CONTINUE
CALL MAT(N,M,A,B )
WRITE(6,22)
22 FORMAT(1H1 )
C WRITE INVERSE MATRIX
DO 9 I = 1,N
9 WRITE(6,10)( I,J,A(I,J), J = 1,N )

```

```

10 FCRMAT(1H / (4( 5H AI(I3,1H,I3,2H)=E15.8)))
11 WRITE(6,23)
23 FCRMAT(1H1)
12 WRITE SOLUTION VECTOR
12 WRITE(6,11)( J, B(J) , J = 1,N )
11 FCRMAT(1H / 4(5H T(I3,2H)=F10.5,9X))
DO 13 I = 1,N
  BC(I) = 0.0
  DO 13 J = 1,N
    BC(I) = BC(I) + (AA(I,J) * B(J))
13 CCNTINUE
DO 15 J = 1,N
  RES(J) = ABS(BI(J)) - ABS( BC(J))
15 CCNTINUE
16 FCRMAT(1H1,30X76H AUGMENTING VECTOR      CALCULATING VECTOR
17 WRITE(6,16)
18 FCRMAT(25X4H B(I3,1H, I3,2H)=E15.8,2X4H BC(I3,1H,I3,2H)=E15.8,
1 6XE15.8 /)
GO TO 101
END
SUBROUTINE MAT (N,M,A,B)
M = N + 1
N = SIZE OF MATRIX TO BE INVERTED
TO SOLVE AX = B, WHERE INPUT A = A, INPUT B = B
OUTPUT B= X, OUTPUTA = A INVERSE
DIMENSION A(50,50),B(50)
N1 = N - 1
TEMP 15 = A(1,1)
A(M,N) = 1.0 / TEMP 15
B(M) = A(1,2) / TEMP 15
DO 1 I=2,N1
  A(M,I-1)= A(1,I+1) / TEMP 15
1 CCNTINUE
A(M,N1) = B(1) / TEMP 15

```

SSHT0073
SSHT0074
SSHT0075
SSHT0076
SSHT0077
SSHT0078
SSHT0079
SSHT0080
SSHT0081
SSHT0082
SSHT0083
SSHT0084
SSHT0085
SSHT0086
SSHT0087
SSHT0088
SSHT0089
SSHT0090
SSHT0091
SSHT0092
SSHT0093
SSHT0094
SSHT0095
SSHT0096
SSHT0097
SSHT0098
SSHT0099
SSHT0100
SSHT0101
SSHT0102
SSHT0103
SSHT0104
SSHT0105
SSHT0106
SSHT0107
SSHT0108

```

DO 10 I=1,N1
  TEMP 6 = A(I+1,1)
  B(I) = A(I+1,2) - TEMP 6 * B(M)
DO 5 J=2,N1
  A(I,J-1) = A(I+1,J+1) - TEMP 6 * A(M,J-1)
5 CONTINUE
  A(I,N1) = B(I+1) - TEMP 6 * A(M,N1)
  A(I,N) = -TEMP6 / TEMP 15
10 CONTINUE
  B(N) = B(M)
DO 15 I=1,N
  A(N,I) = A(M,I)
15 CONTINUE
  REPEATS N - 1 TIMES
DO 100 K=1,N1
  TEMP 15 = B(1)
  A(M,N) = 1.0 / TEMP 15
  B(M) = A(1,1) / TEMP 15
DO 51 I=2,N
  A(M,I-1) = A(1,I) / TEMP 15
51 CONTINUE
DO 60 I=1,N1
  TEMP 6 = B(I+1)
  B(I) = A(I+1,1) - TEMP 6 * B(M)
DO 55 J=2,N
  A(I,J-1) = A(I+1,J) - TEMP 6 * A(M,J-1)
55 CONTINUE
  A(I,N) = -TEMP 6 / TEMP 15
60 CONTINUE
  B(N) = B(M)
DO 65 I=1,N
  A(N,I) = A(M,I)
65 CONTINUE
100 CONTINUE
  RETURN
  END

```

SSHOT0109
 SSHOT0110
 SSHOT0111
 SSHOT0112
 SSHOT0113
 SSHOT0114
 SSHOT0115
 SSHOT0116
 SSHOT0117
 SSHOT0118
 SSHOT0119
 SSHOT0120
 SSHOT0121
 SSHOT0122
 SSHOT0123
 SSHOT0124
 SSHOT0125
 SSHOT0126
 SSHOT0127
 SSHOT0128
 SSHOT0129
 SSHOT0130
 SSHOT0131
 SSHOT0132
 SSHOT0133
 SSHOT0134
 SSHOT0135
 SSHOT0136
 SSHOT0137
 SSHOT0138
 SSHOT0139
 SSHOT0140
 SSHOT0141
 SSHOT0142
 SSHOT0143
 SSHOT0144

TABLE 1

Separation Radius Comparison - Single and Two Plate Models

(see Figs. 12 - 17)

$\frac{A}{B}$	$\frac{B}{A}$	R_o/A		Percent Discrepancy Between Models
		Single Plate Model	Two Plate Model	
1	3.1	4.2	3.7	13.5
	2.2	3.3	2.7	22.2
	1.6	2.7	2.1	28.6
	1.3	2.4	1.7	41.7
.75	3.1	4.5	3.8	18.5
	2.2	3.6	2.8	28.9
	1.6	3.0	2.2	36.4
	1.3	2.7	2.0	35.0
.5	3.1	5.1	4.1	24.4
	2.2	4.2	3.2	31.3
	1.6	3.6	2.8	28.6
	1.3	3.3	2.5	32.0

TABLE 2

Test and Analytical Results for Radii of Separation of Bolted Plates (see Fig. 5)

Case	D in.	2B in.	Separation Diameters, 2 R _O - in.					% Discrepancy Between Computed Values and Tested Values	
			"Rubbing Test"		Autoradiographic Test		Computed		
			Range	Average	Range	Average		Rub. Test	Autorad. Test
1	.065	.422	.42-.48	.45	.41-.46	.44	.488	7.8	9.8
2	.124	.422	.50-.53	.51	.4 - .6	.55	.554	7.9	.7
3	.191	.422	.58-.64	.62	.76-.81	.78*	.620	0	25.8
4	.253	.422	.70-.76	.72	.68-.73	.7**	.700	2.9	0
5.	Unmatch- ed Pair .124/ .257	.422	.54-.58	.56	—	—	.588	4.8	—
6.	.124	1.0	1.06-1.10	1.09	—	—	1.104	1.3	—
7.	.191	1.0	1.11-1.17	1.16	—	—	1.210	4.1	—

* Original x-ray film shows hole in plate and 0.6 inch diameter zone more distinctly than remainder of area sensitized by the radioactive contamination. Loose radiographic contamination observed during test.

** Assembled and disassembled radioactive and non-radioactive plates without rotating plates relative to each other.

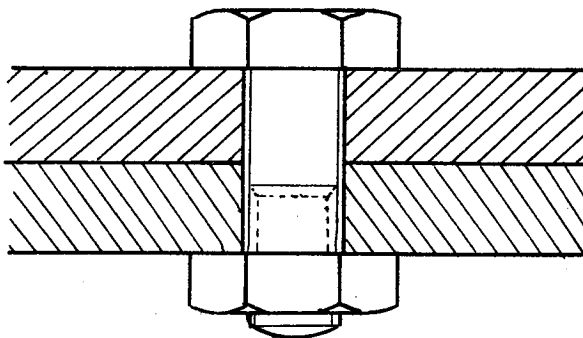


FIG. 1. BOLTED JOINT

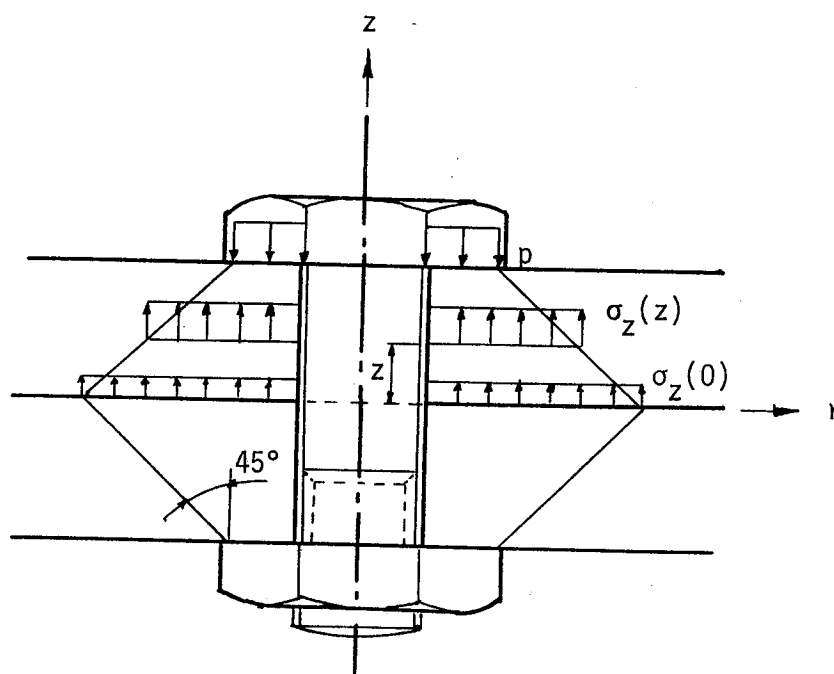


FIG. 2. ROETSCHER'S RULE OF THUMB FOR PRESSURE DISTRIBUTION IN A BOLTED JOINT

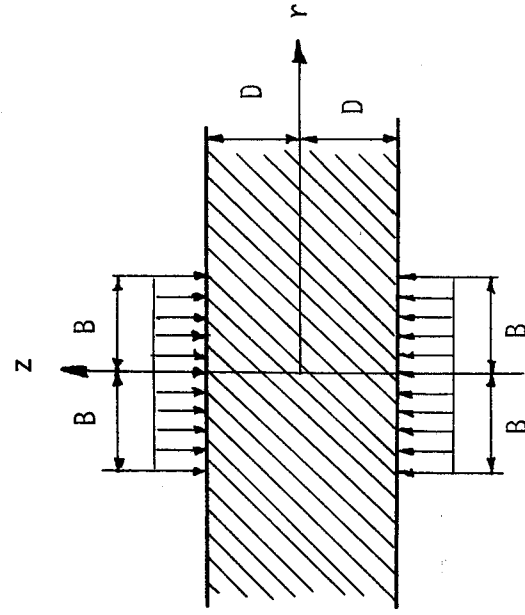


FIG. 3(a)

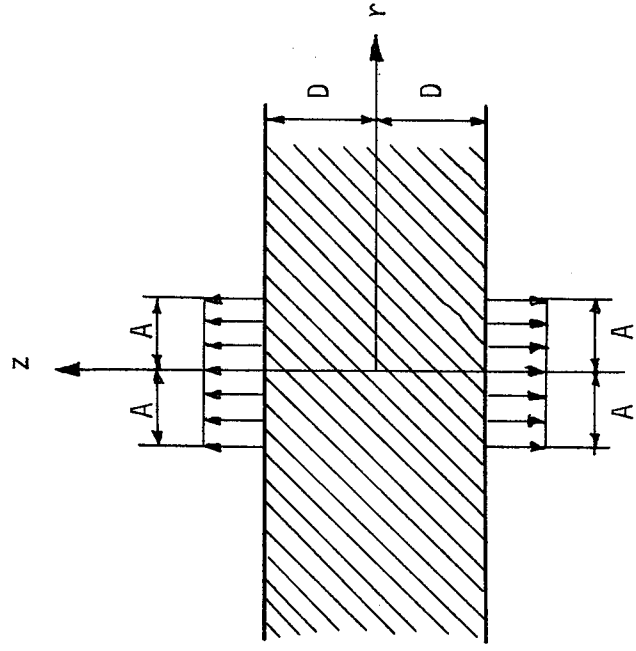


FIG. 3(b)

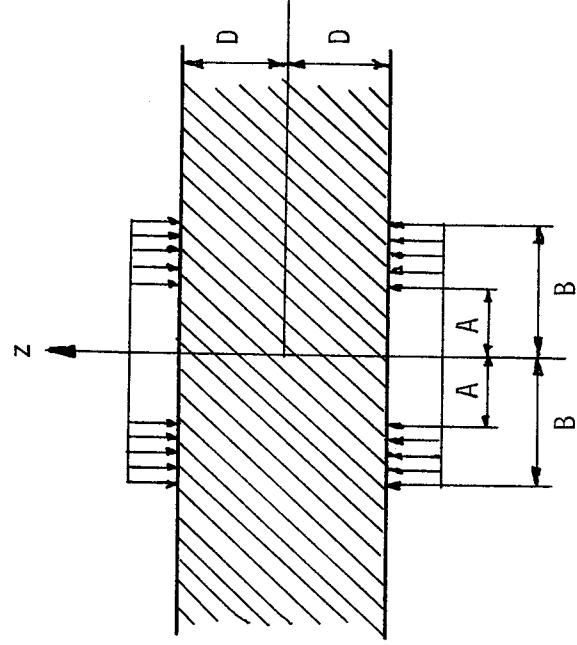


FIG. 3(c)

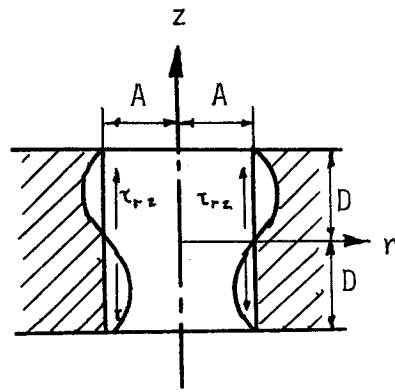


FIG. 3(d)

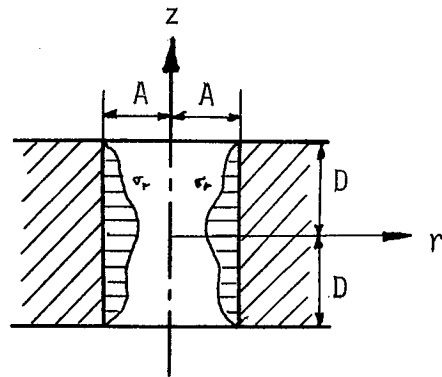


FIG. 3(e)

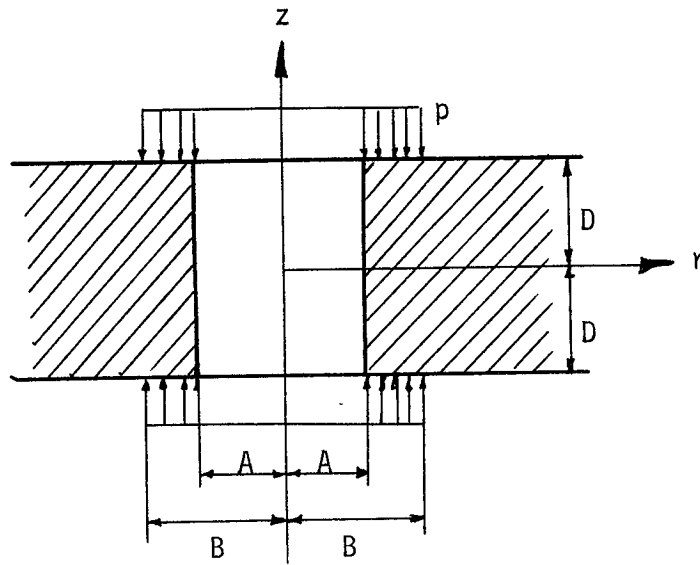
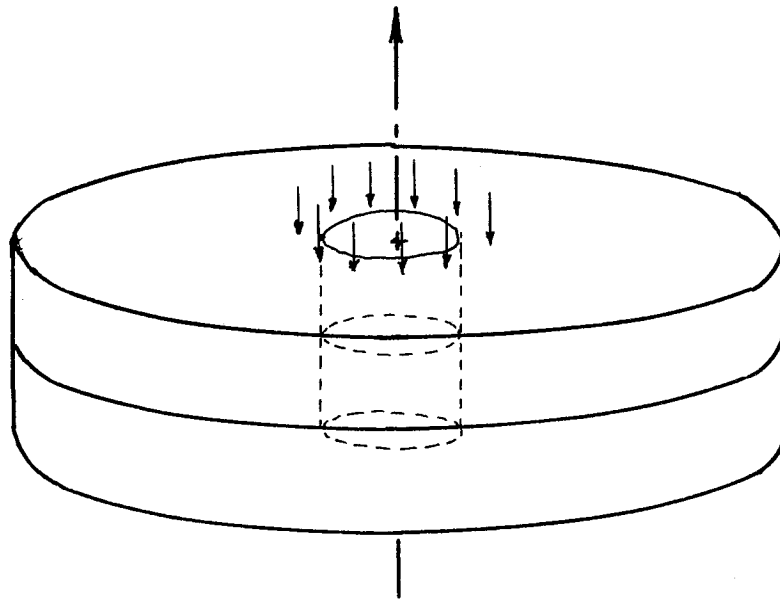


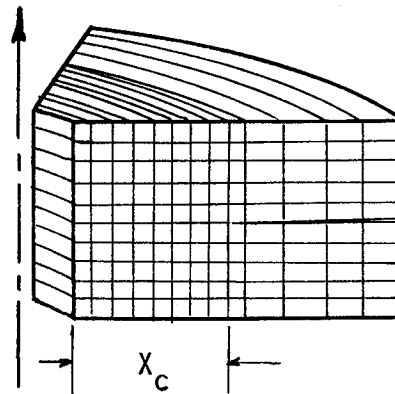
FIG. 3(f)

FIG. 3. FERNLUND'S SEQUENCE OF SUPERPOSITION



(a) Actual Plates

(b) Finite Element
Idealization



(c) Single Annular Ring
Element

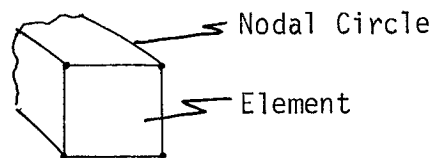
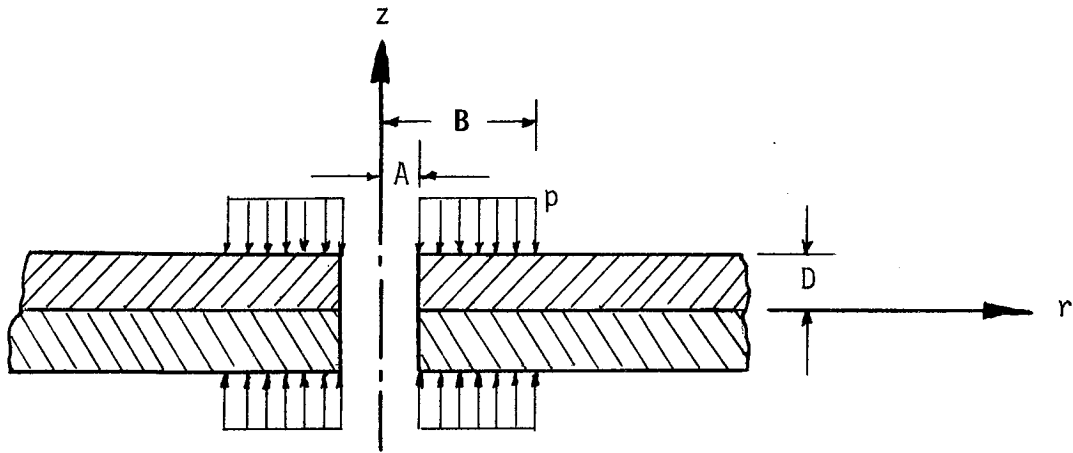
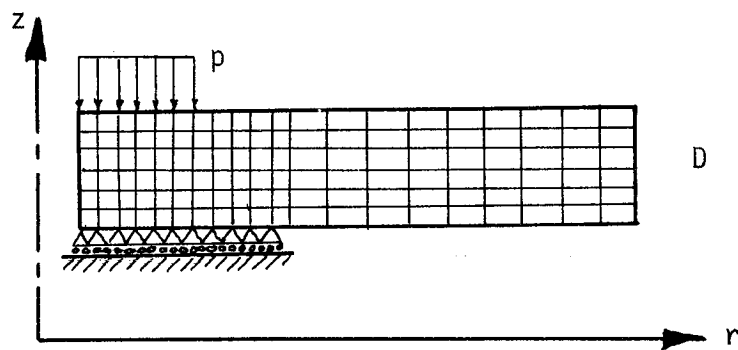


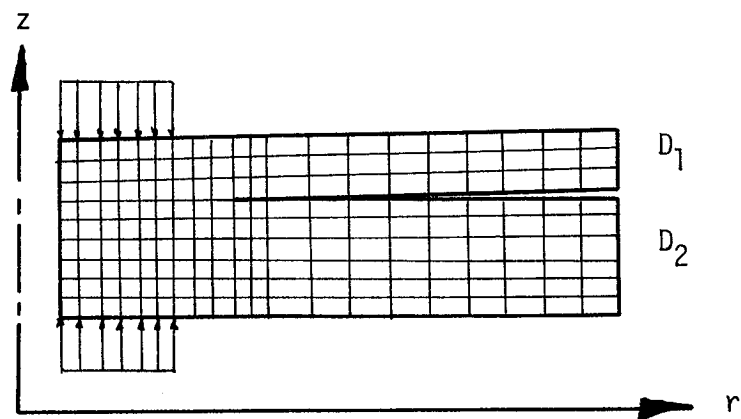
FIG. 4. FINITE ELEMENT IDEALIZATION OF TWO PLATES IN CONTACT



(a) Plates of Equal Thickness Under Load

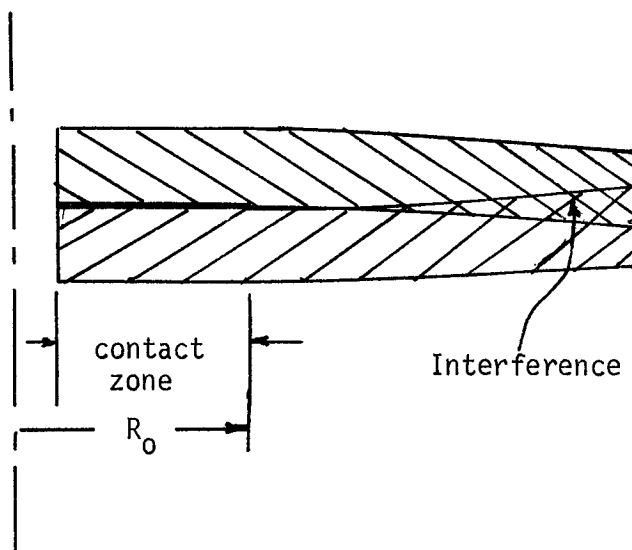


(b) Finite Element Model for Plates of Equal Thickness

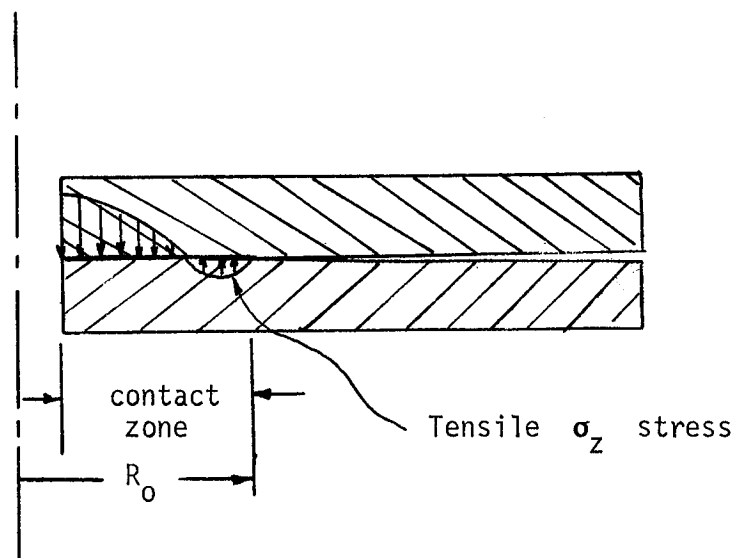


(c) Finite Element Model for Plates of Unequal Thickness

FIG. 5. FINITE ELEMENT MODELS



(a) Plates Intersect, R_0 too small



(b) Contact Zone Sustains Tension, R_0 too large

FIG. 6. EXAMPLES OF UNACCEPTABLE SOLUTIONS

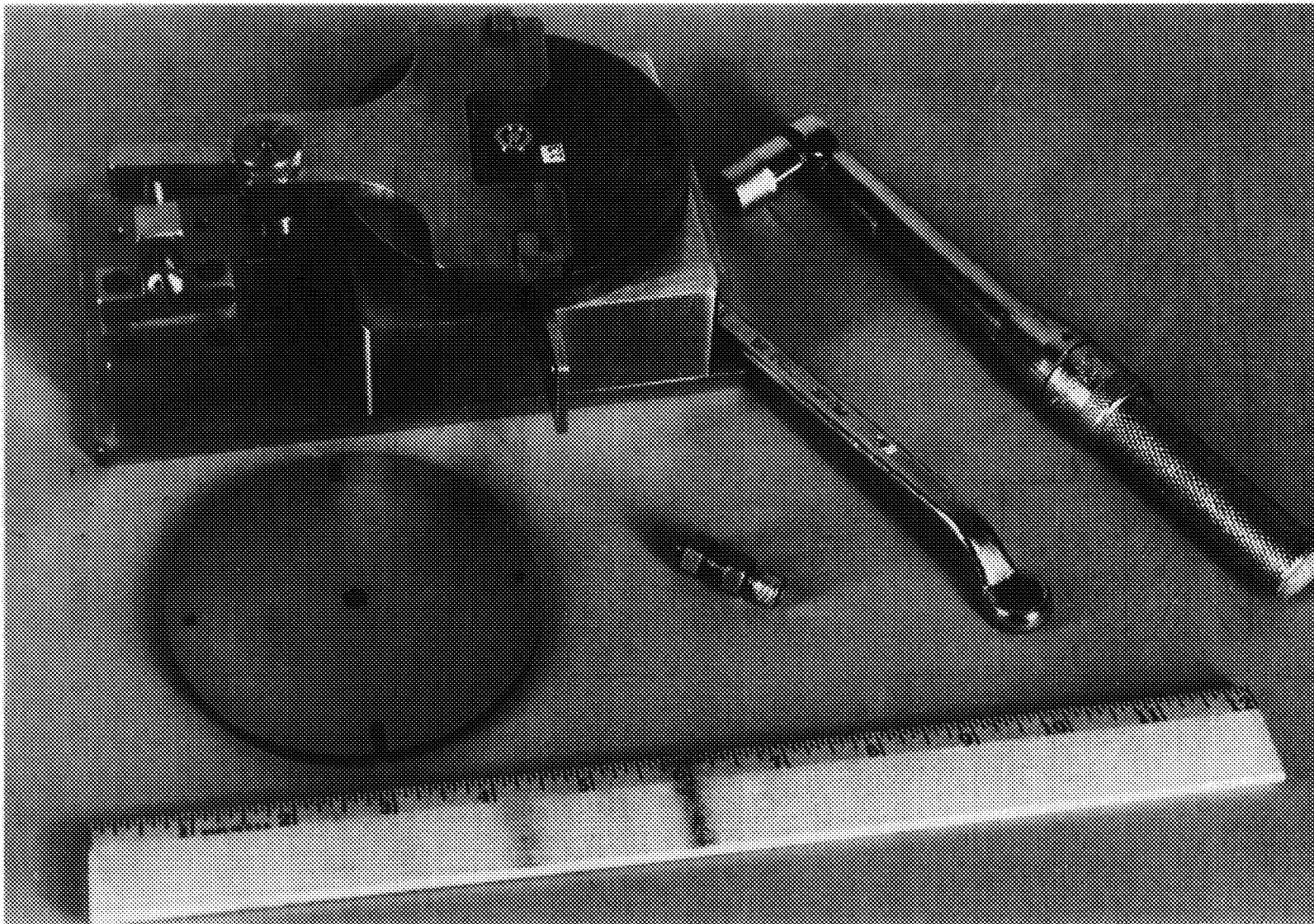


FIG. 7. PLATE SPECIMEN, BOLT AND NUTS, FIXTURE AND TOOLS.

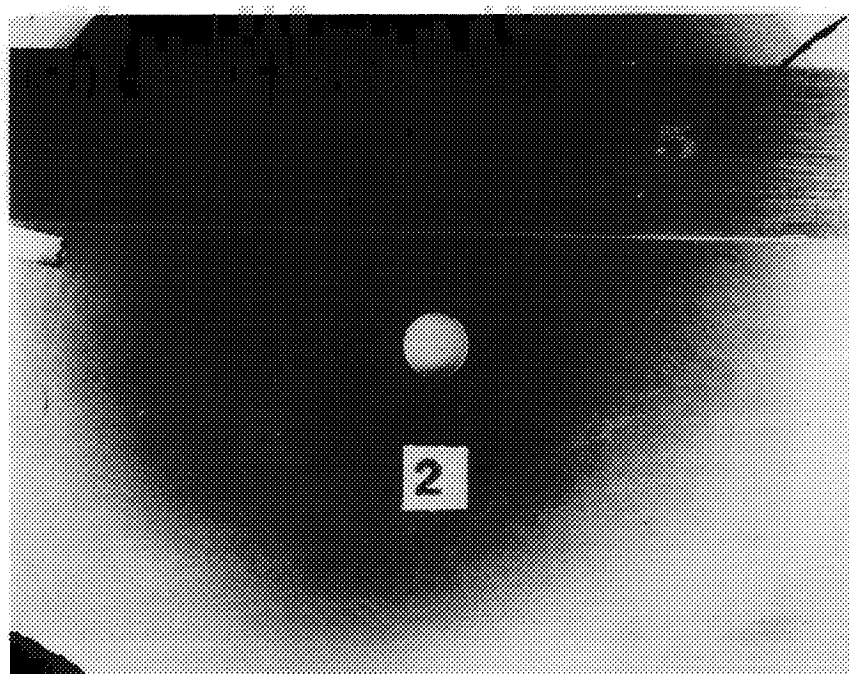
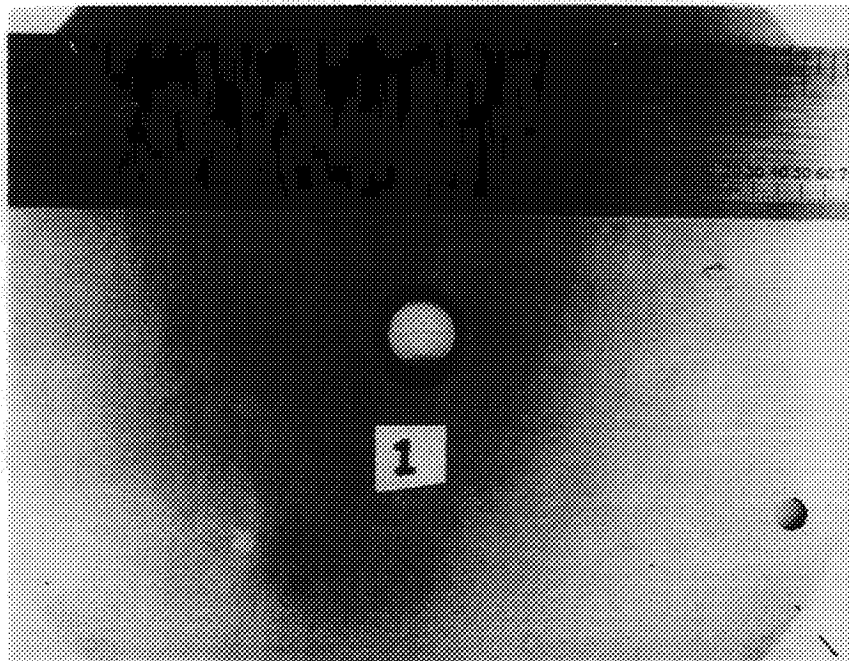


FIG. 8(a). FOOTPRINTS ON MATED PAIR OF 1/16 INCH PLATES.

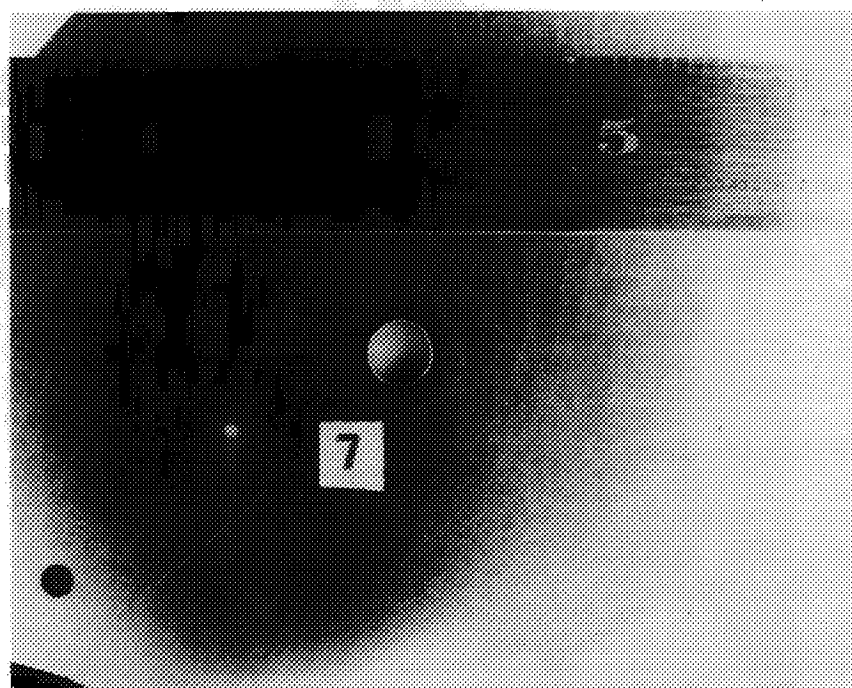
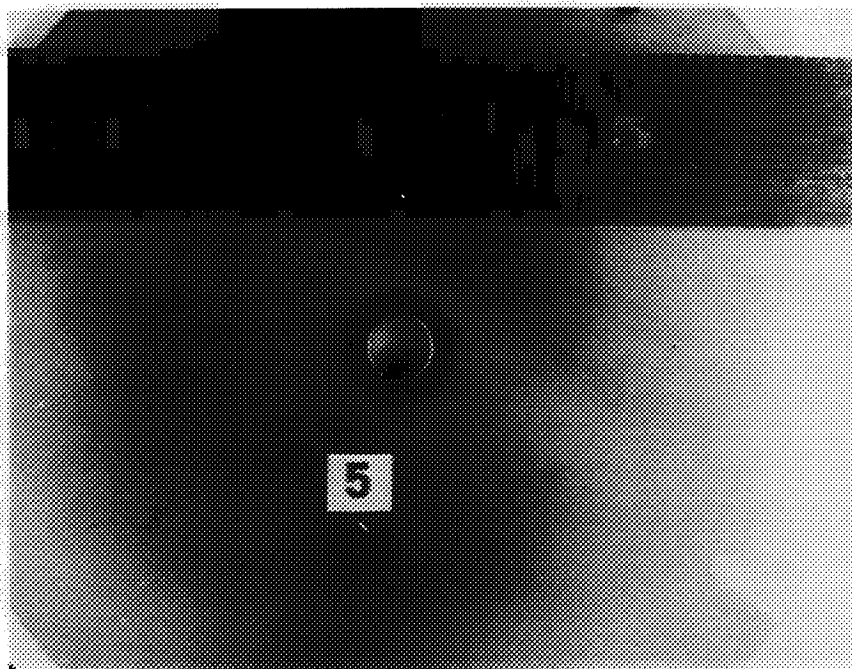


FIG. 8(b). FOOTPRINTS ON MATED PAIR OF 1/8 INCH PLATES.

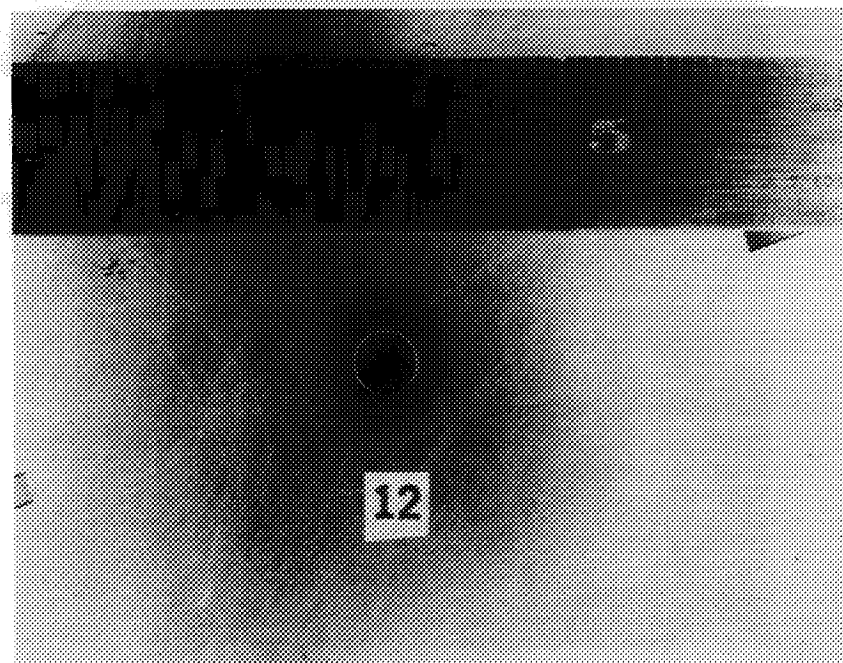
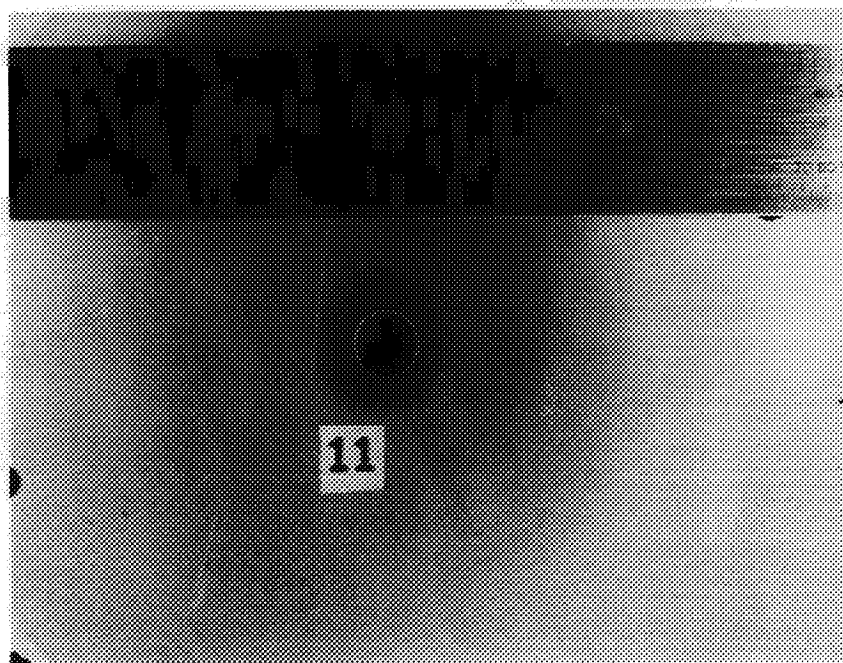


FIG. 8(c). FOOTPRINTS ON MATED PAIR OF 3/16 INCH PLATES.

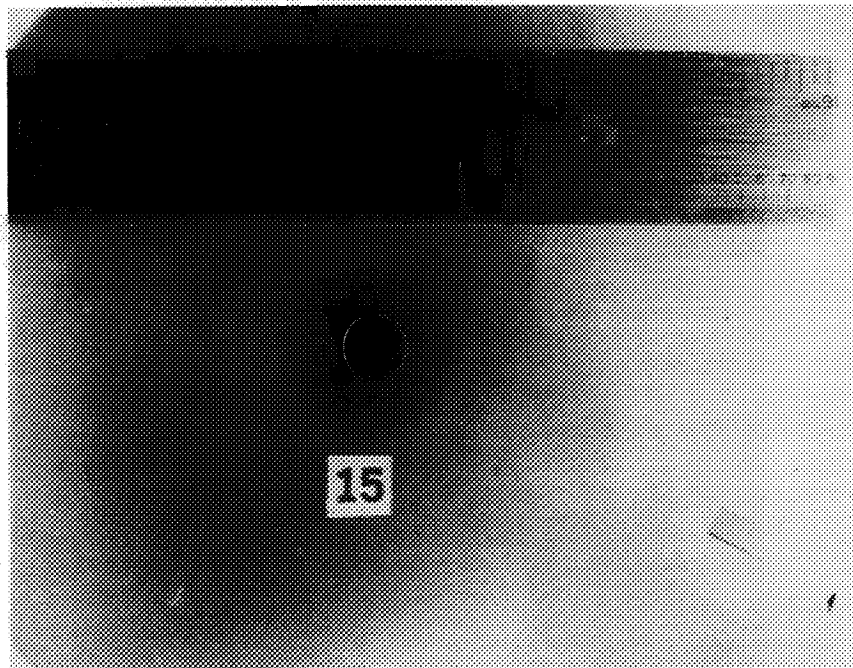
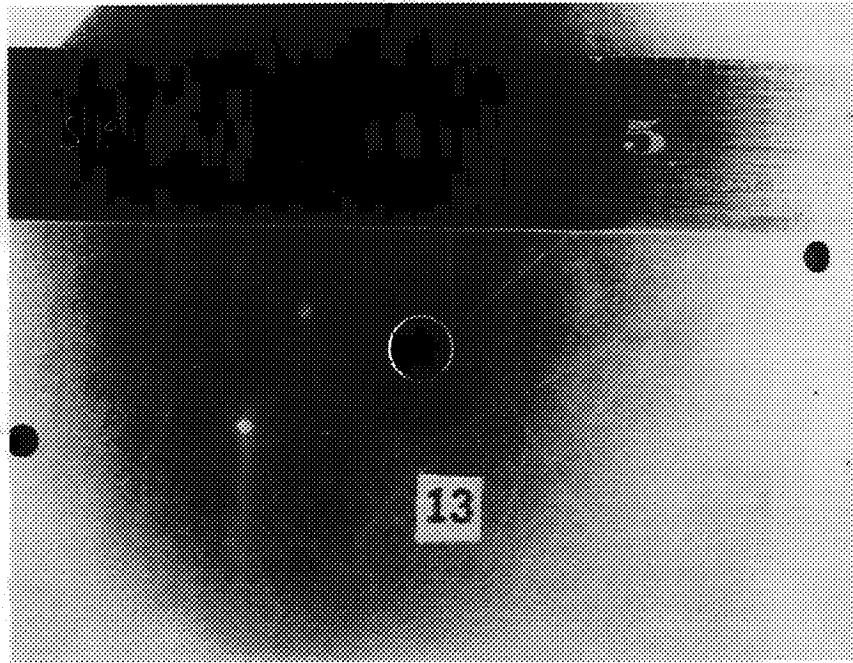


FIG. 8(d). FOOTPRINTS ON MATED PAIR OF 1/4 INCH PLATES.

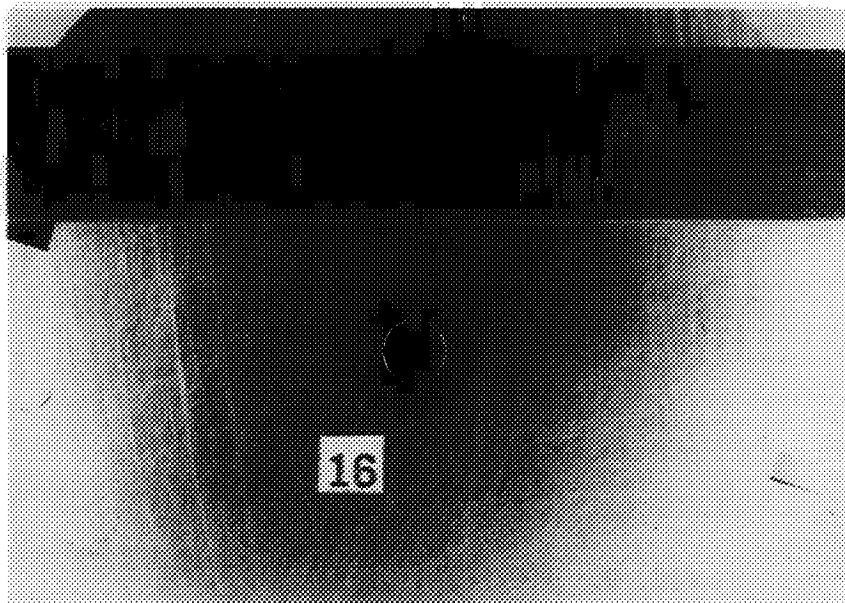
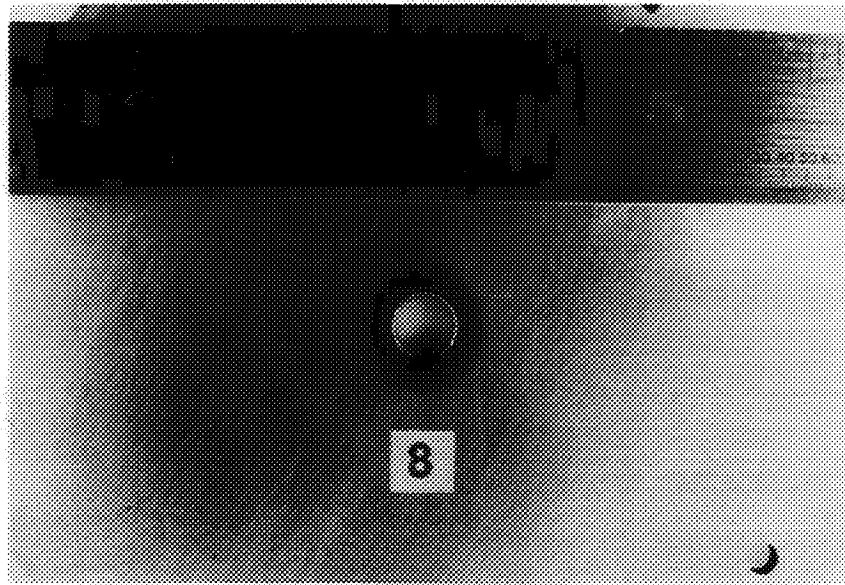


FIG. 8(e). FOOTPRINTS ON MATED PAIR OF $1/8$ AND $1/4$ INCH PLATES.

FIG. 8. FOOTPRINTS ON THE MATING SURFACES OF $1/16 - 1/16$,
 $1/8 - 1/8$, $3/16 - 3/16$, $1/4 - 1/4$, and $1/8 - 1/4$
PAIRS. (A = .128, B = .21)



FIG. 9. FOOTPRINT OF NUT ON PLATE.

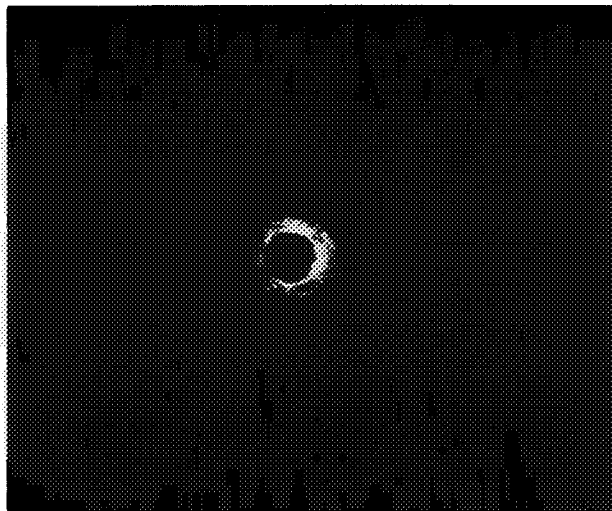


FIG. 10 (a). 1/16 INCH
PAIR

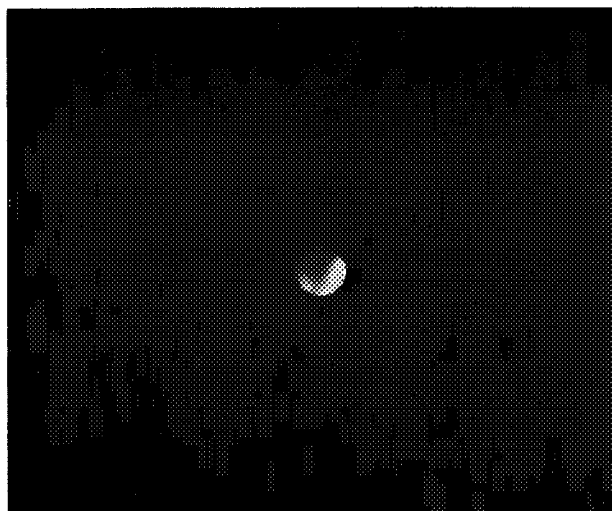


FIG. 10(b). 1/8 INCH
PAIR



FIG. 10(c). 3/16 INCH
PAIR

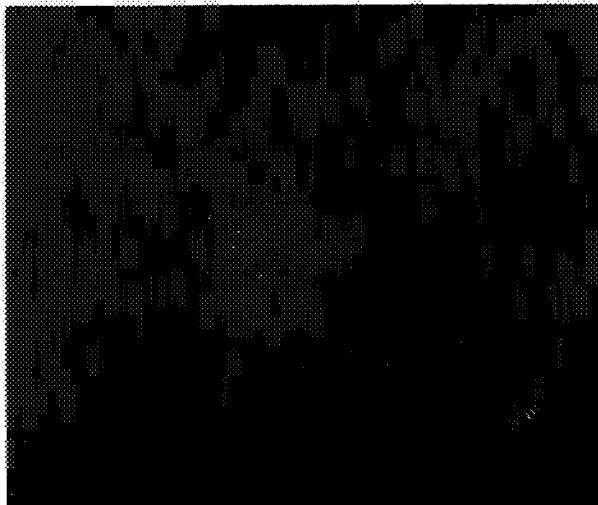


FIG. 10(d). 1/4 INCH
PAIR

FIG. 10. X-RAY PHOTOGRAPHS OF CONTAMINATION TRANSFERRED
FROM RADIOACTIVE PLATE TO MATED PLATE. 1/16, 1/4,
3/16, 1/4 INCH PAIRS. (A = .128 in., B = .21 in.)

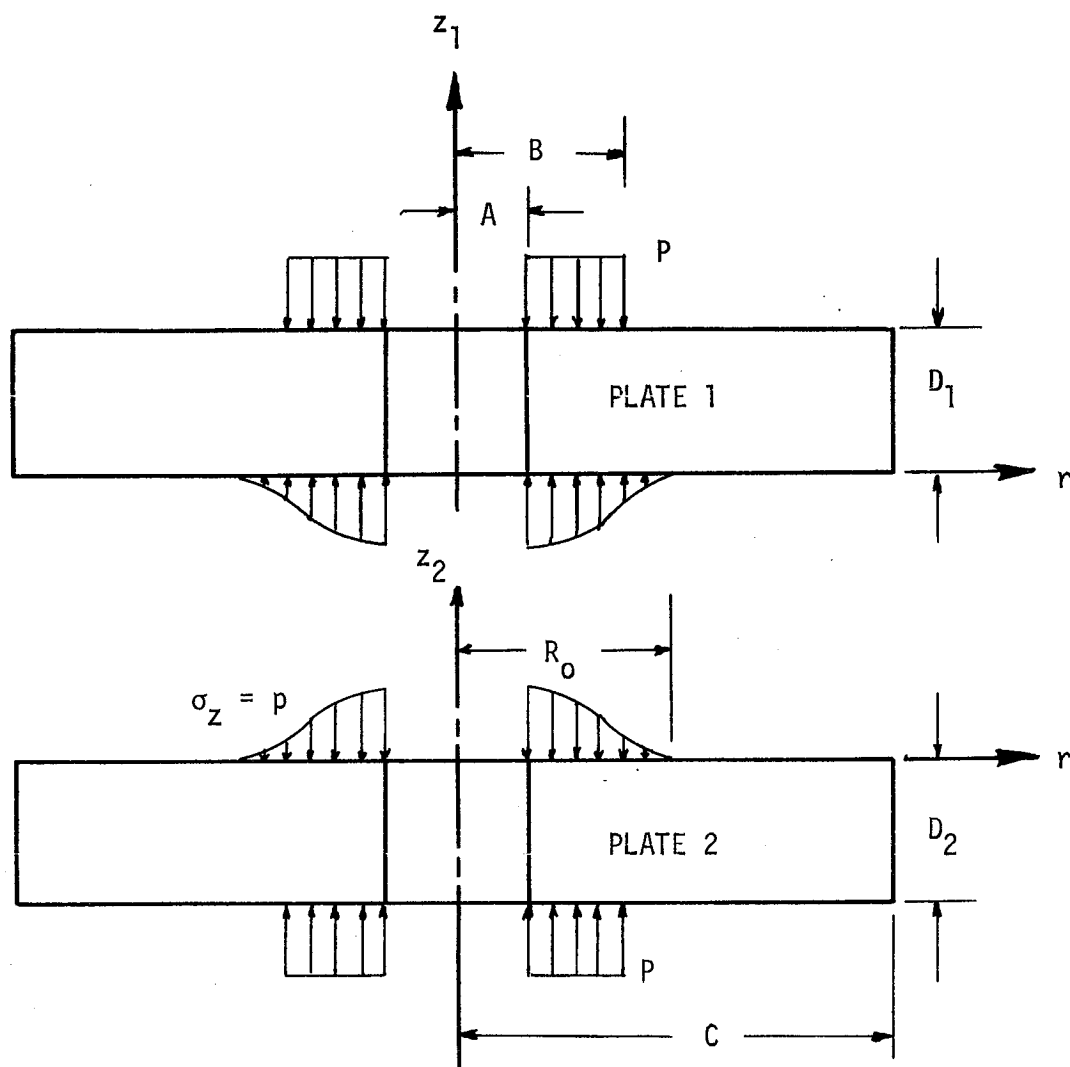


FIG. 11. FREE BODY DIAGRAM FOR TWO PLATES IN CONTACT.

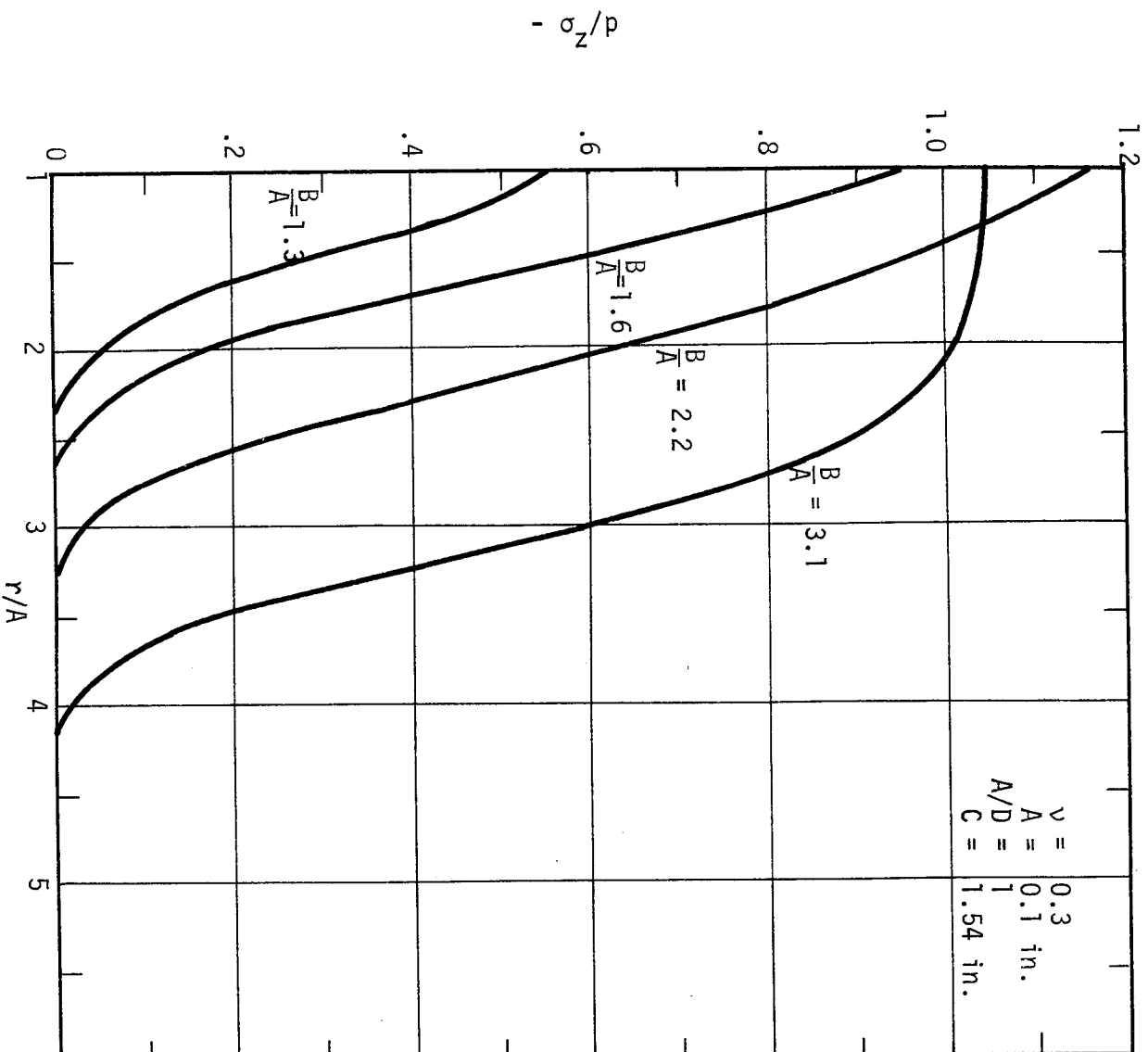


FIG. 12. SINGLE PLATE ANALYSIS-MIDPLANE σ_z STRESS DISTRIBUTION ($D = 0.1$ in.)

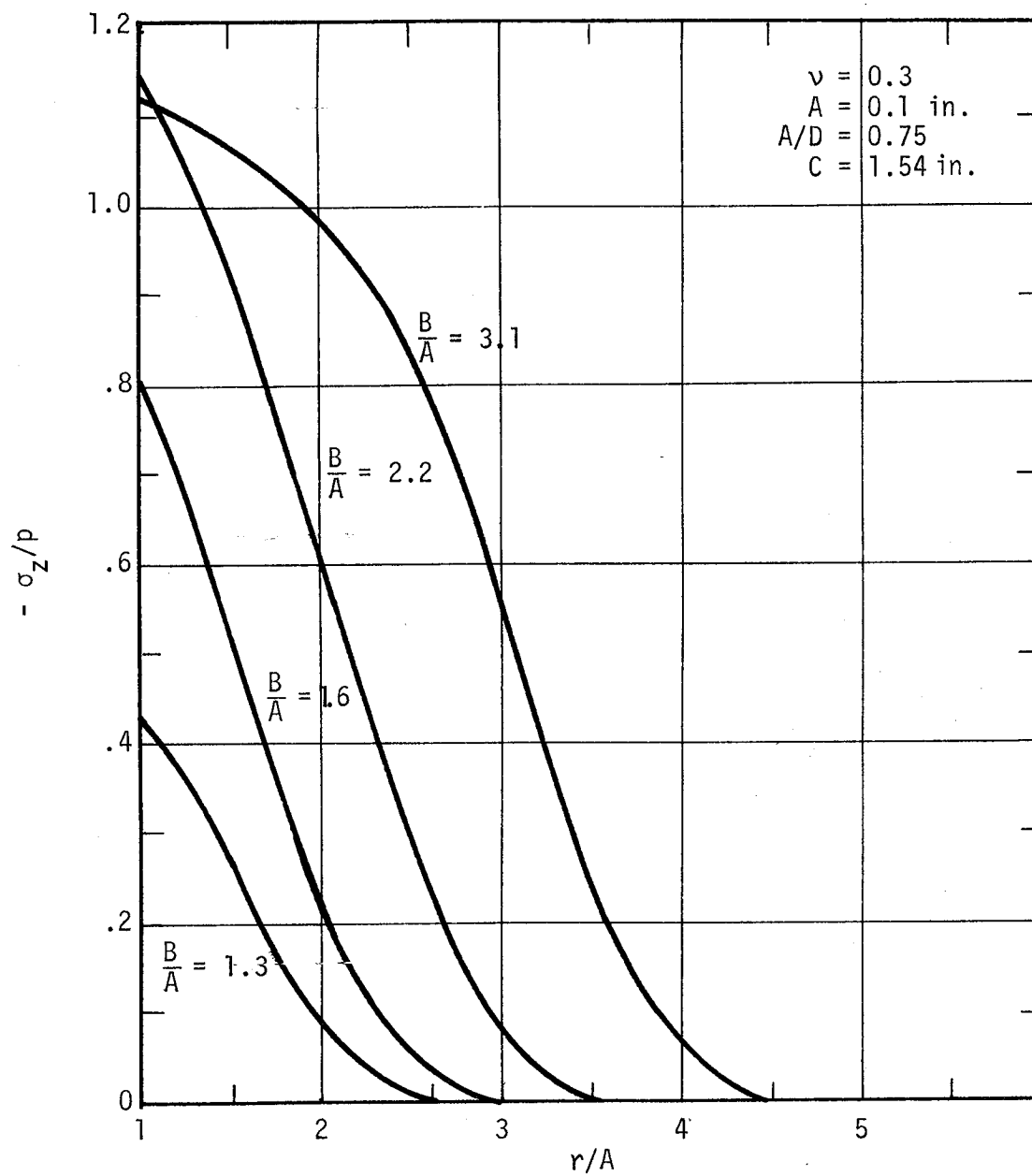


FIG. 13. SINGLE PLATE ANALYSIS-MIDPLANE σ_z STRESS
DISTRIBUTION ($D = 0.133$ in.)

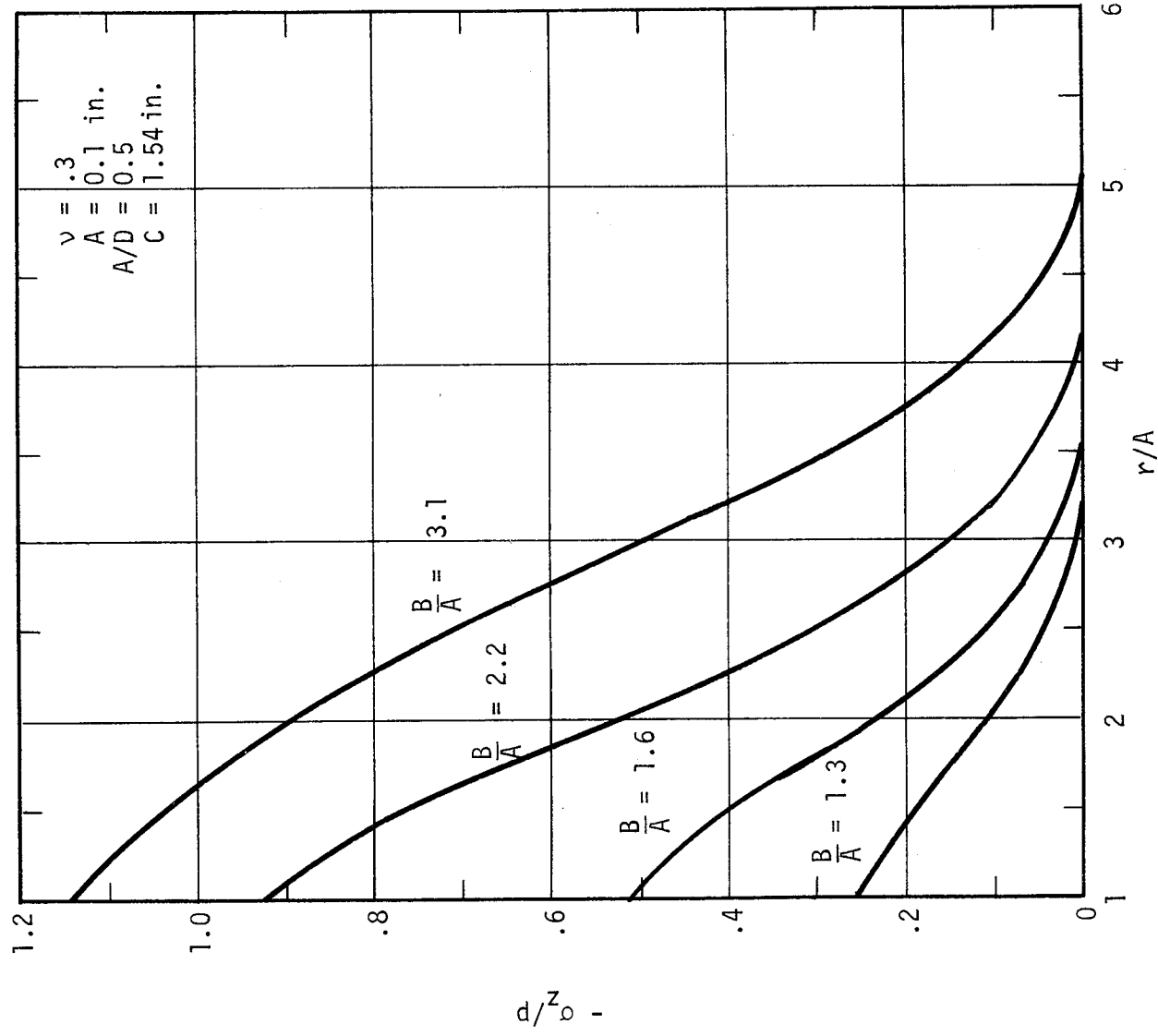


FIG. 14. SINGLE PLATE ANALYSIS-MIDPLANE σ_z STRESS DISTRIBUTION ($D = 0.2$ in.)

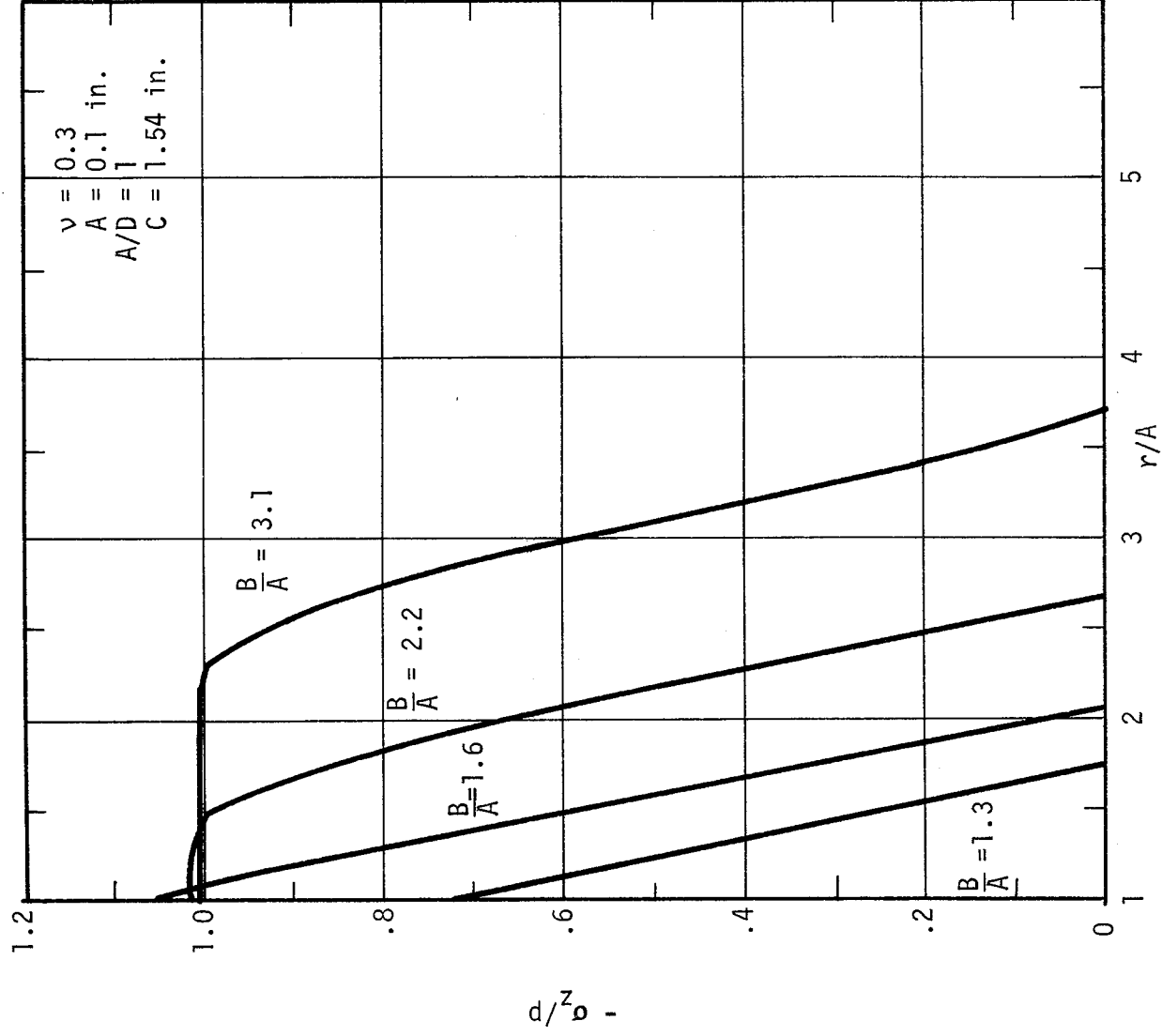


FIG. 15. INTERFACE PRESSURE DISTRIBUTION IN A BOLTED JOINT

($D = 0.1 \text{ in.}$)

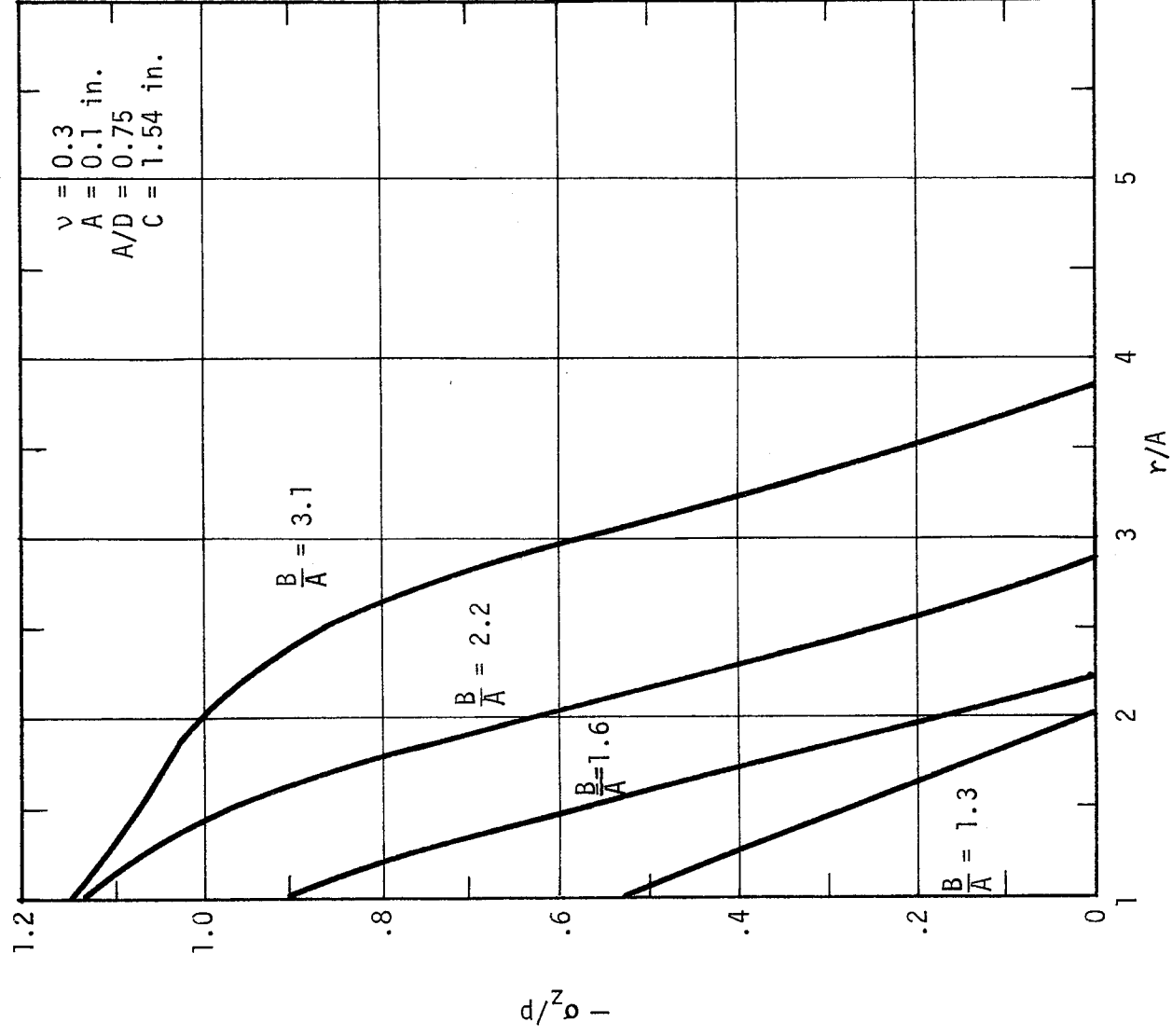


FIG. 16. INTERFACE PRESSURE DISTRIBUTION IN A BOLTED JOINT
($D = .133$ in.)

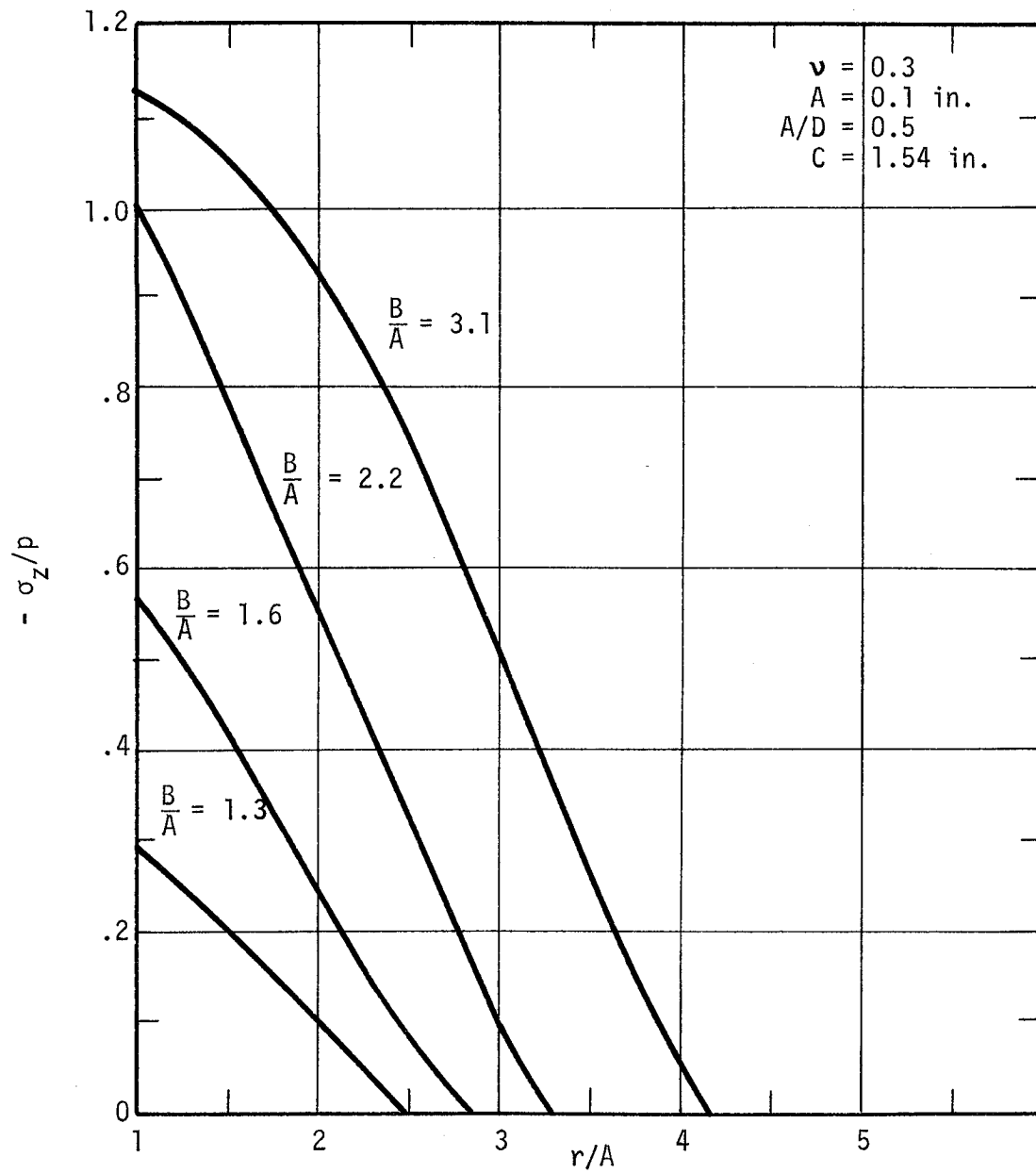


FIG. 17. INTERFACE PRESSURE DISTRIBUTION IN A BOLTED JOINT
($D = 0.2 \text{ in.}$)

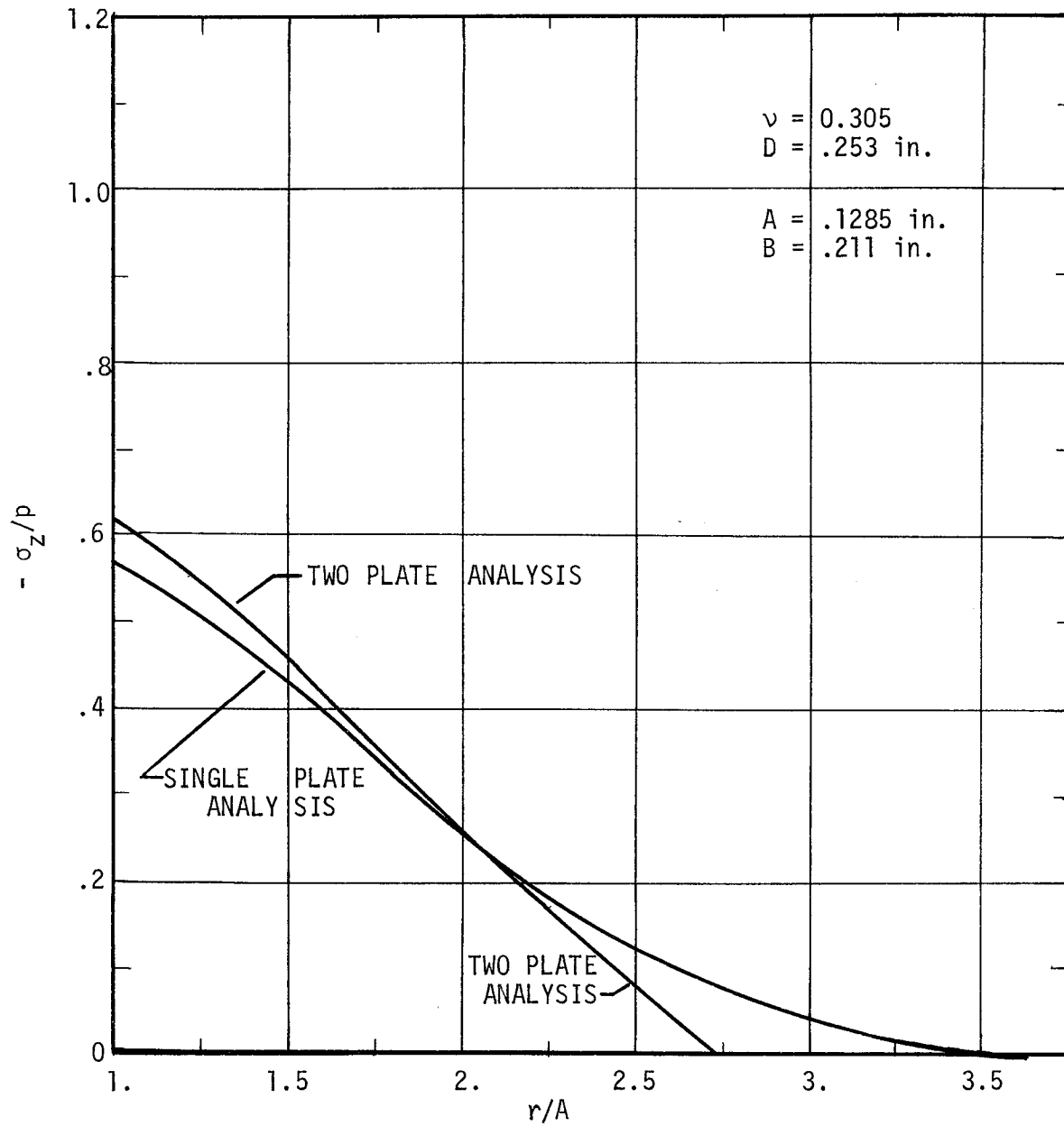


FIG. 18. FINITE ELEMENT ANALYSIS RESULTS FOR 1/4 INCH PLATE PAIR.

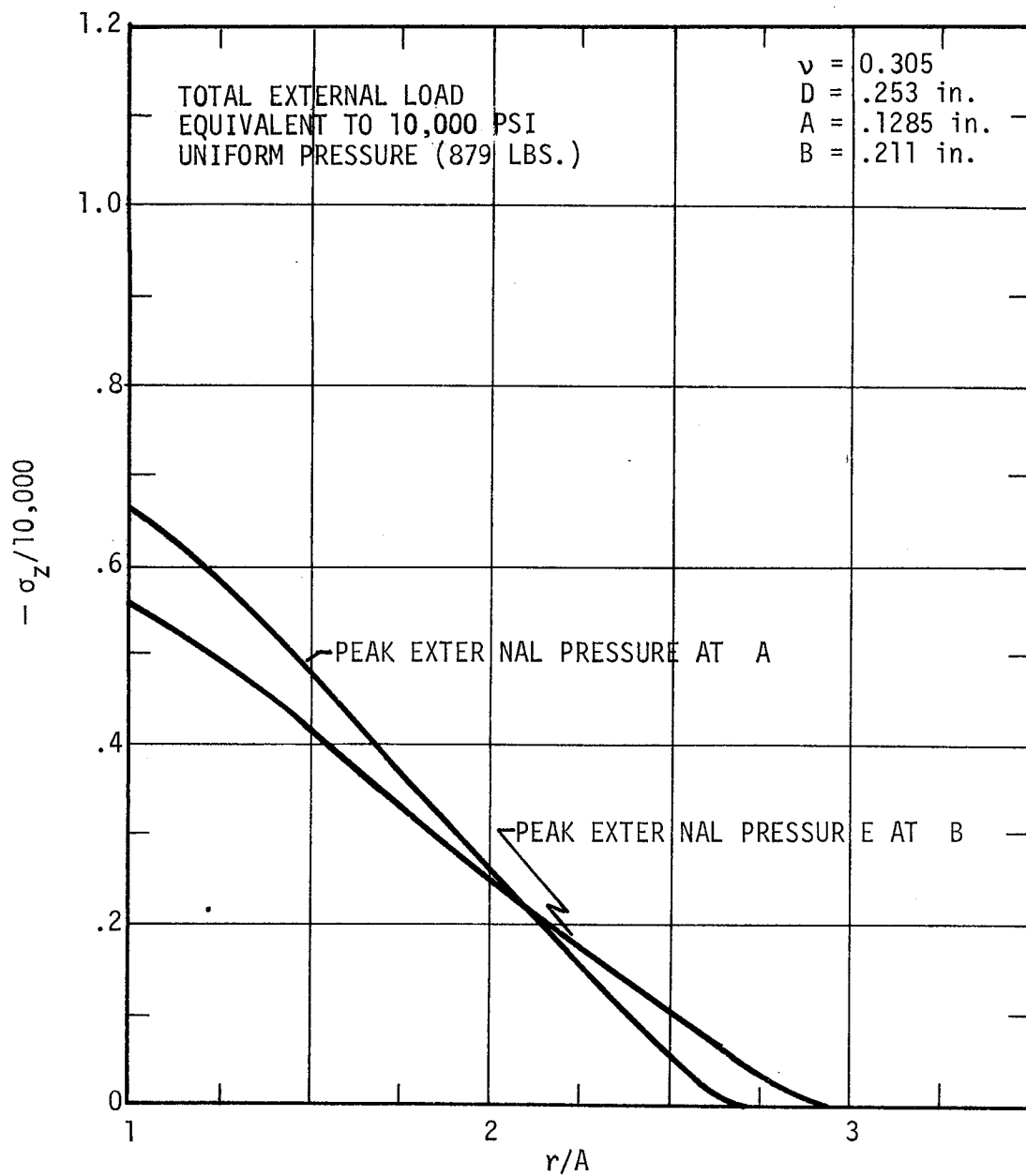


FIG. 19. PRESSURE IN JOINT, TRIANGULAR LOADING

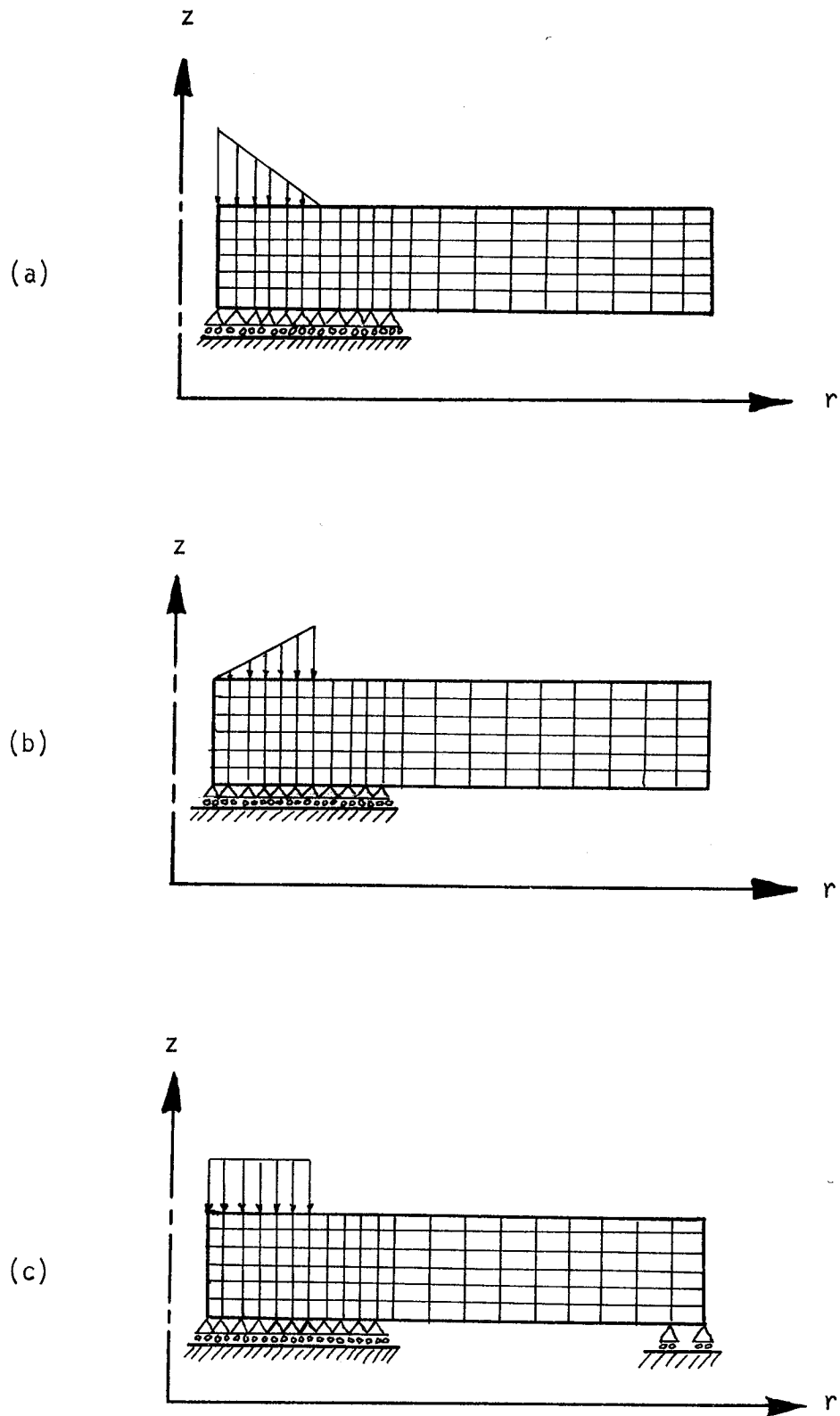


FIG. 20. VARIATIONS OF LOADING AND BOUNDARY CONDITIONS.

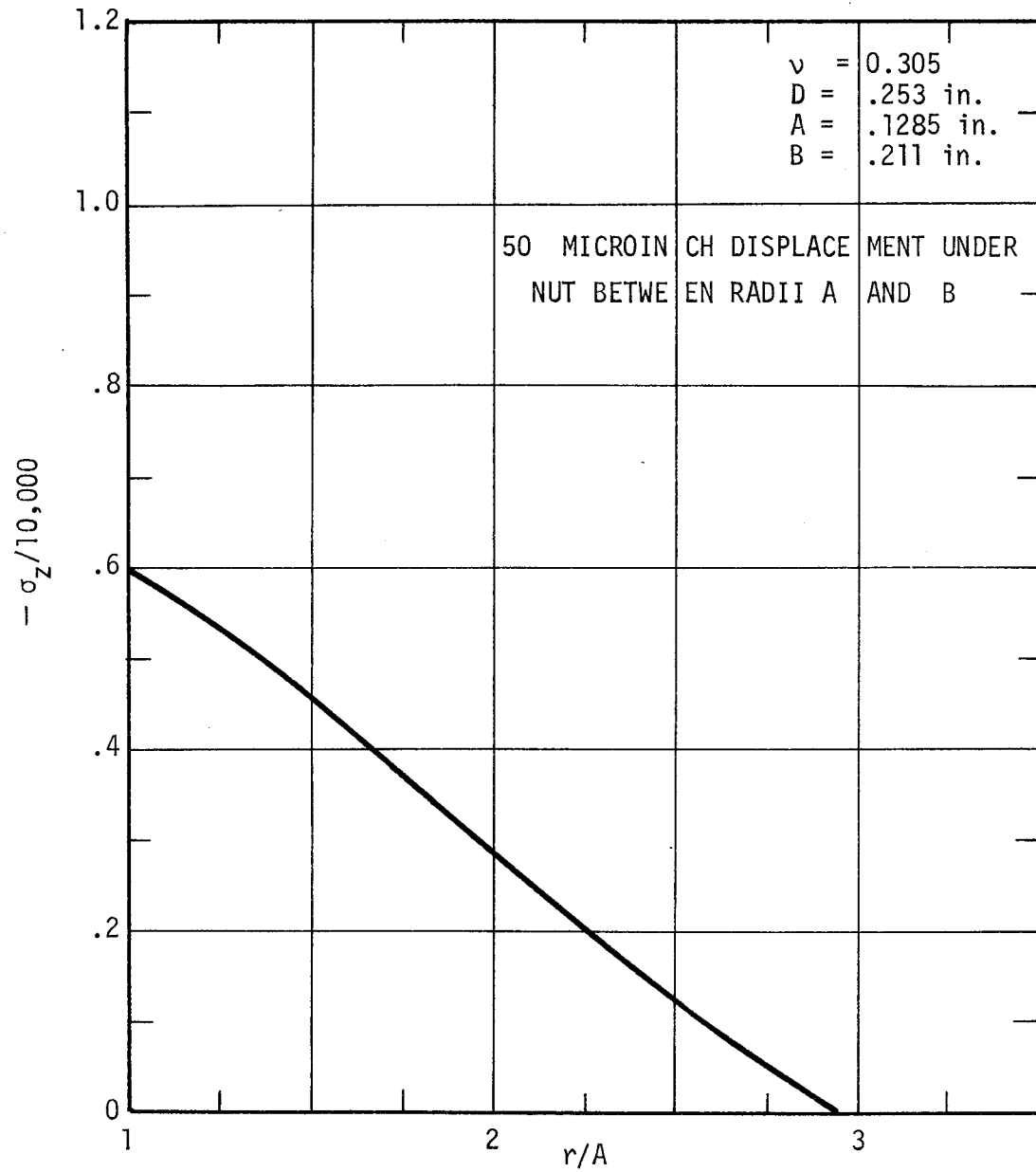


FIG. 21. PRESSURE IN JOINT, UNIFORM DISPLACEMENT UNDER NUT.

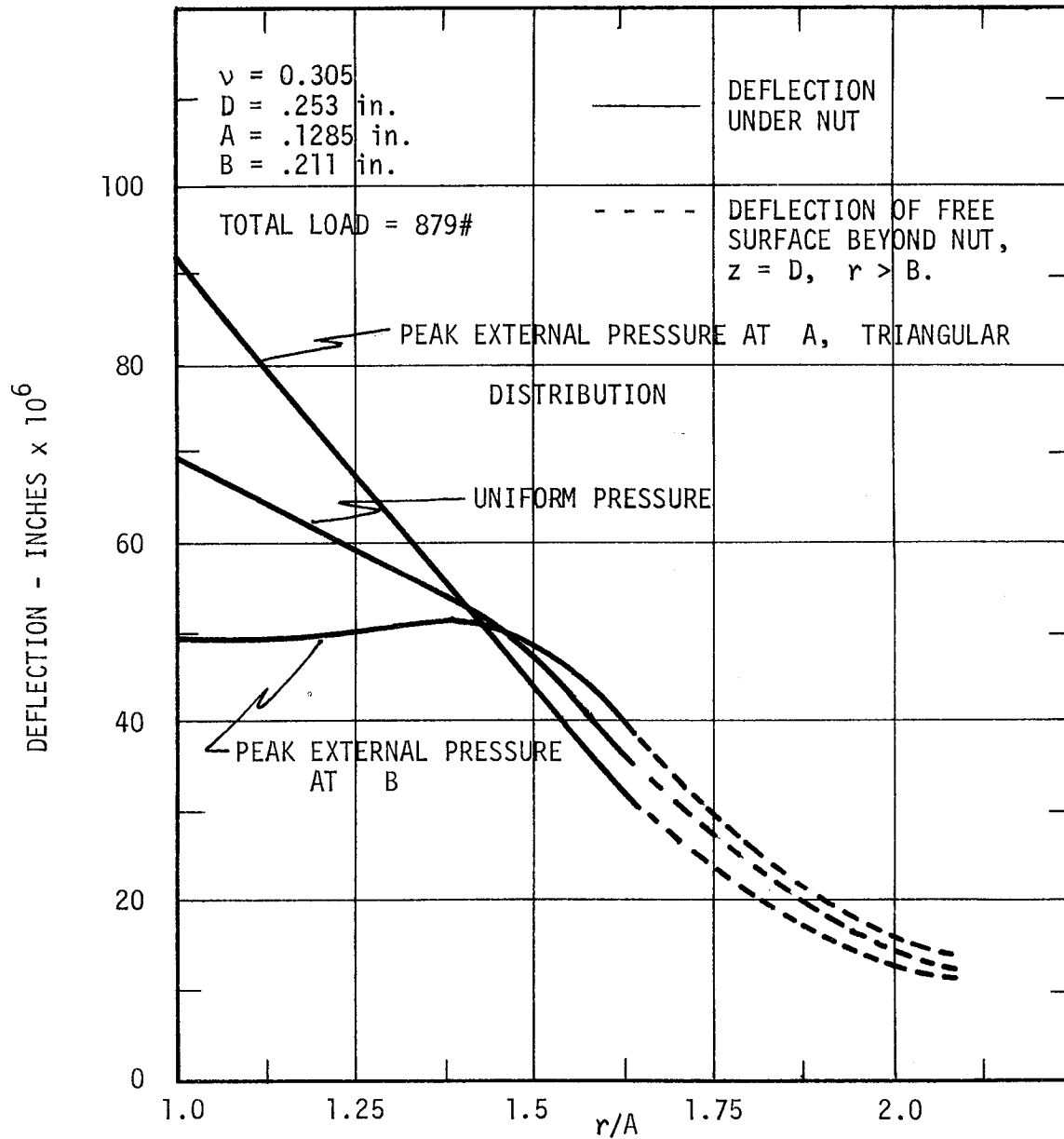


FIG. 22. DEFLECTION OF PLATE UNDER NUT.

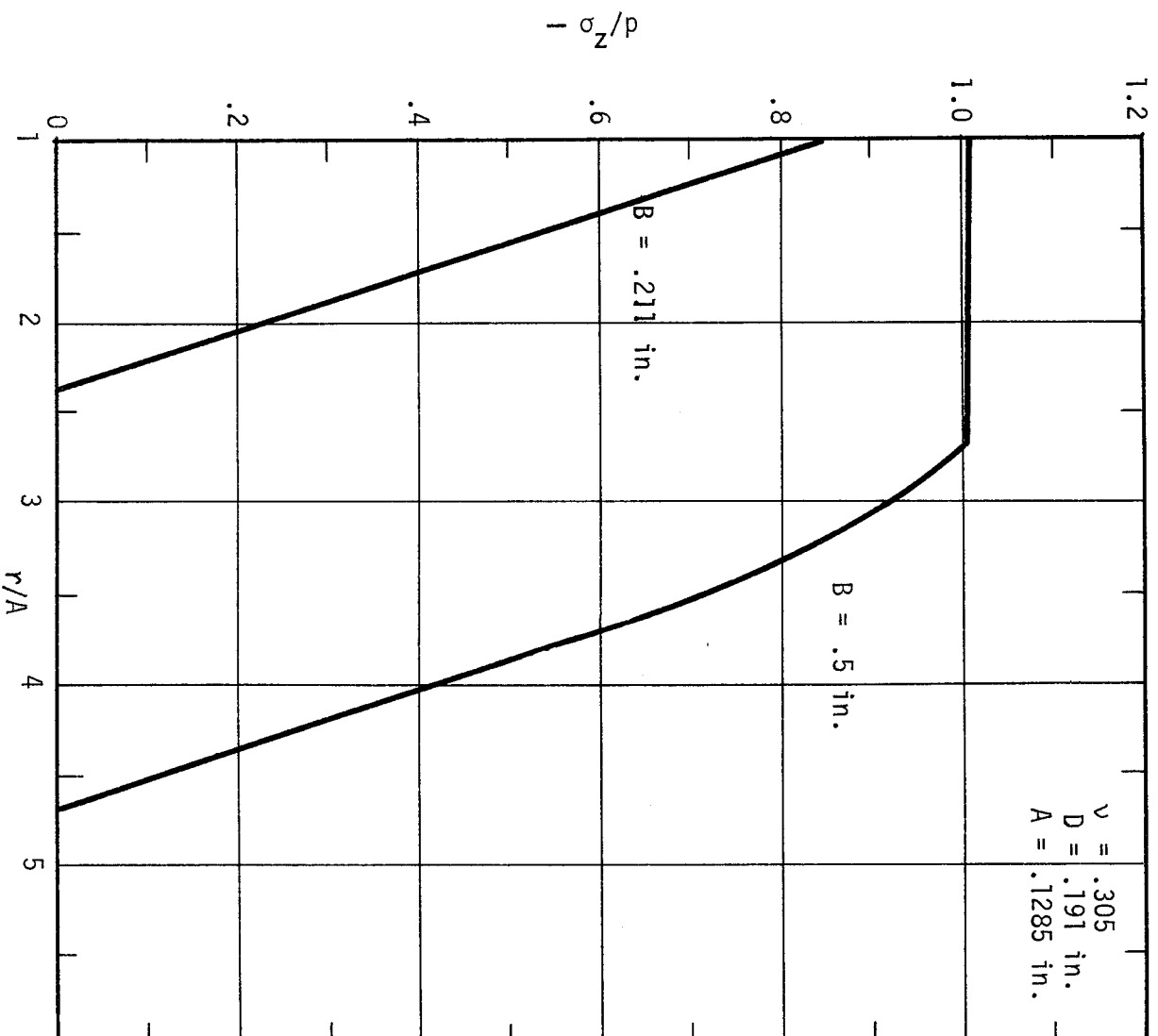


FIG. 23. FINITE ELEMENT ANALYSIS RESULTS FOR 3/16 INCH PLATE PAIR.

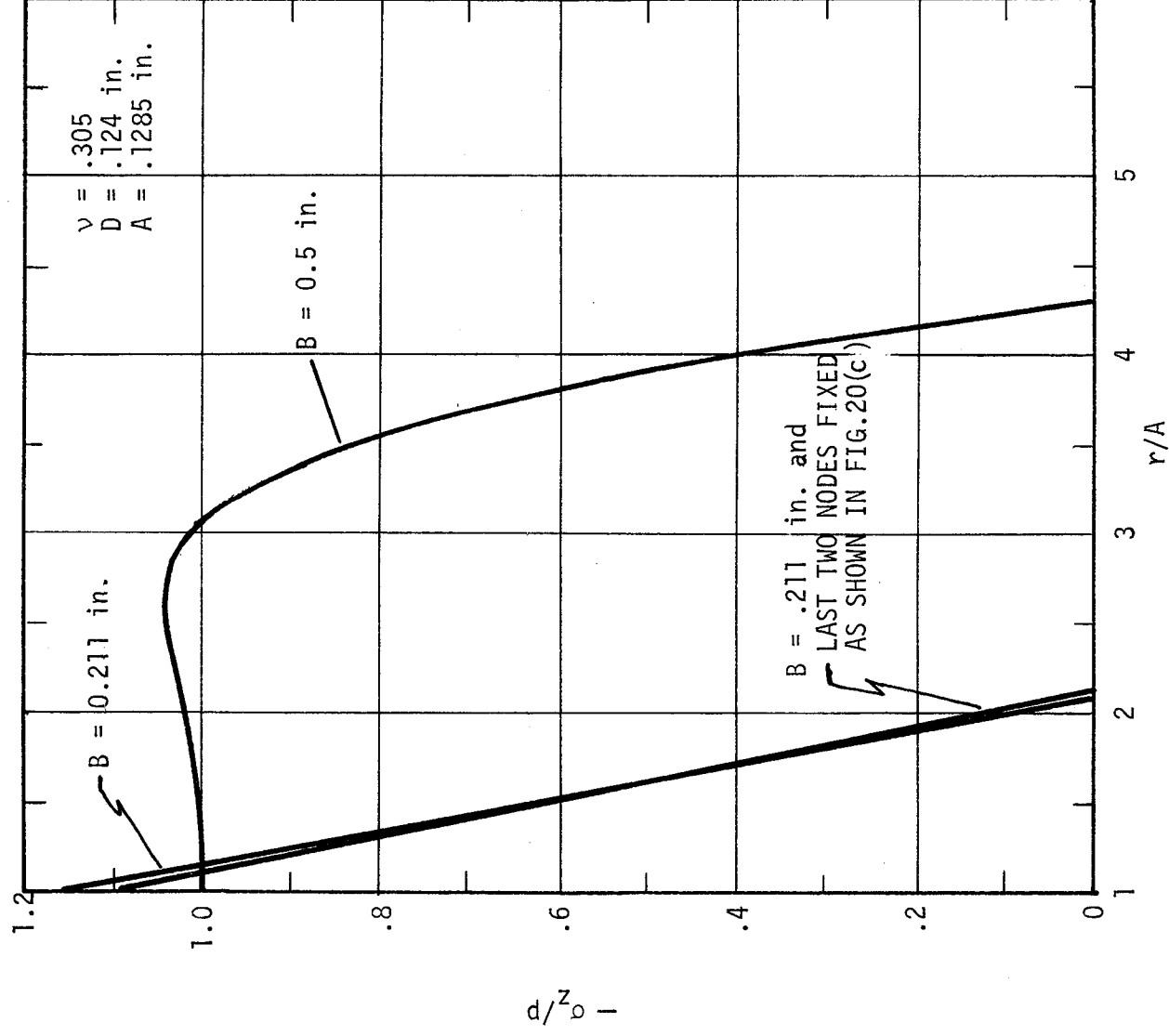


FIG. 24. FINITE ELEMENT ANALYSIS RESULTS FOR 1/8 INCH PLATE PAIR.

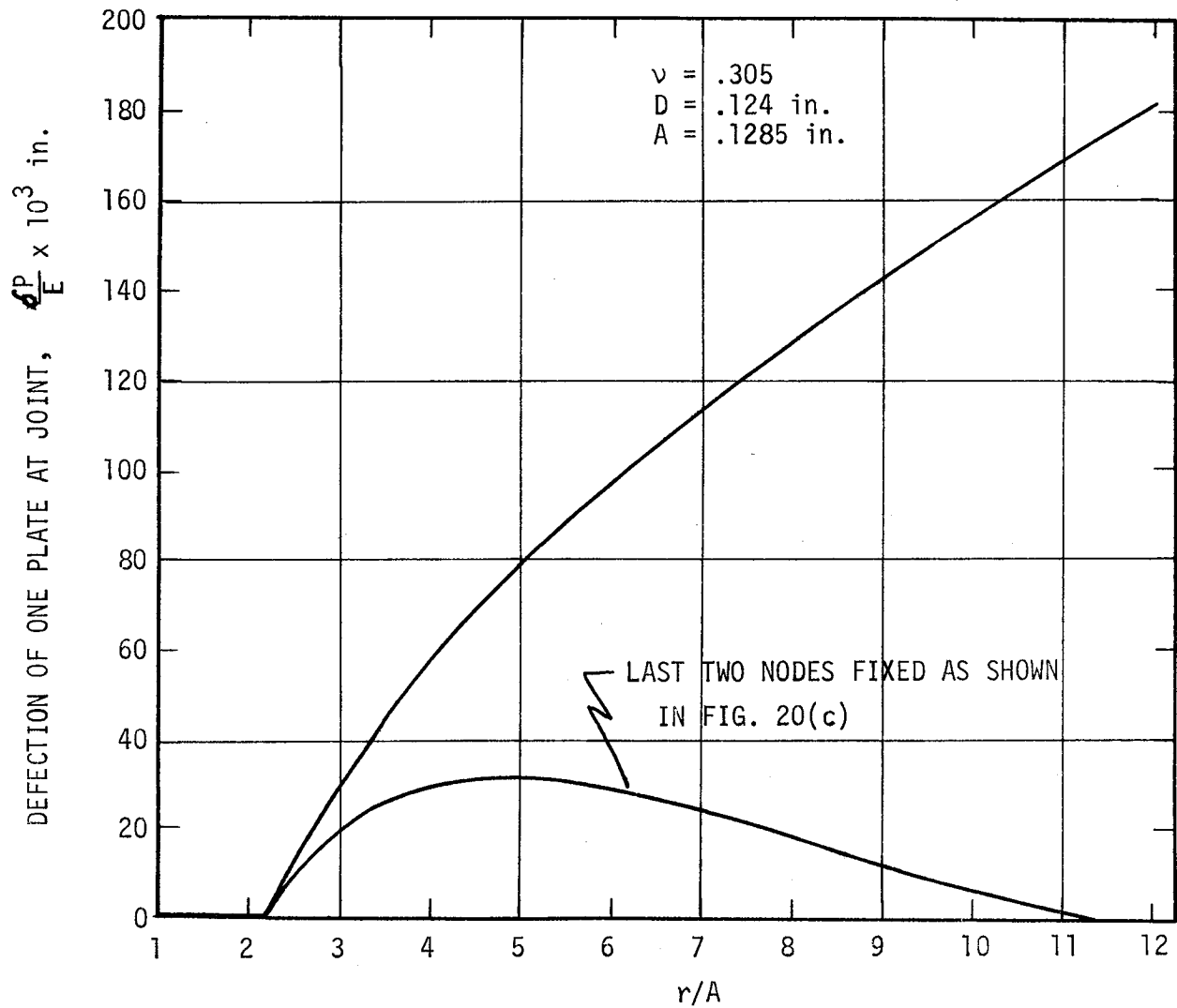


FIG. 25. GAP DEFORMATION FOR FREE AND FIXED EDGES — FINITE ELEMENT ANALYSIS, 1/8 INCH PLATE PAIR.

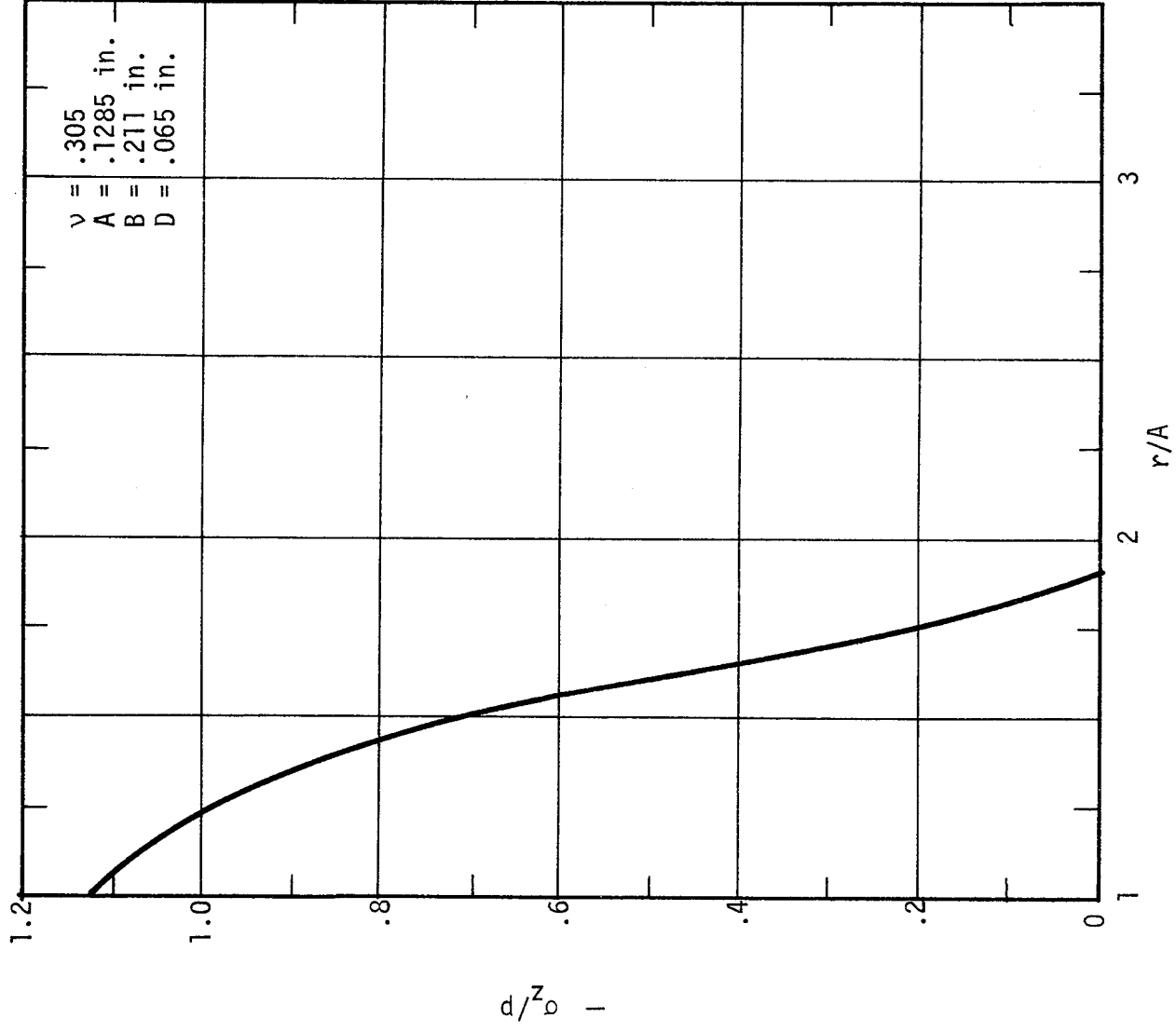


FIG. 26. FINITE ELEMENT ANALYSIS RESULT FOR 1/16 INCH PLATE PAIR.

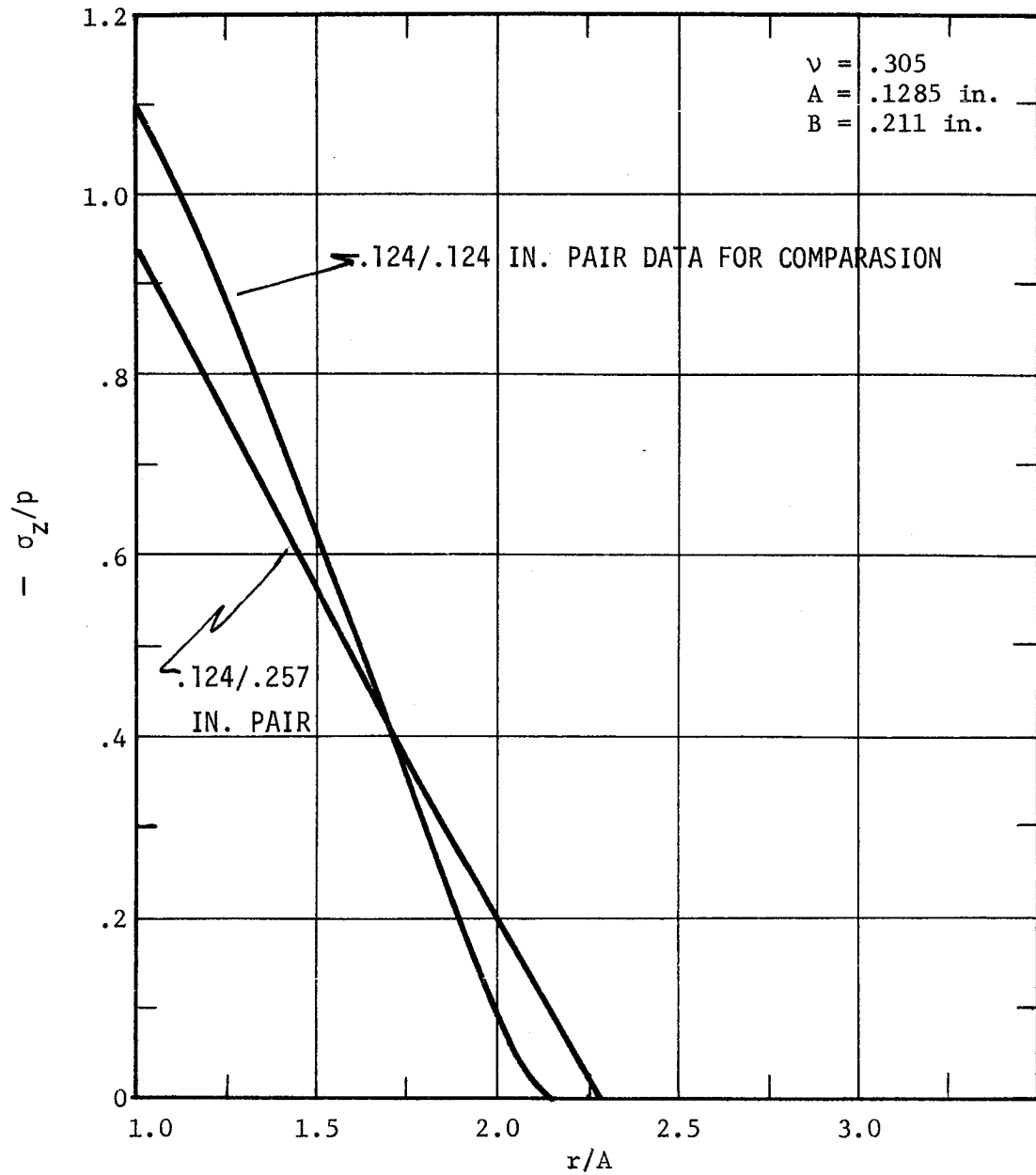


FIG. 27. FINITE ELEMENT ANALYSIS RESULTS FOR 1/8 INCH PLATE
MATED WITH 1/4 INCH PLATE.

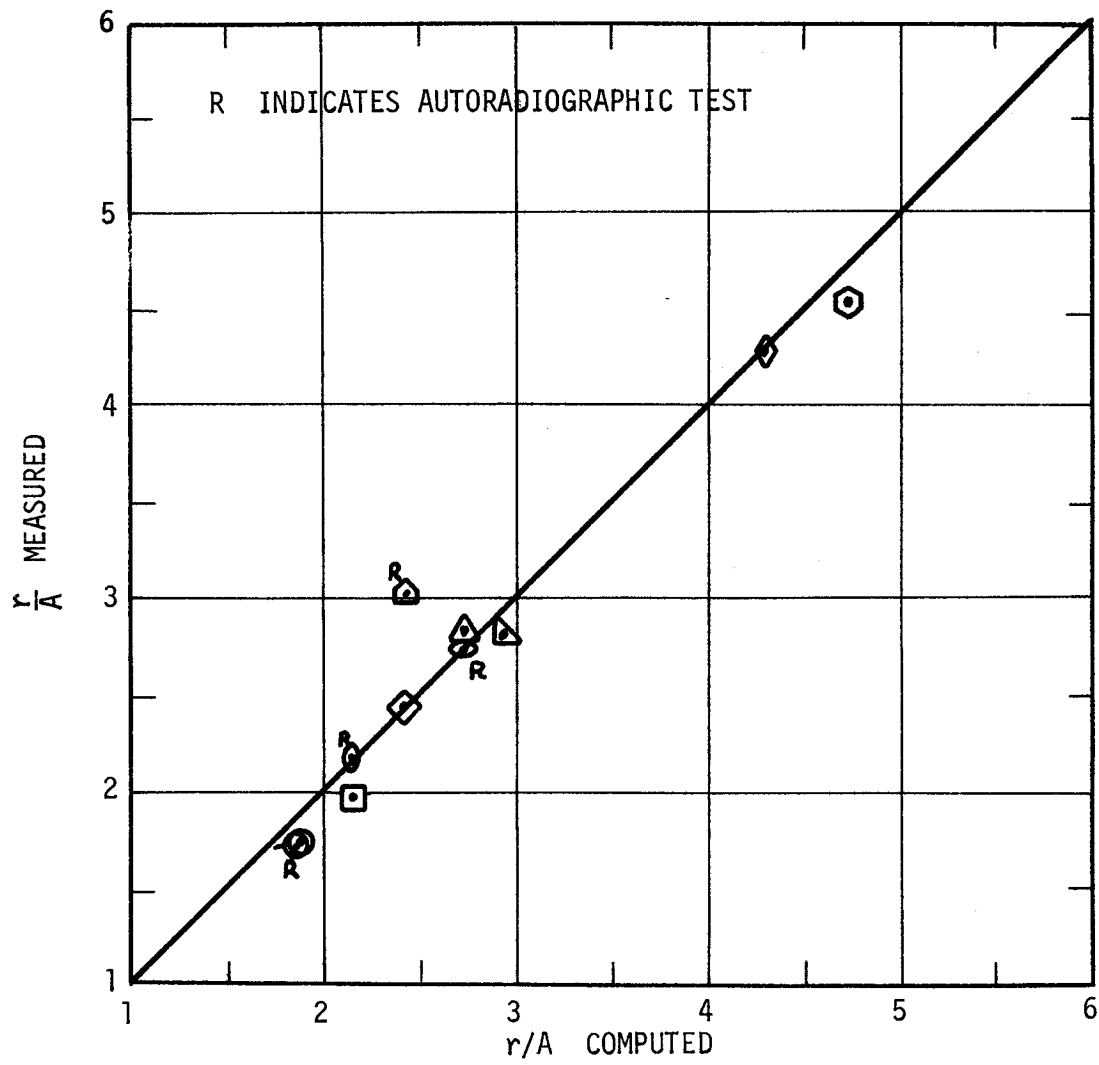


FIG. 28. COMPARISON BETWEEN TESTED AND MEASURED SEPARATION RADII.

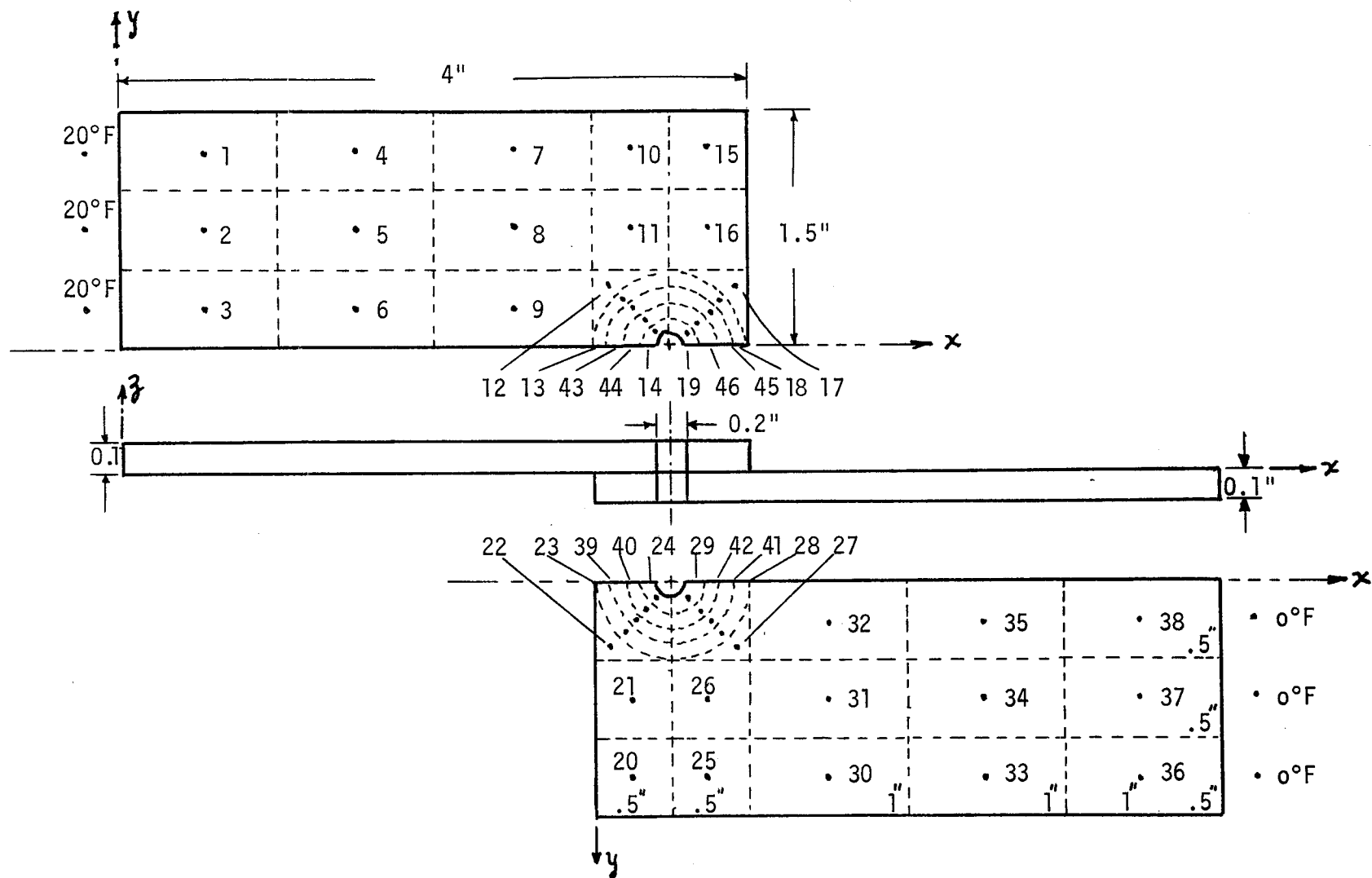


FIG. 29. LOCATION OF NODES — STEADY STATE HEAT TRANSFER ANALYSIS

